2016

Regulatory Architecture of Non-Apoptotic Cell Death Program in C. Elegans

Maxime Jeremie Kinet

REGULATORY ARCHITECTURE OF A NON-APOPTOTIC CELL DEATH PROGRAM IN C. ELEGANS

A Thesis Presented to the Faculty of

The Rockefeller University

in Partial Fulfillment of the Requirements for

the degree of Doctor of Philosophy

by

Maxime Jérémie Kinet

June 2016

REGULATORY ARCHITECTURE OF

A NON-APOPTOTIC CELL DEATH PROGRAM IN C. ELEGANS

Maxime Jérémie Kinet, Ph.D.
The Rockefeller University 2016

Cell death is prevalent in animal development, homeostasis, and disease. While apoptotic cell death has been extensively studied, many dying cells in development do not exhibit apoptotic morphology, and mice lacking core apoptotic regulators have mostly normal rates of developmental programmed cell death. However, little is known about how alternative death programs are set in motion. In the nematode *Caenorhabditis elegans*, most cells fated to die by apoptosis are eliminated as young, undifferentiated cells, for no obvious functional reasons. The male nematode's linker cell, in contrast, dies as an older, differentiated cell, whose life and death subserve precise and important functions. The linker cell first undertakes a long migration along a characteristic path, elongating the male gonad into its proper, mature shape. Once the gonad has attained its final shape and the linker cell has completed its migration, the linker cell then dies to connect the gonad to the environment and allow male fertility. Linker cell death is genetically and morphologically non-apoptotic. Instead, this death program requires the temporal regulator LIN-29, the SARM-like protein TIR-1, the mitogen-activated protein kinase kinase (MAPKK) SEK-1, and the glutamine-rich protein PQN-41. SARM and MAPKKs have been implicated in non-apoptotic degeneration of axon distal segments following axotomy, and some developmental and pathological cell death events in vertebrates resemble the morphology of the dying linker cell. Thus, the molecular mechanism governing linker cell death may be conserved; however, neither the initiating death signals nor the target/s of linker cell death regulators are known. Using classical

genetics, I have investigated the initiating mechanisms of linker cell death. I have characterized the cell-autonomous involvement of a histone 3, lysine 4 methyltransferase complex centered on the Trithorax/MLL-like catalytic subunit SET-16. I then demonstrated that two opposing spatial cues, the Wnt ligands EGL-20 and LIN-44, cooperate with LIN-29 to control linker cell death initiation. I showed that the Abdominal-B-like Hox transcription factor NOB-1 likely acts upstream of these two Wnt pathways, and that the Tailless/Tlx nuclear hormone receptor NHR-67 acts in parallel to these regulators to promote linker cell death in addition to linker cell migration. Finally, I show that the Wnt pathways and all known linker cell death mediators require the heat shock factor HSF-1 for cell death. Importantly, HSF-1 function in linker cell death is distinct from, and competes with, its role in stress responses. My studies demonstrate that HSF-1, previously thought to be primarily protective, is a key downstream regulator of a non-apoptotic cell death program. I have also developed a method to isolate large numbers of linker cells from staged worms populations, to enable a comprehensive characterization of the transcriptional program driving linker cell death.

To my parents.

Sans qui je ne serais jamais arrivé ici.

J’espère qu’aujourd’hui vous serez fiers de moi.

ACKNOWLEDGEMENTS

In truth a whole thesis could, and perhaps should, be written on the people I should thank for supporting, sustaining, and encouraging me during my graduate school years. I can not go over all the friends and family I should thank, but suffice it to say that without their presence in my life, not only would I never have made it through graduate school, but likely I would not never have landed here in the first place.

First and foremost I thank Shai Shaham, my thesis advisor. If from his brilliant example I have picked up a fraction of his ability to ask the right questions and come up with incisive and creative experiments to answer them, my 7 years in his lab have been well worth the time. The collegial academic environment he fosters, the genuine excitement he shows towards his trainees, and his willingness and encouragement to let us explore widely, have enabled me (I hope!) to grow into a confident and ambitious scientist and have kept science truly fun for me, week in and week out.

I also wish to thank all the present and past members of the Shaham lab, whose enthusiasm and generosity with time and ideas have made graduate school a most enriching time. I especially thank Elyse Blum, who initiated me to the ways of the worm and the linker cell; and Menachem Katz, without whose efforts the linker cell sorting project would have never gotten off the ground.

I thank my committee members, Hermann Steller, Cole Haynes, and Elaine Fuchs, for their invaluable scientific input and career advice.

I thank the staff of the Rockefeller Flow Cytometry Resource Center, Svetlana Mazel, Stanka Semova, and Selam Tadesse, for their advice, efforts, and accommodation in developing the cell sorting method.

I thank the Rockefeller Dean's Office, Sid, Emily, Kristen, Marta, Cris, and Stephanie, for their advocacy and all the behind-the-scenes work that make this graduate program such a success.

Finally, I thank the Tri-Institutional MD-PhD program leadership, Olaf Andersen and Ruthie Gotian, for bringing me here and allowing me to pursue my medical and scientific dreams, for their unwavering support in easy and in tough times, for their creation of a true family of colleagues, many of whom I now count among my very best of friends.

Table of Contents

List of Figures

List of Tables

1 Introduction

1.1 Programmed cell death – a historical perspective

In his 1665 tome, *Micrographia,* the British polymath Robert Hooke coined the term "cell" to describe the biological units he observed under the newly invented microscope. Close to 200 years passed before the German zoologist Karl Vogt argued, in 1842, that the regression of the notochord he observed in tadpoles of the midwife toad *Alytes obstetricians* must be physiologic. Two decades later, the great German evolutionary biologist August Weisman, better known as the formulator of the so-called "germ plasm" theory, made essentially the same observation with the degenerating larval structures of pupating insects. During the latter half of the 19th century, cell biologists working in Germany and France accumulated instances of cells dying for no clear pathological reason during the development of organisms representing a wide range of taxa. Ludwig Stieda observed chondrocytes dying during the ossification of growth plates; Elie Metchnikov, the father of cellular immunity, coined the term "histolysis" for the regression of muscles during the metamorphosis of amphibians; Walther Fleming saw cells dying in rupturing and atretic rabbit ovarian follicles; Franz Nissen, in the mammary glands of cats and dogs; Walther Felix, in the uninnervated myocytes of human fetuses; John Beard, in fish sensory neurons[1].

These observations continued into the 20th Century with Rémy Collin, who in 1906 reported on the death of neurons in chick spinal cords, and the concept of cell death as a means to eliminate transient developmental structures became a part of histology textbooks at this time[2]. In the 1930s, Viktor Hamburger and Rita Levi-Montalcini began

their seminal work on cell death in developing nervous systems, and in 1951 Alfred Glucksman published an influential review of cell death in developing vertebrates, organizing it by organ system and developmental function, thus establishing that cell death is a widespread and physiologic phenomenon.

Returning to insect metamorphosis, Richard Lockshin and Carroll Williams proposed, in 1965, the concept of "programmed cell death" properly speaking[3], and the next year, Jamshed Tata, applying actinomycin D and cycloheximide to tadpole tails, showed that new RNA and protein synthesis is necessary for their regression, implying an active process[4]. In 1972, Kerr, Wyllie, and Currie coined the term "apoptosis" in reference to a particular morphological type of organized cell death, contrasting it with accidental necrosis, and identifying it as a common phenomenon in development, homeostasis, and disease, particularly cancer[5]. Although chromatin compaction is the morphological feature most associated with apoptosis today, the morphology they observed of membrane-bound blebs "falling away" from the cell corpse reminded them of leaves falling off a tree in the fall.

In 1973 Schweichel and Merker proposed classifying cell deaths into three morphological classes on the basis of electron microscopic studies[6]. Their type I cell death is now associated with apoptosis. Type II cell death exhibits autophagic morphology, with many large cytoplasmic vesicles containing organellar remnants. Type III cell death has a necrotic morphology, with relatively intact chromatin but bloated and vacuolated cytoplasmic contents[6].

While most of these early observations of programmed cell death were restricted to the deletion of temporary anatomical structures during organismal development, today

we recognize that programmed cell death is required for the proper development, homeostasis, and response to pathological insults of virtually all animals, from sponges to humans[7]. Cell death is crucial for the elimination of supernumerary cells produced during development, as strikingly apparent in vertebrate nervous system, where up to half of all neurons eventually die[8], and especially in certain brainstem nuclei where up to 85% of neurons die[9]. Cell death is also essential in creating a self-tolerant adaptive immune system. Developing lymphocytes with auto-reactive T-cell or B-cell-receptors must killed to prevent autoimmunity, and more than 96% of all T-cell precursors are deleted in the thymus[10,11]. The extra cells produced during an acute inflammatory response must also be eliminated once the instigating insult is over[11]. Many tissues within our bodies, including most of our epithelia, as well as more static tissues such as bone, turn over with varying frequency over the course of our lifetime[5]. Finally, cells that have suffered some pathological insult, whether a viral infection, DNA damage, or excessive metabolic stress, are eliminated via programmed cell death[12]. Thus, a broad understanding of programmed cell death is likely to yield valuable insights into, and, ultimately, treatments for human pathologies.

1.2 Apoptosis

1.2.1 C. elegans perspective

Over the past three decades, the nematode *Caenorhabditis elegans* has proved an invaluable tool for dissecting the molecular mechanisms behind programmed cell death. Several aspects of this remarkable organism make it so well suited to cell death research. Like most or all nematodes, *C. elegans* has a virtually invariant cell lineage, where death features as a prevalent, pre-determined fate[13]. The 131 somatic cells that die in a

developing *C. elegans* hermaphrodite come in several waves. The earliest and largest wave occurs in the embryo, where 113 cells die. Eighteen more cells die during the first two larval stages. In the male worm, a third wave of cell deaths helps sculpts the elaborate tail fan, the male's mating structure, just before the last molt into adulthood. In both sexes, a last, more prolonged wave of programmed cell deaths occurs in the adult gonad, but these deaths do not manifest as the deterministic events of the somatic lineage[13].

The worm being small and transparent, these cell deaths are easy to observe in the intact, developing organism. Combined with simple genetics and culture methods[14] as well as a fully sequenced and well-annotated genome[15], these attributes of *C. elegans* have enabled investigators to conduct large-scale, forward genetic screens to search for genes involved in programmed cell death in an biased manner and to ask precise molecular questions regarding the expected deaths of individual cells.

Indeed, the foundations of our molecular understanding of programmed cell death were laid in the worm. In the 1980s, Horvitz and colleagues screened for mutants abrogating the death of several pharyngeal cells. The mutants isolated in these screens came to define the four core genes[16] of the program known as apoptosis. In the nematode worm, the core apoptotic pathway consists of just four proteins. EGL-1, a Bcl-2 Homology (BH)-3-domain-only protein, is transcriptionally induced in cells fated to die[17]. In these cells, it binds CED-9[18], a pro-apoptotic Bcl-2 family member which contains all four Bcl-2 homology domains (BH1-4). CED-9, when free, binds and sequesters CED-4, an Apaf1-like protein[19,20]. Upon binding of EGL-1 to CED-9, newly liberated CED-4 molecules assemble into octamers known as apoptosomes which force

two CED-3 molecules into such close proximity that they cleave and activate each other[21]. CED-3 is a protease that is translated as an inactive precursor, or zymogen, which must be cleaved to be activated. Active CED-3 uses a catalytic cysteine residue to cleave other proteins specifically after aspartyl residues, a property which led to the common name "caspase". Activated CED-3 cleaves to activate or degrade a multitude of downstream targets, leading to controlled shut-down and eventual destruction of the cell[16,22]. These interactions are summarized in Figure 1A.

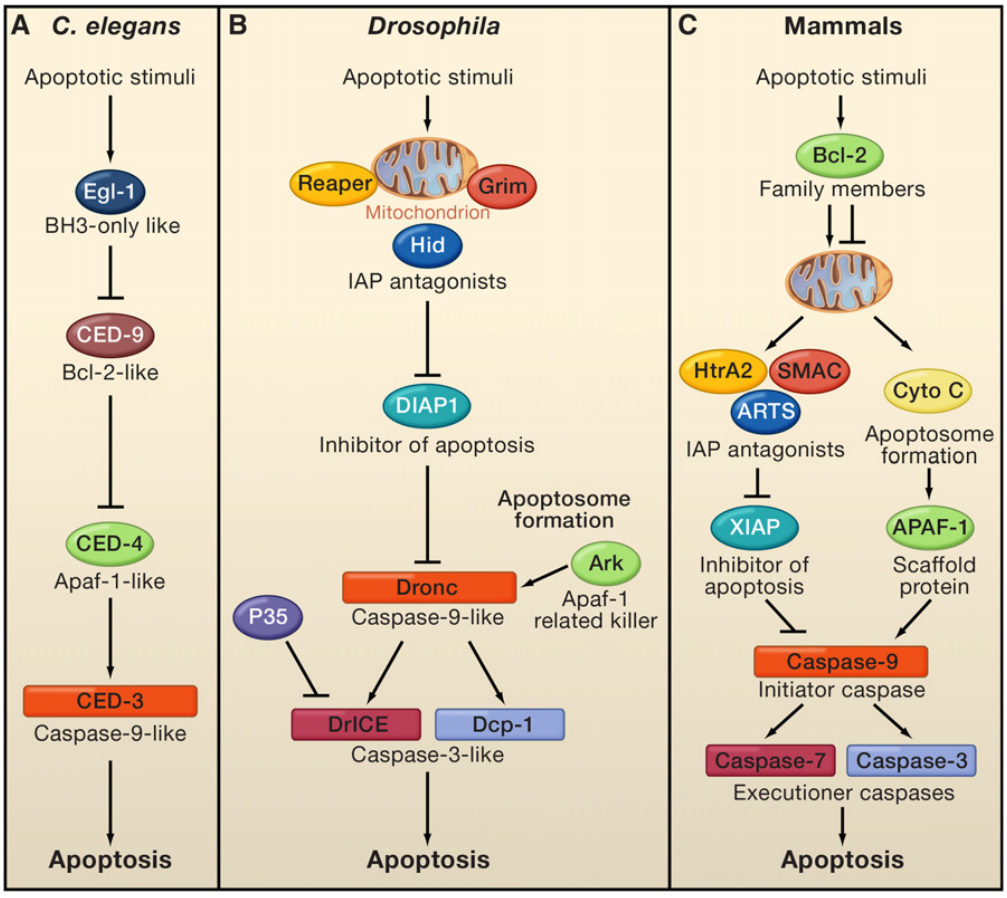

Figure 1: Summary of core apoptotic pathway in *C. elegans*, *Drosophila*, and mammals. Adapted from Fuchs and Steller, 2011[12].

How is cell death initiated in *C. elegans*? Upstream of this conserved pathway, transcription factors have been identified which activate death in specific cells by transcriptional upregulation of *egl-1*, for example, in the M4 sister cell[23,24] or in hermaphrodite-specific neurons in the male[25,26]. Some of these transcription factors appear to be specific for a select cell type, while others appear to function more generally in several cells that are fated to die[24]. While upstream transcriptional signals that instruct cell death are known for a few cells in *C. elegans*, the molecular requirements for proper induction of *egl-1* transcription across the embryo, especially in the early lineage branches, where divisions and deaths happen quickly, are not well understood. The elucidation of these rules awaits a detailed functional analysis of *egl-1* regulatory regions. In at least a few cells, however, proper execution of cell death requires a more complex regulatory strategy involving regulation of cell death genes downstream of *egl-1*.

1.2.1.1 Tail-spike cell death

The *C. elegans* tail-spike cell is a binucleate cell, which arises by cell fusion and sends a slender posterior process that seems to serve as a scaffold for molding the *C. elegans* tail. *ced*-3 and *ced-4* are absolutely required for tail-spike cell death, but *egl-1* plays only a minor role, and a gain-of-function mutation in *ced-9* has no effect[27]. Studies of *ced-3* transcription revealed that its expression is induced in the tail-spike cell about 25 minutes before morphological signs of cell death are apparent. The homeodomain transcription factor PAL-1 promotes *ced-3* expression in the tail-spike cell by binding to three redundant sites upstream of the *ced-3* gene. These results suggest that transcriptional induction of *ced-3*, and not of *egl-1*, may be the key regulatory event promoting tail-spike cell death.

Additional layers of control also exist. A recent study demonstrated that tail-spike cell death requires the F-box protein DRE-1[28]. Genetic and molecular evidence supports the idea that DRE-1 functions in a Skp/Cullin/F-box (SCF) complex in parallel to EGL-1 and likely upstream of CED-9. An attractive model is that DRE-1 substitutes for EGL-1 by inactivating CED-9 through ubiquitination and degradation, thereby creating a permissive environment for newly translated CED-3. Support for this model comes from studies of human FBX010 and BCL2, proteins similar to DRE-1 and CED-9, respectively. In a subset of B-cell lymphomas, FBX010 expression can promote BCL2 degradation. Furthermore, in these same lines, FBX010 expression promotes cell death[28].

Mutations in FBX010 are found in some patients with B-cell lymphomas, and expression of the gene is reduced in many others. Furthermore, RNAi against FBX010 in tumor cells promotes their survival[28]. These results suggest that FBX010 may function as a tumor suppressor gene. Mutations in Cdx2, the human homolog of *C. elegans pal-1* promote intestinal tumors[29], suggesting that this gene is a tumor suppressor as well. These observations raise the intriguing possibility that while tail-spike cell death control exhibits non-canonical features in *C. elegans*, similar regulatory mechanisms may play integral roles in controlling tumorigenesis in humans.

1.2.1.2 Sex-specific death of CEM neurons

The sexually dimorphic CEM cells survive in males, differentiating into neurons that help orchestrate the male's complex mating behavior[30]. In hermaphrodites, which do not exhibit this behavior, the neurons die[13]. CEM cell death requires all four core cell death genes. Yet, as in the tail-spike cell, CEM cell death regulation appears to require

transcriptional activation of the *ced-3* caspase gene. Although *egl-1* expression is still induced in CEM neurons, this induction is not always sufficient to promote CEM death. In males carrying mutations in *unc-86*, a gene encoding a POU homeodomain transcription factor, *egl-1* expression is unaltered, but CEMs fail to die. Genetics and expression studies revealed that UNC-86 protein, LRS-1, a tRNA synthetase, and UNC-132, a novel protein, control CEM demise by promoting *ced-3* transcription [25,26]. Nonetheless, whether *ced-3* or *egl-1* transcription is the rate-determining step in CEM cell death remains unclear.

ced-3 transcription in CEMs seems to be counteracted by CEH-30, a BarH1-related transcription factor. CEH-30 functions genetically downstream of *egl-1* and *ced-9*[25,31]. A *ceh-30* gain-of-function allele alters an intronic consensus sequence for binding by TRA-1A, a Gli-related protein that is an effector of the sex determination machinery promoting hermaphrodite identity[32,33]. This observation suggests that TRA-1A normally represses *ceh-30* in hermaphrodites.

CEM neurons and the tail-spike cell survive for an extended duration after they are generated and before succumbing to cell death. Likewise, both cell types actively control transcription of *ced-3*. This correlation raises the possibility that in these long-lived cells destined to die, there is a need to replenish CED-3 protein to promote cell death. Indeed, *ced-3* transcriptional reporter studies suggest that while the gene is widely expressed, its transcription is mainly confined to early embryogenesis[34], before most cell death takes place. Thus, cells that are longer lived may need to re-express the gene to promote their demise.

1.2.1.3 The use of alternate caspases in dying cells

The *C. elegans* genome contains three caspase-encoding genes in addition to *ced-3*: *csp-1, csp-2,* and *csp-3*[35]. While CSP-1 protein has caspase activity *in vitro*[35], and its overexpression can promote cell death in *C. elegans*[36], neither *csp-2* nor *csp-3* seem to encode catalytically active enzymes. CSP-2 has a catalytic cysteine, but lacks conserved residues surrounding the active site, and CSP-3 lacks the large caspase subunit and its active site.

csp-1 may play a minor role in somatic cell death. While mutants in the gene have no obvious cell death defects, enhanced cell survival is observed in conjunction with weak mutations in *ced-3* caspase[36]. Enhancement is cell-specific, as only some cells destined to die, such as the sister of the pharyngeal M4 neuron, are affected. The activity of CSP-1 does not appear to be regulated by CED-4, as *ced-4* lesions do not inhibit ectopic cell death mediated by CSP-1. It seems, therefore, that if CSP-1 has a role in cell death, it may respond to different cues than CED-3.

Loss-of-function mutations in the *csp-2* and *csp-3* genes have been reported to enhance cell death in the germline[37] and soma[38] respectively, although this observation has been challenged[36]. A suggested mechanism for these effects is that these caspase-related proteins bind CED-3 or CSP-1 to inhibit their activities[37,38]. However, given the weak cell death effects of mutants in these genes, testing models regarding their activities remains challenging.

1.2.1.4 Germ line cell death

In well-fed, unstressed worms, about half of all germ cells born die within the gonad before reaching maturity. Importantly, due to the relatively undifferentiated and syncytial

nature of the germ line, the deaths of germ line nuclei do not appear as the deterministic events of the somatic lineage. How are germ line deaths initiated? ras/*let-60*/MAPK signaling, perhaps modulated by ephrin signaling through the VAB-1 receptor[39] or insulin signaling through the DAF-2 receptor[40], promotes exit from the pachytene stage of meiosis I[41] and subsequent death[39,41]. However, ras/*let-60(gf)* mutations do not increase the amount of death[42]. Therefore, MAPK signaling likely imparts germ cells with competence for death, without being instructive. Germ line deaths, like most somatic deaths, require *ced-3* and *ced-4*. Similarly, *ced-9* functions in a protective capacity. However, *egl-1(lf)* does not prevent germ line cell death, and *ced-9(gf)*, which in the soma blocks cell death, has no such effect in the germ line[43]. Thus, in the healthy, fed state, *ced-9* must be regulated differently in the germ line than in the soma.

Mutations in the Pax2-related genes *egl-38* and *pax-2* promote excess germ cell death[44]. Genetically, *egl-38* and *pax-2* function upstream of *ced-9*, a model supported by the observation that EGL-38 and PAX-2 proteins bind to regulatory sequences near the *ced-9* gene and promote transcription at this locus. This protective role of *egl-38* and *pax-2* extends to the soma, likely through the same mechanism, because these mutants also exhibit enhanced somatic apoptosis that is suppressed by *ced-3, ced-4,* and, perhaps because the *egl-38* and *pax-2* alleles used are not nulls, by *egl-1*[44]. An interesting possibility is that MAPK signaling directly controls the activity of *egl-38* and *pax-2*, transcriptionally or post-translationally. Alternatively, MAPK signaling could control levels of CED-9 translationally, similarly to how MAPK activity determines Mcl-1 levels to control the amount of breast tissue during puberty and lactation[45].

The amount of germ cell death increases in response to a variety of stressors, including DNA damage[42], starvation[46], infection[47], and osmotic, oxidative, and heat insults[48], presumably as a way to ensure the propagation of the fittest and most intact genomes and to focus resources on fewer but healthier germ cells[49]. Interestingly, hypoxia suppresses germ cell death[50], perhaps because worms are often but transiently exposed to hypoxia as they feed on aerobic bacteria, their preferred source of food. In the stressed state, a role for BH3-only proteins in the germ line comes into focus. The worm homolog of p53, *cep-1*, is activated in response to various stressors, including DNA damage and infection, in a manner that is modulated positively and negatively by MAPK signaling[42]. Following activation, CEP-1 directs the transcription of two BH3-only genes, *egl-1* and *ced-13*[51], much like mammalian p53 directs the transcription of a number of BH3-only genes in response to stressors. As mutants for both *egl-1* and *ced-13* block DNA damage-induced germ line death, these genes may perform non-redundant functions, perhaps responding to different genome-integrity meiotic checkpoints[52].

Whether dying germ line nuclei succumb to stochastic fluctuations around the baseline permissiveness to death set by MAPK, *egl-38,* and *pax-2*, or whether they deterministically signal their own death, is unknown. The involvement of genes acting in gonadal sheath cells in germ cell death competence[53,54] raises the possibility that regulation of germ cell death could have cell-autonomous and non-autonomous components. Individual nuclei could instruct their own death, depending on CEP-1/p53's assessment of their own genomic integrity. How faithfully this signal is obeyed could depend on its strength relative to the gonad-wide permissiveness to death. This permissiveness, as we have seen, might in turn be set by diffusible insulin-like-peptides

or Ephrins, originating in the gonad sheath and controlling MAPK pathway activity and levels of CED-9 throughout the death-competent gonad, in a manner that is responsive to certain types of organismal stress. In particular, the observation that germ cells and the gonadal sheath form a bidirectional signaling circuit to control death offers a simple model system to study stromal effects on programmed cell death, a process that is dysregulated in many human cancers.

While we have some idea of how apoptotic pathways are induced and initiated in a variety of cell types in the worm, the picture of what happens downstream of CED-3 is less clear. Indeed, caspases do not simply digest the contents of the cell non-specifically, as cytoplasmic release of calpains or other lysosomal proteases[55] induces a necrotic death rather than an apoptotic one. While a few effector substrates of CED-3, such as the DNA endonuclease NUC-1[56] and the Xk-family transmembrane protein CED-8, which promotes phosphatidylserine exposure[57,58], have been identified, they largely cannot promote cell death on their own. Rather, their mutant phenotypes suggest that they function in efficient corpse clearance. However, removal of individual pieces of the execution machinery downstream of *ced-3* may result in some parts of the dying cell being dismantled appropriately while others persist. This mixed effect may therefore obscure the *prima facie* clear demarcation between cell killing and corpse clearance. Furthermore, Jagasia *et al.* found that in the course of developmental apoptosis, the characteristic mitochondrial fragmentation requires *egl-1* and *ced-9* but not *ced-4* or *ced-3*[59], showing that not all features of apoptosis need be caspase-mediated. Clearly, much remains to be learned about how apoptotic demise is orchestrated downstream of the core pathway.

1.2.2 Drosophila perspective

The study of apoptosis in the fruit fly *Drosophila melanogaster* has revealed a number of important regulatory layers not obviously present in worms. In contrast to *C. elegans,* where a single major apoptotic caspase, CED-3, exists, the fly genome encodes seven caspases. These fly caspases can be classified into two groups based upon the length of their N-terminal pro-domain. Long prodomain caspases, such as Dronc (or, in fact, CED-3), contain Caspase activation and recruitment domains (CARDs), which mediate recruitment of caspases to the apoptosome[60,61] and are also present on CED-4/Apaf-like proteins. Other long-prodomain caspases, such as Dredd[62], contain death effector domains (DED)[63,64] which recruit caspases to another type of activation complex, the death inducing signaling complex (DISC). These complexes are usually, but not always, scaffolded on a transmembrane receptor[65,66]. However, the relevance of DISCs and DED-domain caspases in initiating apoptosis in *Drosophila* is not clear[62,67]. Upon activation, the initiator caspase Dronc[68,69] cleaves and activates the caspases Drice[70], Dcp-1[71], or others, which then perform the executioner functions associated with CED-3. This two-step caspase activation sequence allows for signal amplification of the cascade, as one activated Dronc can activate many molecules of Drice. The fly genome encodes a CED-4-like protein, Dark[72], which also forms octameric apoptosomes[73]. However, unlike in the worm, *Drosophila* Dark does not appear to be regulated by Bcl-2 family members in most developmental or pathological deaths[74,75]. Curiously, *Drosophila* Debcl, a homolog of the mammalian pro-apoptotic Bcl-2 family members Bax and Bak, does appear to promote developmental cell death specifically in the nervous system[75]. The reason for this tissue-specific Bcl-2 requirement is unclear.

How is this cascade regulated in flies? Steller and colleagues isolated a deletion mutant spanning the gene *reaper* in which most developmental cell deaths in the fly were abolished[76]. However, in *reaper* mutants, cells are still able to undergo apoptosis in response to X-ray irradiation, showing that *reaper* does not affect the core execution machinery. Still, overexpression of *reaper* is able to cause ectopic cell death[76]. A first clue to how *reaper* promotes cell death came from the isolation of loss of function mutations in *thread,* a gene encoding Drosophila Inhibitor of Apoptosis (Diap1), which dominantly enhanced *reaper*-overexpression-induced cell death[77]. Other IAPs were identified in vertebrates[78-80], and form a family of proteins which are able to bind to and inhibit the action of caspases[81-83]. *Drosophila* Diap1 is a RING-finger E3 ubiquitin ligase, which targets the initiator caspase Dronc for proteasomal degradation, but which can also auto-ubiquitinate in response to apoptotic stimuli to allow Dronc accumulation[77,84]. Reaper and its homologs Hid, Grim, and Sickle[76,85-87] can physically sequester IAPs, and Reaper also stimulates the auto-ubiquitinating and proteasomal destruction of Diap1[84], thereby freeing caspases to kill cells. These interactions are summarized in Figure 1B.

Interestingly, certain viruses that primarily infect arthropods, the baculoviruses, encode caspase inhibitors of uncertain evolutionary origin[88]. One such inhibitor, p35, prevents apoptosis in diverse phylae[89-91]. P35 is as direct caspase inhibitor whose cleavage by executioner caspases results in the formation of an extremely avid direct caspase inhibitor[92-94].

Unlike in the worm, where transcriptional induction of *egl-1* appears to be the main avenue for induction of apoptosis, in *Drosophila*, transcriptional induction of *reaper*-family IAP inhibitors[76], in response to a variety of developmental or homeostatic

impulses[95-97], seems to be the primary mediator of the decision to die. In addition, *hid* is subject to inhibitory phosphorylation, notably through epidermal growth factor receptor (EGFR)-Ras-MAPK signaling[98].

In some cases, apoptosis in the fly can be induced from another cell by the TNF family ligand Eiger, through its receptor Wengen[67,99]. However, unlike its mammalian counterparts (see below), this extracellular pathway does not involve a DED-domain caspase such as Dredd, but rather functions through JNK signaling, and, like most other fly programmed cell deaths, transcriptional upregulation of an IAP inhibitor gene, in this case, *hid*[99].The developmental significance of this pathway in flies is unclear, and it may be relevant mostly in pathological settings[99,100], but studies of this pathway in flies has implications for the synchronization of cell death across a structure that must be deleted[100,101], a problem first raised by early zoologists observing developmental programmed cell death and one with clear pathological correlates.

1.2.3 Vertebrate perspective

Vertebrates have evolved a sort of synthesis of the worm and fly models. Although vertebrates have conserved the essential architecture of the core worm pathway, the core genes have accrued various family members, the molecular details of their interactions have diverged, and additional regulatory layers have emerged. Importantly, apoptosis in mammals can be initiated through two parallel, though interacting, pathways. In one, the intrinsic pathway, analogous to the worm pathway, signals originating from within the cell entrain the apoptotic machinery. In the other, extrinsic pathway, signals from outside

the cell are relayed within to activate the death program. Both pathways converge on the same central event, the activation of caspases[102].

In mammals, a number of caspases have been identified. Some perform functions primarily unrelated to cell death; indeed, *C. elegans* CED-3 was first identified as a caspase through its homology to mammalian caspase 1, also known as interleukin converting enzyme for its role in the proteolytic activation of the cytokine interleukin-1β[103]. Like in flies, two or three mammalian caspases are needed to recapitulate the role of worm CED-3: caspase 9, the initiator caspase, is activated by Apaf1[104] and can proteolytically activate executioner caspases 3, 6, and 7[105,106]. Interestingly, although worm and fly apoptosomes are octamers, mammalian Apaf1 appears to form a heptameric apoptosome[107]. The functional significance of this difference is unclear.

Further upstream, a number of Bcl-2 family members have been described, which fall into three broad structural categories. In the first, the proteins Bcl-2[108,109], Bcl-X_L[110], and Mcl-1[111] contain all four BH domains[112-115], similarly to worm CED-9. Like CED-9, these proteins also antagonize apoptosis[116-118].

Two mammalian Bcl-2 family members, Bax[119] and Bak[120], lack the BH4 domain. Under physiological conditions, these are bound by the CED-9-like, full-length Bcl-2 proteins[119]. Upon release, Bax and Bak form or promote the formation of large pores in the mitochondrial outer membrane[121,122], an event termed mitochondrial outer membrane permeabilization (MOMP). MOMP depolarizes mitochondria and allows for the cytoplasmic release of mitochondrial-resident factors that promote apoptosis through a variety of mechanisms. These include the *reaper*-like Second mitochondrial activator of caspase / Direct inhibitor of apoptosis-blocking protein with low pI (Smac/DIABLO)[123-

[125]; Omi/HTRA2, a serine protease that binds to and cleaves IAP-type direct caspase inhibitors, including XIAP[126-128]; the flavoprotein apoptosis inducing factor (AIF)[129,130], which further permeabilizes mitochondria and also translocates to the nucleus to induce chromatin condensation and DNA fragmentation through unclear mechanisms; and cytochrome *c*[131]. The latter, in particular, is required for the formation of mature Apaf1 apoptosomes[132], caspase 9 activation[104] and apoptosis.

Mammalian BH3-only-domain proteins make up the third class of Bcl-2 family members, and appear to fall into two sub-classes. One, comprised of Bid[133] and Bim[134], is able to induce, through direct physical interaction, oligomerization of Bax/Bak and their insertion into the outer mitochondrial membrane[135,136]. The other, comprised of Puma[137,138], Noxa[139], Bik[140], and Hrk[141], activates Bax/Bak indirectly, by binding to and inactivating the full-length Bcl-2 family members[142]. Although such a classification suggests a functional hierarchy where the indirect activators act upstream of the direct activators, different models exist for how indirect and direct inducers interact functionally to promote Bax/Bak-mediated MOMP[143,144]. Which one is correct or predominates may depend on the cellular context.

Regardless of the precise biochemical mechanism, the different BH3-only-domain proteins appear to be regulated by a variety of transcriptional and post-translational mechanisms to signal death in response to various stressors and external signals. Indeed, in contrast to the situation in flies, where somatic cells are killed primarily by transcriptional induction of IAP-antagonists, mammalian IAP antagonists seem to be ubiquitously expressed. Rather, the mammalian intrinsic pathway largely reprises the

somatic worm model of requiring transcriptional induction of BH3-only proteins to induce death[145]. These interactions are summarized in Figure 1C.

As discussed above, in the extrinsic apoptotic pathway, the core pathway can be activated from without the cell. This is accomplished by ligation and activation of death receptors such as Fas/CD95 or TNF-R[146], recruitment of adaptor molecules including FADD[66] and TRADD[147], and activation of DED-domain relay caspase 8 or 10[64,148]. These relay caspases can then activate the initiator and executioner caspases, thus bypassing mitochondria, as is demonstrated by the fact that Bax/Bak double-knockout T cells can be killed by Fas ligation[149]. Caspase 8 can also proteolytically activate the BH3-only protein Bid, thus engaging the intrinsic pathway[150]. This cross-talk between the extrinsic and intrinsic pathways appears to be most important in cells expressing high levels of IAPs[151].

The mammalian cellular immune system can also directly induce caspase activation. Cytotoxic lymphocytes, such as $CD8^+$ T cells or NK cells, upon activation, release their cytoplasmic granules containing perforins and granzyme proteases onto their target cells[152]. Perforins insert into the plasma membrane of the target cells[153], forming large pores through which granzymes[154,155] then enter to proteolytically activate caspases in the target cell cytoplasm[156].

1.3 Cell death without caspases – evidence for alternative death programs

As we have seen, apoptosis is an essentially conserved cell death program throughout the animal kingdom with important clade-specific variations. However, evidence from a range of taxa suggests that other forms of cell death exist. Indeed, 19th century zoologists observed a range of morphologies in dying cells, and we are beginning to appreciate that

these varied morphologies may reflect different molecular underpinnings. Here I briefly review candidate models for non-apoptotic cell death programs.

1.3.1 Non-apoptotic cell death in mammals

Apaf1 knockout mice have greatly sub-Mendelian survival, but this reduced viability appears to be mostly due to exencephaly caused by accumulation of neuronal precursors in one particular brain region, rather than a general overabundance of neurons or other cells. Furthermore, this overabundance may be caused by excess proliferation rather than decreased cell death[157]. In these mice, intra-uterine regression of inter-digital webbing is only briefly delayed[157]. If able to survive past the perinatal period, Apaf1 mutants generally are able to survive into adulthood, with no gross anatomical or physiological abnormalities. Indeed, male infertility is caused by increased death of sperm precursor cells, and females are fertile[158]. Finally, Apaf1-deficient mice do not harbor excessive neurons in their spinal cords or in dorsal root ganglia[159].

Similarly, Bax/Bak double mutant mice are also able to survive to adulthood, albeit, again, at greatly sub-Mendelian frequencies[149]. These mice exhibit a phenotype distinct from the Apaf1 mutants. Notably, although Bax/Bak and Apaf1 mutants appear to share the neuronal precursor hyperproliferation defect[149], the exencephaly that causes most of the perinatal death in Apaf1 mutants is absent. Bax/Bak mutant mice do have increased numbers of leukocytes, manifesting as peripheral leukocytosis, hypercellular lymphoid organs, and lymphocytic infiltrates in various organs; females also have imperforate vaginas[149]. Further, Bax/Bak mutants retain some amount of inter-digital webbing into adulthood[149]. However, this latter phenotype remains quite weak when compared to the frank syndactyly that mutants for certain Wnt and BMP pathway

regulators exhibit[160-162], suggesting that, in Bax/Bak mutants, much of the cell death necessary to separate digits[163] can take place.

How, in these mutants, the cell death undoubtedly necessary for proper animal development occurs remains a mystery. One possibility is that none of the mouse mutants created to date fully blocks apoptotic, caspase-dependent cell death. Indeed, the extrinsic and intrinsic pathways function through a set of caspases that only partially overlap, and to date no mutant has been created that could truly be considered a pan-caspase molecular null mutant. However, some evidence suggests that the deaths seen in Apaf-1 and Bax/Bak mutants, where apoptosis can safely be said to be substantially impaired, are not due to redundancy in the apoptotic machinery.

Chautan *et al.* described the physiological occurrence of a necrotic death morphology in the same mouse inter-digital cell death[164] which seemed, from the Apaf-1 and Bax/Bak knockouts, to rely at least partially on non-apoptotic mechanisms. These authors first treated wild-type limb buds with a stimulator of BMP signaling, to promote the death fate, and a pan-caspase inhibitor, to block apoptosis, and subsequently observed dying cells with necrotic morphology. They then showed that this morphology was prevalent in untreated Apaf1 mutants. Finally, Chautan *et al.* examined untreated wild-type mice, and found roughly equal rates of morphologically necrotic and apoptotic cell deaths in the inter-digital spaces[164]. Thus, at least in this tissue, a non-apoptotic cell death program may act not simply as a backup to apoptosis, but as the primary mechanism for killing a subset of cells.

Oppenheim *et al.* found that in mouse Apaf1-mutant embryonic spinal cords, neuronal death was delayed by a few days, but final numbers of all types of neurons

examined were unaffected[159]. Cells in the process of dying were present in these tissues, suggesting that the normal cell numbers were not exclusively due to an adjusted production of cells. Furthermore, when examined by electron microscopy, dying motor neurons in these mutants exhibited non-apoptotic morphology, with many large cytoplasmic vesicles, organellar swelling, and nuclei and chromatin that remained intact until late in the death process[159].

In another setting, Oppenheim and colleagues showed that in caspase 9 and caspase 3 mutant mice, neuronal cell death in the peripheral nervous system seems relatively unaffected, with normal numbers of spinal interneurons and sensory, motor, and autonomic neurons[165]. Again, dying cells did not exhibit apoptotic morphology, with little chromatin condensation and cell blebbing, but extensive cytoplasmic vacuolation and organellar swelling[165], as in Apaf1 mutants.

Even in wild-type animals, non-apoptotic morphology can be observed. Pilar and Landmesser surgically removed the optic vesicle from chick embryos[166] and examined the morphological consequences of this treatment on the ciliary ganglion neurons which normally innervate this organ. Interestingly, they find structures reminiscent of those seen in apoptotic mutants: dilated ER, swollen mitochondria, but also highly crenelated nuclear envelopes with relatively open chromatin[167]. These studies argue that non-apoptotic death could occur in a wild-type developing nervous system, just as they seem to occur in wild-type inter-digital tissue removal.

Indeed, some authors have argued, based on cell culture results showing that cells supposedly blocked for apoptosis have reduced clonogenic potential, that apoptotic processes only speed or organize death, without acting as the *bone fide* life/death

switch[168,169]. However, these cell culture results belie the fact that both in *C. elegans* and in mammalian nervous systems, extra cells due to blockade of apoptosis are able to survive and differentiate into functional neurons[170,171] and extra cells in mammalian hematopoietic lineages can differentiate into functional lymphocytes and erythrocytes[149,172].

Schweichel and Merker also proposed a third type of cell death, or Type III cell death, characterized primarily by cytoplasmic changes[6]. Recently, a signaling pathway resulting in morphological similarities to necrosis has been reported[173] and termed necroptosis[174]. Necroptosis requires signaling through any of a variety of receptors such as Fas, TNF-R1, TRAIL-R, Toll-like-receptors 3 or 4, all receptors implicated in mutually inhibitory apoptotic and inflammatory signaling. Downstream of these receptors, in the absence of caspase 8 activity, a DISC-like "necrosome" is formed, composed, at a minimum, of the death-domain-containing kinases RIP1[173] and RIP3[175]. The latter appears to act on the pseudokinase MLKL[176] to induce its oligomerization and insertion into cell membranes[177], permeabilizing them and causing necrotic cell death. Given the requirement for low caspase 8 activity, the relevance of necroptosis in normal development is still an open question. However, this pathway may be engaged in pathological situations where caspase 8 is inactive, either because it has been inactivated by mutation or by pathogens, or because the cell of interest does not express sufficient caspase 8 to inhibit necroptosis[178].

1.3.2 C. elegans and Drosophila non-apoptotic deaths

Other types of programmed cell death have been proposed to act at least to some extent independently of apoptosis. Schweichel and Merker described a "Type II" autophagic cell death morphology 1960s[1]. Recently, interest in the role of autophagy in cell death has revived, and a genetic program controlling autophagy is being pieced together[179]. However, it is not clear to what extent autophagy is a true cell death program capable of killing cells. Autophagy is a cellular survival program, which, when overwhelmed, may result in dead cells with autophagic morphology. Alternatively, autophagy may accompany apoptosis in cases where large-scale tissue destruction is required. This appears to be the case in *Drosophila* salivary gland regression, where inhibition of autophagy delays, but does not ultimately prevent, cell death[180]. Even here, caspases are crucial in tissue lysis[181]. In most cases, perhaps, canonical apoptotic features develop more quickly, but in cases where these are inhibited or slowed, autophagic features develop. However, genetic evidence that autophagy *per se* can kill cells is unconvincing: mice defective in autophagic genes exhibit defects in corpse clearance but not cell death[182]; in *C. elegans*, inactivating autophagy genes promotes cell death[183]. Thus, perhaps except in rare cases, autophagy is unlikely to constitute *bona fide* cell death program, backup or otherwise[184].

In *Drosophila*, the TNF family member Eiger has been shown to promote apoptosis, but may also function through a caspase-independent mechanism[185]. Interestingly, this caspase-independent death requires JNK signaling and dysregulation of energetic homeostasis, a set of requirements similar to that observed in at least some forms of axonal degeneration[186]. However, the physiological relevance of this pathway in *Drosophila* cell death is unclear.

One *bona fide* non-apoptotic pathway appears to play an important role in the adult male *Drosophila* testis, where about a quarter of developing spermatogonial cysts physiologically undergo programmed cell death through a mechanism that does not appear to require effector caspases[187]. Indeed, Drice and Dcp appear to inhibit this cell death program, although whether this inhibition occurs at initiation or execution remains unclear. Conceptually, though perhaps not mechanistically, this role of caspases parallels the protective effect of caspase 8 against necroptosis (see above). Interestingly, the initiator caspase Dronc appears to promote this germ cell death, independently of Dark and, presumably, of the apoptosome.

How then does *Drosophila* male germ cell death proceed? Using electron microscopy, the authors found that dying germ cells exhibited morphological features of both necrosis and apoptosis, including cytoplasmic contraction and chromatin condensation, consistent with the latter, and swollen mitochondria and vesicular, membranous structures, consistent with the former. Genetically, the authors found several pathways that appear to promote germ cell death. In the first clear involvement of Bcl-2 family members in *Drosophila* programmed cell death, the authors found that Debcl and Buffy are required for efficient execution. In addition to these molecules, the authors identify several other mitochondrial proteins: the kinase Pink1, the serine protease Htra2/Omi, and endonuclease G, as being required for germ cell death. In a partially parallel pathway, the authors find that lysosomes and lysosomal-resident hydrolases, including the protease cathepsin D and the nuclease Dnase II, promote germ cell death. How this program is initiated, how its effectors are coordinated, and what their targets might be remains unclear. Omi and endonuclease G have previously been implicated in

apoptosis, and cathepsins in necrosis (see section 1.3.2.4), suggesting that the mixed morphological features reminiscent of these two pathways may have specific molecular underpinnings.

In worms, null and even dominant-negative *ced-3* alleles do not prevent all cell death. Even in quadruple caspase mutants, a few inconsistent cell corpses are occasionally visible[36] in hatched L1 larvae, and these corpses exhibit many features of wild-type apoptotic corpses, including phosphatidyl serine exposure, engulfment, cytoplasmic contraction and chromatin condensation. Additionally, these corpses persist for longer than wild-type corpses, suggesting that engulfment or processing of these corpses is less efficient than for wild-type corpses. While *ced-3* can promote the activity of engulfment genes[58], another explanation for this delay in corpse clearance is that these cells die by a process fundamentally different from apoptosis, which promotes fast clearance.

How apoptotic morphology can be generated in *C. elegans* in the absence of a functional core apoptotic pathway is unclear. One possibility is that engulfment pathways can kill cells fully independently; quadruple caspase mutants that are additionally mutant for both arms of the engulfment pathway were not examined. Alternatively, other backup pathways may exist. Whether either of these two backup mechanisms is able to bypass caspases and engage mechanisms that caspases normally activate, or whether they generate apoptotic morphology entirely independently of events normally downstream of caspases, is unknown. Some evidence suggests that there may be non-*ced-3*-dependent death mechanisms that are part and parcel of apoptosis. RNAi against *icd-1*, the *C. elegans* beta subunit of the nascent polypeptide associated complex (β-NAC), causes

widespread ectopic cell death resembling apoptosis[188]. Loss of *ced-4,* but not of *ced-3*, suppresses this *icd-1*(RNAi)-mediated death, suggesting that *ced-4* can promote caspase-independent killing activities*,* or that *ced-4* can function through other caspases. However, other pro-apoptotic caspases in the worm play only minor roles in cell death and do not seem to function through *ced-4*[36]. Therefore, *ced-4* may indeed be able to kill without caspases, and morphologically apoptotic death may not require caspases in all situations.

1.3.2.1 lin-24/lin-33 mutants

Dominant mutations in two genes, *lin-24* and *lin-33*, were initially isolated in screens for the vulvaless phenotypes. These mutations were found to cause the inappropriate death, late in the L1 larval stage, of P*n.*p cells, the descendants of some of which eventually form the vulva[189].

Morphologically, dying cells in *lin-24* and *lin-33* mutants are refractile and oval by Nomarsky optics. By electron microscopy, corpses exhibit electron-dense nuclear puncta but otherwise normal nucleoplasm, dilation of the nuclear envelope, dense membranous cytoplasmic whorls, and disrupted mitochondria. While the last two in particular are features of the channel-mediated degenerative deaths we will review below, together these four features circumscribe a distinct morphological entity. Interestingly, cells that survive the insult can either recover fully normal morphology or be left with an abnormally small nucleus. Recovered, surviving cells exhibit cell fate defects in P*n.*p cells. Deletion alleles of these genes, presumably representing the molecular null phenotype, are phenotypically wild-type, suggesting that *lin-24* and *lin-33* are not involved in the fate of P*n.*p cells. Rather, recovered cells may have experienced the insult

during a period critical for the reception of some developmental signal. Indeed, P3-8.p commit to a vulval fate at this time period in a process that requires the homeodomain-encoding (HOX) gene *lin-39*[190].

The gene product of the *lin-24(d)* allele contains a domain similar to bacterial toxins, and most recovered alleles contained mutations in this conserved domain. While the *lin-33* gene is not homologous to any known genes, wild-type activity of each gene is required to express the dominant mutant phenotype of the other, which suggests that LIN-33 may traffic or otherwise activate LIN-24. Bacterial toxins homologous to LIN-24 kill eukaryotic cells by forming oligomeric pores in the plasma membrane, a mechanism shared with the membrane attack complex of the vertebrate blood complement system[191] as well as with the perforins of cytotoxic lymphocytes[152].

Galvin *et al.* note that wild-type *lin-24* is primarily expressed in the gut. However, the reporter used may be incomplete, and the gut does not show ectopic death in the gain of function mutants. Still, adhering to this result, one possibility is that the gain-of-function mutations in both genes cause selective ectopic expression in the P*n*.p cells in addition to the novel gene product function. Because the two mutations were isolated independently, this explanation seems highly unlikely.

A second, perhaps more plausible explanation is that *lin-24* and *lin-33* are more widely expressed than previously thought, and that certain cells are somehow more susceptible to death by the *lin-24/lin-33* system. Supporting the idea of cell-type-dependent variability in propensity towards death is the observation that in weak *ced-3(n2427)* mutants, the surviving cells are not randomly distributed but appear to form a consistent subset of cells normally fated to die. In a similar way, *lin-24* and *lin-33* gain of

function might be able to kill only a certain subset of cells as a consequence of some particularity of those cells.

lin-24(d) and *lin-33(d)*-mediated death proceeds efficiently in the absence of functional CED-3 caspase. However, alleles of *egl-1, ced-4*, and of the two classical engulfment pathways were able to suppress this death, albeit weakly, with the suppression being especially apparent in *lin-24(d)* and *lin-33(d)* heterozygotes. Therefore, *lin-24* and *lin-33* could be downstream of *ced-4* or of *ced-3* in some cells, with the gain-of-function mutations reducing, but not eliminating their *ced-4* dependence.

A related explanation for the action of *lin-24* and *lin-33* is that they are downstream of the engulfment genes. Mutations in the engulfment pathways enhance the inappropriate phenotype of weak *ced-3* alleles, and may frankly block the death of one cell, the B.al/rapaav, a death which is nonetheless also *ced-3*-dependent[192]. Reddien *et al* showed that this killing function of engulfment genes resides in the engulfing cell themselves. *lin-24/lin-33*-mediated death is also very sensitive to perturbations in the engulfment pathway. Therefore, in a scenario that would be closer to a cytotoxic T cell's use of perforins, *lin-24* or *lin-33* might function in neighboring cells to kill the P cells, either both, or with one acting as the receptor for the other on the P*n.*p cells. Perhaps *lin-24* and *lin-33* act as downstream mediators of the death-promoting effect of the engulfment pathway, able to kill the P*n.*p cells because of some pre-existing susceptibility of these cells to death.

1.3.2.2 pvl-5 mutants

The results of Joshi and Eisenmann corroborate the idea that *lin-24/lin-33* mediated death may have more in common with apoptosis than initially appears. They identify loss of

function mutants in a gene, *pvl-5,* which also cause inappropriate death of P*n.*p cells, at the same developmental time as the *lin-24*- and *lin-33*-mediated deaths, and frequently with the same ovoid morphology and shrunken nucleus after recovery[193].

The two processes are not identical. *pvl-5(lf)* sometimes causes a swollen, necrotic morphology not reported in *lin-24/lin-33* animals. Moreover, while neither death process preferentially targets any specific subset of the 11 P*n.*p cells, the cell fate defects resulting from the two lesions are likely to be different: *lin-24* and *lin-33* animals are vulvaless, whereas *pvl* stands for protruding vulva. It is also not clear to what extent *pvl-5* surviving or recovered P*n.*p cells are able to assume their normal fate.

Strikingly, while *lin-24/lin-33*-mediated death does not require *ced-3*, *pvl-5*-mediated death does. Further, *pvl-5(lf)*-mediated death is suppressed by *ced-9(gf),* but not by *egl-1(lf)* or by *ced-4(lf),* whereas *lin-24(d)* and *lin-33(d)* can be suppressed, though weakly, by alleles of all core apoptotic genes except *ced-3*. Finally, *pvl-5* mutants suffer a small number of *ced-3*-dependent ectopic cell deaths in tissues other than the P*n.*p cells, something that was not reported one way or the other in *lin-24* and *lin-33* mutants.

Notably, these other ectopic deaths exhibit more varied morphologies than the dying P*n.*p cells, suggesting that the ovoid morphology of the dying P*n.*p cells seen in *pvl-5, lin-24,* and *lin-33* mutants may result in part from some pre-existing aspect of those cells rather than from the death process *per se,* and lending additional support to the idea that death processes affect different cells in different ways.

Unfortunately, the molecular identify of *pvl-5* is unknown to this day. Genetically, *pvl-5* functions upstream of *ced-3* and in parallel to *ced-9.* PVL-5 could represent a worm caspase inhibitor. However, the worm genome has not been found to contain caspase

inhibitors like the IAP proteins[194]. Still, it is possible that nematodes independently evolved an IAP-like function, obscuring its identification by primary sequence homology. Alternatively, *pvl-5* may control *ced-3* at a pre- or co-translational level. It is difficult to explain why *pvl-5* is suppressed by the *ced-9(gf)* and *ced-3(lf)* but not by *ced-4lf)*. Xue and Horvitz described a direct inhibition of CED-3 by CED-9[195]. As Joshi and Eseinmann note, if the *ced-9(n1450gf)* allele also affects this function of CED-9, their results might be evidence that this function of CED-9 is particularly relevant in P*n.*p cells.

1.3.2.3 A latent apoptotic pathway in Pn.p cells?

How can we reconcile the results of these two papers? Comparative anatomy may be useful. In *Pristionchus pacificus* and other distantly related nematodes, some or all P*n.*p cells that are not destined to take part in the vulva die by *ced-3*-dependent apoptosis[196,197]. Additionally, in *Pristionchus,* all P*n.*p have the capacity to die: *Ppa-lin-39* mutants are vulvaless because all P*n.*p cells die, and this phenotype can be suppressed by *Ppa-ced-3* mutations. Thus, in *Pristionchus*, *lin-39* functions as a cell-specific inhibitor of *ced-3.* How might *Ppa-lin-39* inhibit cell death? One possibility is that it antagonizes the activity of *Ppa-egl-1* or *Ppa-ced-4*, or that it promotes the activity of *Ppa-ced-9.* Since none of these genes were cloned at the time of these studies, this possibility was not investigated. However, some clue may be gained from the method of isolation of the *Ppa-ced-3* alleles. Sommer *et al.* identified *Ppa-ced-3* in a screen for suppressors of the vulvaless phenotype of *lin-39*. After screening over 60,000 genomes, 22 of 24 isolated alleles exhibit lesions in *Ppa-ced-3*, suggests that *Ppa-lin-39*'s main function may be to transcriptionally repress *Ppa-ced-3.* It is striking that *pvl-5(lf), lin-24(gf), lin-33(gf)* and *Ppa-lin-39(lf)* all cause the death of the same cells, at the same developmental time.

Perhaps these alleles, rather than being evidence of separate processes, affect the same process in different ways.

1.3.2.4 Degenerative necrosis

Forward mutagenic screens have generated several classes of mutants, most of which were isolated in search of phenotypes other than cell death, that cause inappropriate cell death in the course of the worm's development. Early work from the Chalfie lab isolated alleles of *mec-4*[198], *deg-1*[199], and *unc-8*[200] that dominantly cause certain neurons to swell and eventually die with a vacuolar morphology reminiscent of necrosis. Upon closer inspection, these cells accumulate progressively larger electron-dense membranous whorls and vacuoles, and in parallel begin to form chromatin clumps and nuclear crenellations[46]. Later, organelles may swell, lyse, and disappear.

All three genes encode ENaC-type cation channels that conduct predominantly sodium[201], but also small amounts of calcium[202]. The causative mutations have been shown to increase channel open probability[203]. Gain of function mutations in the nicotinic acetylcholine receptor DEG-3, an ionotropic receptor subunit that functions as a cation channel, also cause necrosis[204].

In screens for suppressors of the channel-mediated necroses, Xu *et al*. identified mutants in the *C. elegans* homolog of the ER calcium-binding chaperone calreticulin, *crt-1*, as being required for MEC-4(d)-mediated necrosis[205]. Mutations in another endoplasmic reticulum (ER) calcium-binding protein, the calnexin CNX-1, also suppress necrosis, as do mutations in the ER-resident IP_3 receptor, ITR-1, and in the ryanodine-receptor ER calcium release channel, UNC-68. Moreover, necrosis could be restored in these mutants by thapsigargin, a drug that both blocks the ER calcium influx pump and

causes calcium release from the ER. Finally, EGTA, a calcium chelator, blocked necrosis. These results establish that cytosolic calcium elevations are required for this type of necrosis. Interestingly, thapsigargin treatment of wild-type worms occasionally caused the necrosis of several other cells in the worm apparently at random, suggesting that sustained cytosolic calcium elevation may be sufficient to cause necrosis in many cell types. Indeed, the *deg-3(gf)* mutations, which likely directly cause cytosolic calcium increase without the need for additional ER calcium, cannot be suppressed by any mutations that block ER calcium release[205].

Is elevated cytosolic calcium inherently toxic to cells? Syntichaki *et al.* instead show that cytosolic calcium activates two classes of proteases, the calcium-activated calpains CLP-1 and TRA-3, and the cathepsin E-like aspartyl proteases ASP-3 and ASP-4, which are responsible for killing the cell[55]. Indeed, overexpression of these proteases was sufficient to cause death in some cells. How might these two classes of proteases interact? RNAi-mediated knockdown of both calpains synergized over the RNAi of the single calpains, and knockdown of both cathepsins synergized over the single cathepsins. However, knockdown of one calpain and one cathepsin did not show enhancement over either single gene knockdown, suggesting that the calpains and the cathepsins could function in a linear pathway. In such a pathway, the elevated cytosolic calcium might activate the calpains, which would in turn activate the cathepsins to kill the cell; however, the evidence for such a genetic pathway has not been rigorously tested. Additionally, several other cytoplasmic cathepsin genes are present in the worm. It is not clear if the requirement for just two of these in neuronal necrosis reflects cell-type-specific

expression of various cathepsins or substrate specificity. If the latter, finding the relevant substrates of cathepsins becomes of paramount importance.

These same authors also show that alleles for subunits of the vacuolar-H+-ATPase (V-ATPase) are able to suppress degenerin-mediated death as well as thapsigargin-induced necrosis[206], suggesting that acidification of the cytosol contributes to channel-mediated necrosis downstream of calcium elevation, and possibly in parallel to cathepsin activation. This is in contrast to mouse studies that suggest that acid may be upstream of calcium release[207], although the two could be mutually enhancing. Further, Artal-Sanz *et al.* propose that the source of this acid in the worm is lysosomes, as treating worms with lysotropic weak bases as well as impairing lysosomal biogenesis could prevent necrosis[208]. We do not yet know if, in *C. elegans*, cytoplasmic acidification is sufficient for cathepsin activation, and, in turn, necrosis.

Interestingly, neuronal necrosis can also be induced by expression of a constitutively active $G_{\alpha s}$[209,210]. Death by such a protein requires the adenylyl cyclase ACY-1, which transmits signals from metabotropic neurotransmitter receptors, and is more modestly dependent on voltage-gated calcium channel subunit UNC-36 and the vesicular glutamate transporter EAT-4[209]. Together, these data suggest that neuronal activity modulates sensitivity to necrosis. Our evolving understanding of stroke pathophysiology suggests that the primary hypoxic injury depletes cellular ATP, which powers the Na^+/K^+ ATPase that maintains the electrochemical gradient across neuronal membranes. Later, an equally dangerous secondary insult occurs upon reperfusion, when the weakened electrochemical gradient allows massive glutamate-mediated neuronal

excitation occurs[211], leading to a rise in cytoplasmic calcium. Necrotic brain foci are also observed in epilepsy[212], which is perhaps more clearly an excitotoxic injury.

In the worm, as in humans, it is still unclear whether necrosis by activation of cytosolic and lysosomal proteases leads to a rather general, poorly controlled digestion of the cell, or whether specific sequences of proteolytic events are required. Elucidating this question may provide insights into the progression of excitotoxic injury after stroke.

1.3.2.5 Other necrotic mutants

Several mutations have been found to cause necrotic cell deaths in cell types other than neurons. In *pnc-1* mutants, the uterine *uv1* cells die in mid-to-late L4 stage with a vacuolated morphology in a process that is dependent on necrotic calpains and aspartyl proteases[213]. Since supplementing wild-type worms with NAM reproduces the *uv1* necrosis phenotype of *pnc-1*[214], this necrosis is likely due to an overabundance of nicotinamide (NAM), which the protein PNC-1 converts to nicotinic acid. It is unclear why these uterine precursor cells are so sensitive to NAM. Other cells whose energy requirements are likely much higher than those of *uv1* cells, such as muscle cells, do not necrose in *pnc-1* mutants. Further, boosting EGFR signaling, which is normally active in *uv1* cell specification, suppresses the death, suggesting that a specific EGFR-repressible NAD+ consumer, or its product, may be involved. However, how such an NAD+ consumer would cause calpain or aspartyl protease activation is unclear.

Other types of mutations also cause cell-type-specific necroses. Loss of the transcription factor *lin-26* causes hypodermal-specific vacuolated necroses through an unknown mechanism[215]. Generally, since downstream events of differentiation are not guided by a single transcription factor, discord between pieces of a cell's differentiation

program may set up energetic, mechanical or other imbalances that facilitate necrosis. Necrosis in the worm has come to be defined by the vacuolar morphology seen in degenerin mutants, but we do not know whether this morphology always requires cathepsin activation. It would be interesting to know whether *lin-26(lf)*-mediated necrosis requires calcium or cathepsins.

Chelur *et al*. observed vacuolated, necrotic morphology after reconstituting human caspase-3 activity in body wall muscle using the strong *hsp-16.2* promoter. In contrast, this system caused the more classical, refractile morphology in other cells[216]. Whether the muscle vacuolations resulted from cathepsin activation is unknown. Regardless, the phenomenon supports the notion that apoptosis is not simply wholesale caspase-mediated digestion of the cell, but rather a precise sequence of events, with cell-type-specific idiosyncrasies, that can been overwhelmed by excessive caspase activity. Additionally, other forms of necrosis, secondary to some catastrophic cellular disruption distinct from cathepsin-mediated destruction, may not result in a vacuolated morphology.

One such example might occur in *unc-83* and *unc*-84 mutants, where the nuclei of the P epithelial blast cells fail to migrate ventrally along with the rest of the cell body, causing the cell to die in a *ced-3*-independent manner[217,218]. This death is not classically necrotic, in that the corpse morphology is refractile rather than vacuolated. *unc-83* and *unc-84* encode KASH and SUN domain proteins, respectively, that anchor the nucleus to the cytoskeleton[219]. Alone, the absence of *unc-84* does not kill, since double mutants of *unc-84* with genes that block all aspects of P cell migration do not cause death[217]. Conversely, the failure of nuclear migration itself is not lethal in all cases, since, in *unc-83* mutants, other nuclei fail to migrate correctly without entraining cell death[218].

It is not immediately clear, then, what kills the P cells in these mutants. Neurons span much greater distances between their distal appendages and their somata but employ special adaptations to bridge this distance efficiently; perhaps the mutant P cells die because they do not harbor these mechanisms. Alternatively, the particular location of the P cells might expose them to mechanical stress that a cell so stretched is unable to sustain. Supporting the latter hypothesis is the observation of large cellular fragments disconnected from the nuclear position. By analogy with the requirement for cathepsins in necrosis, the question of whether this death requires any action of the part of the P cells remains open. In other words, is it possible to interrupt the death without restoring proper nuclear migration, or are the two inherently linked? Here, a simple forward mutagenic screen might uncover yet additional death mechanisms.

1.4 Linker cell death: a non-apoptotic programmed cell death in *C. elegans*

At least one cell in the worm dies by a mechanism that does not appear to require any known cell death gene. The male worm's linker cell is born at the beginning of the second larval stage, L2, near the middle of the animal. Over the course of the next 36 hours, the linker cell migrates along a stereotyped path, leading the developing male gonad behind it, thereby inducing the gonad to adopt the proper, reflexed morphology (Figure 2). Upon reaching the cloaca at the middle of the fourth larval stage, the linker cell dies, and its corpse is engulfed by one or both of two occasionally fused rectal epithelial cells, the Ul/r.p cells (Figure 3)[220]. The death and clearance of the linker cell is usually complete just prior to the animal's final molt from the fourth and last larval stage (L4) into adulthood. This cell death is thought to be necessary to fuse lumen of the *vas deferens*, a channel connecting the gonad's sperm maturation compartments to more

distal structures, with the cloaca, the worm's excretory orifice, thereby enabling sperm exit and male fertility[220].

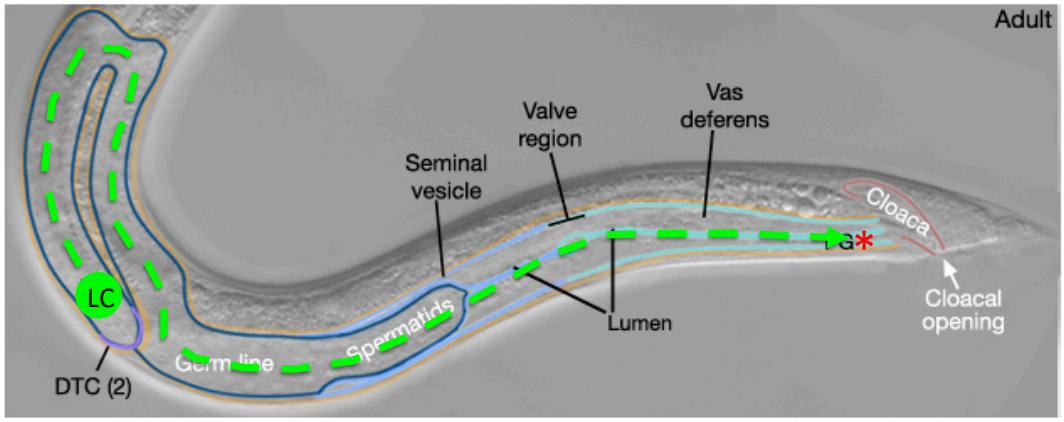

Figure 2: Wild-type young adult male showing linker cell migration path and gonad morphology. The linker cell is born at the beginning of the L2 stage near the middle of the animal (green circle, LC), and then migrates along a stereotyped path (dashed green arrow), leading the developing male gonad (blue outlines) behind it. At the end of the L4 stage, the linker cell dies (red asterisk) near the cloaca. Figure adapted from Wormatlas, 2009.

Although *C. elegans* males comprise only about 0.1% of a healthy wild-type population[221], male mating provides clear fitness benefits to stressed populations[222]. Furthermore, other closely related nematodes are gonochoristic[223], a sexual strategy where males are absolutely required for the propagation of the species. Thus, the death of the linker cell, which gates rhabditid male fertility, is likely under strong selective pressure.

The death of the linker cell is remarkable for several reasons. Unlike most cell deaths in *C. elegans*, which occur in young (~30 min), undifferentiated cells, the linker

cell dies after a long life spent performing a defined, differentiated function. Ellis and Horvitz, in their initial characterization of *ced*-3 mutants, found that the linker cell died efficiently in *ced-3* mutants[16]. Abraham *et al.* confirmed and extended this finding, showing that the death of the linker was not blocked by any alleles that normally block apoptosis, and additionally did not require known engulfment genes or proteases involved in the worm necrotic processes discussed previously[224]. Denning *et al.* confirmed the caspase-independent nature of linker cell death by finding no surviving linker cells in quadruple caspase *csp-3; csp-1; csp-2 ced-3* mutant males[36]. Sulston initially described the death of the linker cell as a "murder", suggesting that its execution is carried out by U.l/rp rectal epithelial cells, which also abut the terminal vas deferens[13,220]. However, Abraham *et al.* disproved the "murder" hypothesis, at least by the Ul/r.p cells, as ablating their grandmother cell did not cause the linker cell to survive[224].

In addition to being genetically non-apoptotic, the death of the linker is morphologically distinct. In contrast to the condensed chromatin, persistently (until late) spherical nucleus, delaminating nuclear envelope, and compacted cytoplasm seen in apoptosis, linker cell corpses maintain an open chromatin, with a mostly tight adherence between nuclear envelope leaflets, while the contour of the envelope progressively crenellates, as in degenerative death (Figure 4). Additionally, early mitochondrial and possibly endoplasmic reticulum (ER) swelling can be observed, as well as large, membrane-bound vesicles containing what may be organellar remnants. Occasionally, large vesicles appear in or near the linker cell, reminiscent of the vesiculated appearance of necrotic cells, although the death does not require calpains or cathepsins[224].

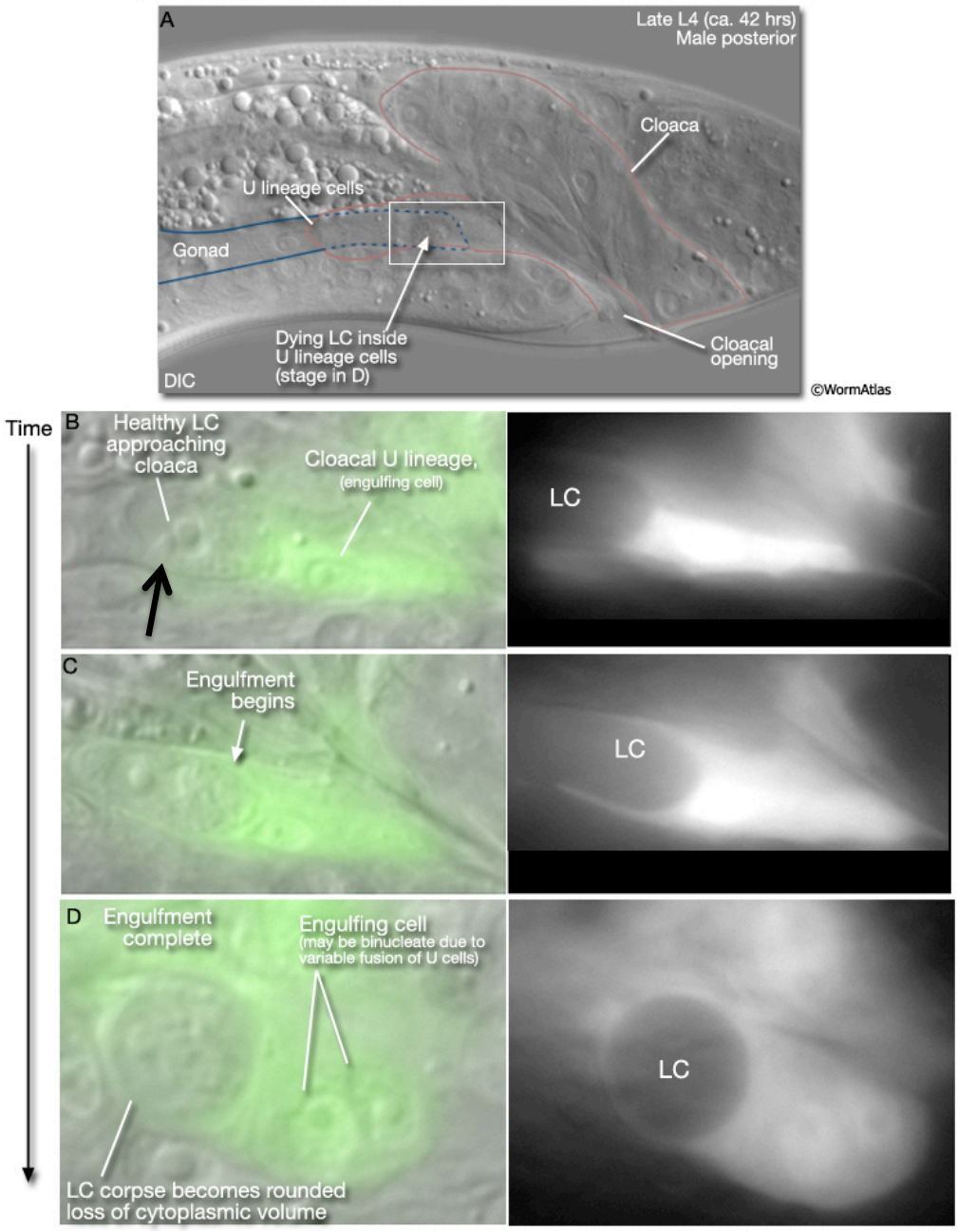

Figure 3: Progression of linker cell death in a late L4 male. A. Late L4 male with an engulfed linker cell. B-D. Closer view of linker cell death and engulfment over time. Note that in B, although the linker cell appears generally healthy, the nucleus envelope harbors a notch on its ventral aspect (black arrow), indicating that the death process has likely begun. Left column, DIC and GFP overlay. Right column, *lin-48*p::GFP, marking the engulfing U.l/rp cells. Figure adapted from Wormatlas, 2009.

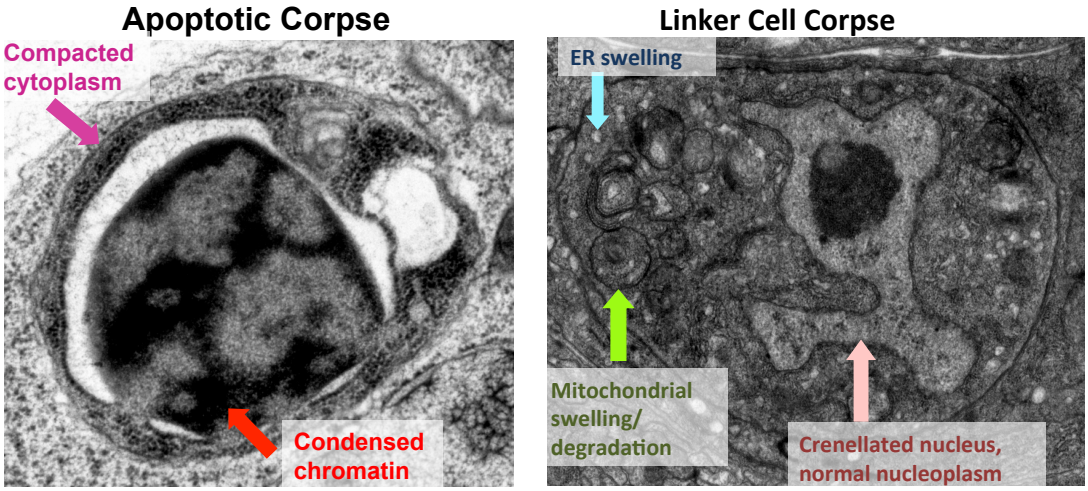

Figure 4: Linker cell death is morphologically non-apoptotic. Electron micrographs adapted from Abraham et al. (2007)[224]. Salient contrasting features are indicated.

How is linker cell death initiated? Abraham *et al.* found that the death requires the heterochronic genes *let-7* and *lin-29*[224]. Heterochronic genes function to ensure that developmental processes occur at the right time in the worm, and a variety of heterochronic mutations have been isolated in which certain events happen too early, too late, not at all, or repeatedly instead of once[225]. As *lin-29* controls many events occurring at the transition to adulthood[226], its involvement in linker cell death is consistent with a temporal signal being required to specify the death of the linker cell. Harris *et al.* extended these findings by showing that it is specifically a function of LIN-29 dependent on its cofactor MAB-10, which interacts with the C-terminus of LIN-29, that controls linker cell death[227]. However, both LIN-29 and MAB-10 are present in the nucleus of the linker cell during its migration, at least as early as the L3 stage. Further, *lin-41*, which negatively regulates *lin-29* and is in turn antagonized by *let-7*[228], has no effect on linker cell death[224]. In contrast, for events, such as seam cell division, in which *lin-29* is

instructive, *lin-41(lf)* causes precocious expression of developmental fates[228]. Thus, LIN-29 may act permissively or redundantly for linker cell death.

While the linker cell is but one cell in the male worm, several pieces of evidence suggest that the molecular mechanisms behind linker cell death may be conserved. Interestingly, the morphology of linker cell death is reminiscent of the peripherally deprived chick ciliary ganglion neurons observed by Pilar and Landmesser, suggesting that linker cell death[167]. Furthermore, these morphological features have also been observed in dying neurons of patients with poly-glutamine expansion diseases, such as Huntington's or some spinocerebellar ataxias, as well as in mouse models for those disease[229].

In a genome-wide RNAi screen for linker cell death regulators, Blum *et al.* found that the gene *pqn-41*, which encodes a protein containing N-terminal coiled-coils and a C-terminal polyglutamine region, the conserved mitogen activated protein kinase kinase (MAPKK) SEK-1, and its adapter TIR-1 may function together to promote linker cell death[229]. The morphological parallels with polyglutamine diseases are striking in light of the involvement of PQN-41, itself a poly-glutamine protein. However, *pqn-41* is not required for other cell deaths, nor can ectopic expression of the rescuing PQN-41C isoform precociously kill the linker cell or other cells. Thus, *pqn-41* cannot be the *ced-3*-like executioner of the linker cell. Nonetheless, it is possible that human neurodegenerative polyglutamine proteins cause disease by reactivating a cryptic linker-cell-death-like program. Additionally, the occasional appearance of vacuoles in wild-type linker cell death suggests that linker cell death may share some downstream events with necrosis, although upstream initiating events are different.

Finally, the TIR-1 homolog SARM1 has been implicated in the Wallerian degeneration of severed axons in both flies and mammals[230], a caspase-independent process which may involve SEK-1 in a MAPK cascade[186]. Intriguingly, SARM1 gain-of-function mutations can also induce non-apoptotic neuronal death[231]. Thus, the study of linker cell death may yield insights into both normal human development as well as several types of pathology. However, little is known about how linker cell death is initiated or executed.

1.5 Methodological primer on the study of linker cell death

The linker cell dies at a very specific time and place in the worm. Therefore, to reproducibly score linker cell death, we utilize a two-step synchronization process. First, we collect a population of worms where numerous eggs are present, either laid on the plate or within gravid hermaphrodites, and treat that population with an alkaline bleach solution that kills larvae and adults but leaves embryos intact. Then, we let these embryos hatch overnight in sterile M9 salts buffer. Because no source of food is present in this medium, newly hatched larvae arrest their development in the early L1 stage, and a synchronized population is obtained. Once released on an *E. coli* lawn, these animals resume their development approximately synchronously. However, two days later, by the L4 stage, synchronized animals are no longer at precisely the same developmental stage. Therefore, we pick late L4-larval-stage males, as identified by their retracted tail tip and developing adult rays visible under the still-unshed L4 cuticle (Figure 5D), to a new plate, and wait for exactly two hours before mounting the animals on a microscope slide for scoring under DIC and widefield fluorescence. Because animals exibit the morphological criteria we use to define the very late L4 stage for a maximum of two

hours, at the time of scoring, all males are newly molted adults at most 2 hours old (Figure 5E). The strains we use all contain a cytoplasmic marker for the linker cell driven either by a *mig-24* or a *lag-2* promoter fragment, allowing us to quickly identify the linker cell and assess its shape.

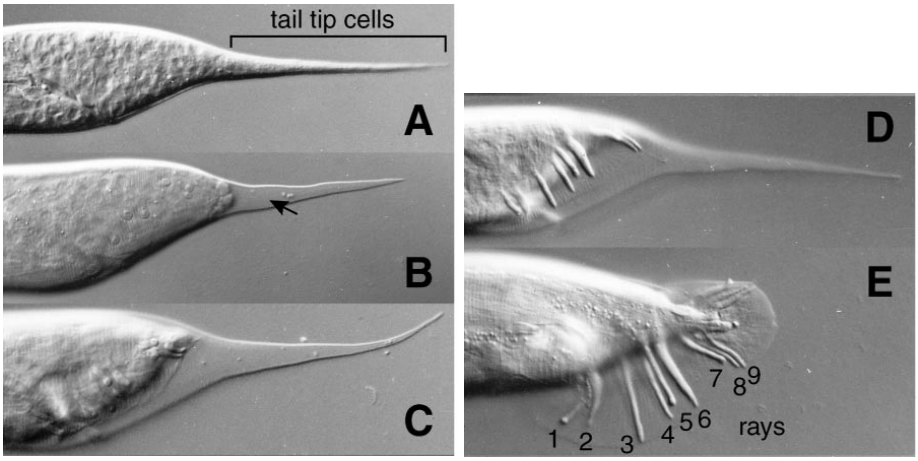

Figure 5: Morphological changes in the male tail at the L4-adult molt. A. Early L4 stage. B-D. Progression of adult tail tip morphogenesis in mid-late L4. E. Adult tail tip. To score linker cell death, animals are picked as in (D) and scored two hours later, as (E). Compare tail morphology in (D) with Figure 3A. Figure 3A, where linker cell is already dying and engulfed, is earlier than (D). Images from Nguyen *et al.*[232].

We use a strictly binary scoring system. To score a linker cell as surviving, we use a strict set of criteria, all of which must be met. A linker cell is counted as surviving if it is not rounded, does not have any large cytoplasmic blebs, and has not appreciably shrunk its volume, as assessed by a cytoplasmic fluorescent protein; and if its nuclear envelope is still round and contains a prominent nucleolus, as assessed by DIC. Other cells containing any of the defects outlined here are counted as dead or dying. Almost all linker cells are dead in newly molted adults (**Table 1**), whereas various mutants have

inappropriate linker survival in varying percentages of animals. To perform RNAi, animals are fed dsRNA-expressing *E. coli*[233] from the L1 stage onward to avoid possible embryonic lethality or other early developmental defects.

2 SET-16, an MLL-type histone methyltransferase, promotes linker cell death

2.1 Preliminary studies on *swd-2.2*

I began my work studying the role of another hit from the genome-wide RNAi screen conducted by Blum *et al.*, *swd-2.2*. Importantly, the complex migration of the linker cell, as well as the expression of the *lag-2* marker gene, is unaffected by RNAi against *swd-2.2*(RNAi) (Figure 7), suggesting that *swd-2.2* controls death specifically, and not linker cell fate generally. I confirmed that RNAi against *swd-2.2* results in reproducible linker cell survival, using two different RNAi clones, in an RNAi-sensitized *rrf-3* background (**Table 1**).

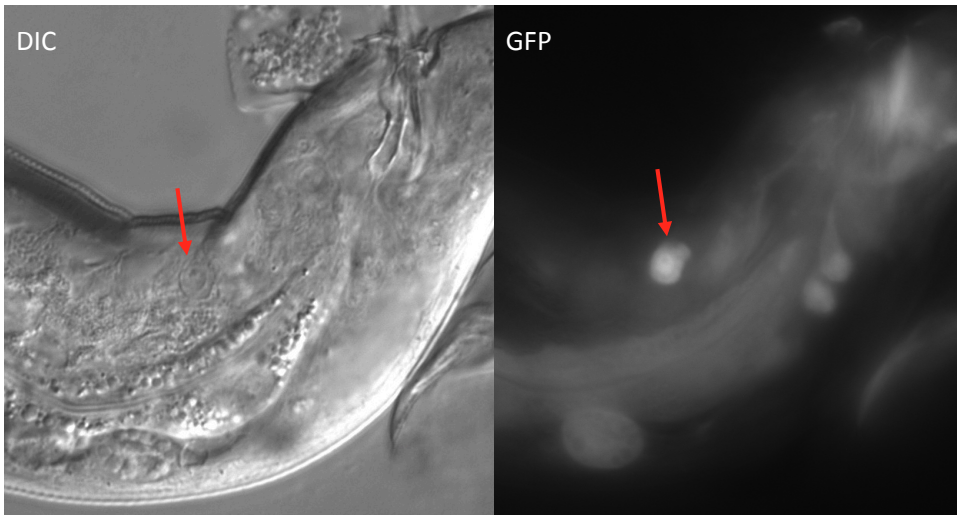

Figure 6: *swd-2.2*(RNAi) causes linker cell survival without other overt defects in linker cell fate. Representative photomicrographs of an *rrf-3(pk1426); him-8(e1489); lag-2*p::GFP animal fed *set-16* RNAi. A 2-hour old adult male is shown. Left: DIC channel. Right: GFP channel. Red arrow: linker cell. As shown, *lag-2*p::GFP marks the linker cell.

Table 1: A SET-16/MLL complex promotes linker cell death.

RNAi*	% LC survival†	n‡
Empty vector	4 ± 2	122
swd-2.2	31 ± 5	90
swd-2.2 24h	16 ± 5	45
swd-2.2 (2) §	22 ± 5	81
swd-2.1	3 ± 2	102
swd-2.2(RNAi) + *mig*-24p::Cbr. *swd-2.2* (1)	7 ± 3	84
+ *mig*-24p::Cbr. *swd-2.2* (2)	8 ± 3	97
+ *mig*-24p::Cbr. *swd-2.2* (3)	9 ± 3	68
set-16	49 ± 5	109
set-16 (2) §	50 ± 6	60
utx-1	18 ± 3	140
ash-2	17 ± 4	90
rbbp-5	10 ± 3	84
wdr-5	10 ± 3	109
pis-1	14 ± 4	70
set-2	2 ± 2	55
hcf-1	0	48
dpy-30	3 ± 2	69
cfp-1	5 ± 3	56

Note: *All strains also contain the *qIs56* reporter transgene to visualize the linker cell; *him-8(e1489)* or *him-5*(*e1490*) to increase the incidence of males; and *rrf-3*(*pk1426*), an RNAi-sensitizing mutation. All un-numbered clones from Ahringer library. †±SEM. ‡Number of animals scored. §*swd-2.2* (2) and *set-16* (2) clones constructed as in methods.

Surviving cells persist until at least 24 hours past their usual time of death, suggesting that *swd-2.2* is able to fully block, rather than just slow, linker cell death. By fusing a 4-kb upstream *swd-2.2* promoter region to GFP, I found that *swd-2.2* is expressed in all cells in *C. elegans*, including the linker cell (Figure 7).

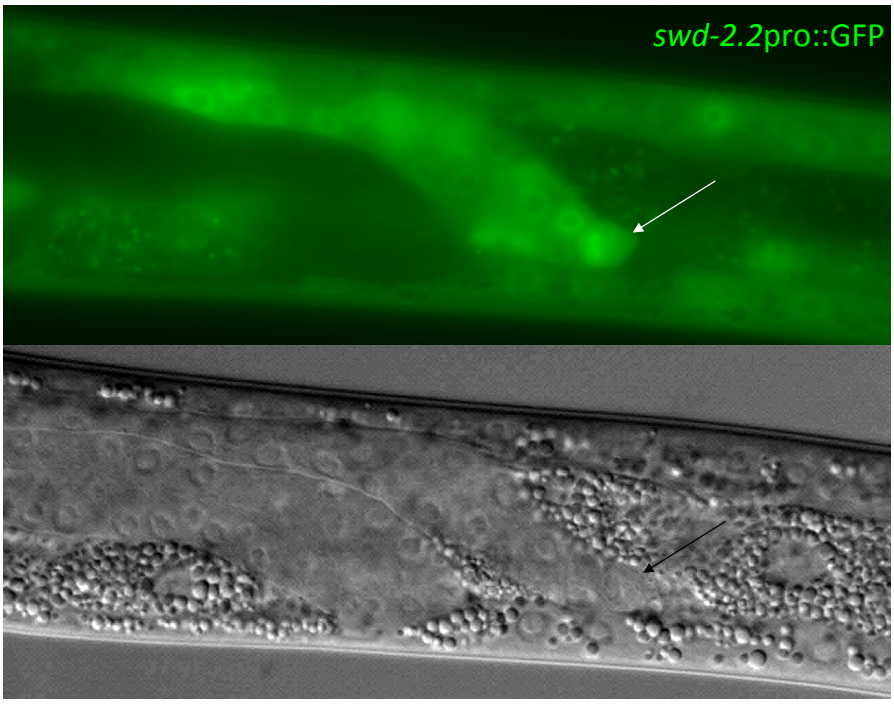

Figure 7: swd-2.2 is expressed in the linker cell. *unc-119; him-8* animals harboring a 4-kb *swd-2.2*p::GFP transgene were examined for GFP expression. An L3 male is shown. Top: GFP channel. Bottom: DIC channel. Arrow: linker cell.

To find out in which cell *swd-2.2* might function, I needed to rescue the *swd-2.2* phenotype in a cell-specific manner. Since *swd-2.2* is essential in the worm, I could not rescue a genetic mutant. Instead, I decided to rescue the RNAi phenotype using a cDNA that encodes a nearly identical protein but which diverged significantly at the primary nucleid acid sequence. I therefore cloned the cDNA for its homolog from a closely related species, *C. brenneri*. This homolog is identical at the protein level to *swd-2.2* but only ~70% homologous at the nucleotide level, with, importantly for preventing RNAi, no stretches of perfect homology longer than 20 nucleotides. Expressing this cDNA in the

linker cell specifically using the *mig-24* promoter[234], I found that *Cbr-swd-2.2* could rescue the *swd-2.2* RNAi phenotype in three independently isolated lines (**Table 1**), strongly suggesting that *swd-2.2* functions cell-autonomously to promote linker cell death.

2.2 Background: *swd-2.2* and histone methyltransferase complexes

swd-2.2 is predicted to encode an homolog of the yeast swd2p and the human Wdr82, a family of highly conserved (>92% from yeast to humans) WD40-repeat-containing nuclear proteins with two still unreconciled functions. I will describe these functions primarily in the context of the yeast *Saccharomyces cerevisiae* literature and nomenclature, as this is where much of the work on these two functions has been carried out. In one function, the protein associates with a histone 3-lysine 4 (H3K4) methyltransferase complex, called the COMPASS or Set1 complex (Set1C), for the catalytic set1p subunit[235,236]. It is thought that swd2-like proteins recruit the Set1C to the 5' end of active genes[237] and promote the addition of a second and third methyl group to the histone tail[238], in a fashion which is dependent on *swd-2*'s own mono-ubiquitylation at the conserved K68/69 residues[239]. In turn, this regulatory activity may be regulated *in trans* by mono-ubiquitylation of H2B at lysine 123 by rad6/bre1[240], aided by the Paf1 complex[241]. The H3K4 trimethyl mark is often present at the 5' end of actively transcribed genes[242], and COMPASS has been implicated in global anti-silencing[243], a function which is not inconsistent with the open chromatin seen in dying linker cells. In addition to swd2, the yeast COMPASS is made of 7 other polypeptides: set1, bre2, swd1, swd3, spp1, shg1, and sdc1[244], most of which have identified human homologs. Sdc1 is

the homolog of *dpy-30*, first identified as part of the *C. elegans* dosage compensation machinery[245].

In yeast, only one catalytic H3K4 methyltransferase subunit, Set1, exists. In higher eukaryotes, a second class of catalytic subunits has been described. The founding member of this class, *trithorax* (*trx*), was isolated in *Drosophila* as a homeotically transformed mutant more than 35 years ago[246], and eventually found to encode a large protein that occupies and activates the promoters of homeodomain genes such as *Antennapedia* and *Bithorax* complex genes[247-249]. Compared to the relatively small Set1-like methyltransferases, Trx-like proteins harbor a long N terminus with a number of regulatory domains, in addition to their C-terminal catalytic SET domain. A *C. elegans trx* homolog, *set-16*, was found by homology after the worm genome was sequenced, but few specific functions have been ascribed to *set-16*. Where worms and flies each encode one Trx-like gene, humans harbor 6, named MLL1-6 for the mixed lineage leukemias in which they are often found translocated to transcriptional elongation factors[250,251]. Set1-type and MLL-type complexes harbor similar, but distinct sets of accessory subunits [251]. Whereas Set1-like complexes are thought to control global levels of H3K4-trimethyl, in flies and humans, Trx complexes are thought to regulate the transcription of a small subset of developmentally important genes, such as Hox genes and Wnt target genes, to ensure the tissue specificity of their expression[252-254]. This may also be the case in *C. elegans*, where the Set1-like *set-2* and the Ash2L-like *ash-2* genes appear to be responsible for most somatic and germline H3K4-trimethylation[255].

Of the 8 yeast COMPASS subunits, only swd2 is essential for cell survival[256], plausibly because of its other described function, in the RNA cleavage and

polyadenylation factor (CPF), which is involved in polyadenylating pre-mRNAs to form the mature message. In yeast, the holocomplex is composed of many subunits assembled into sub-complexes as defined by their co-elution under increasingly stringent conditions[257]. Swd2p may be the subunit which holds the various subcomplexes together[258].

2.3 *set-16* promote linker cell death cell-autonomously

Which *swd-2.2*-containing complex, then, promotes linker cell death? To answer this question, I performed a targeted RNAi mini-screen for other subunits of both complexes. Strikingly, RNAi against many H3K4 methyltransferase complex components (**Table 1**), but not CPF components (**Table 2**), caused inappropriate linker cell survival.

Table 2: RNA cleavage and polyadenylation factor subunits are not involved in linker cell death

RNAi*	% LC survival†	n‡
ztf-1	4 ± 2	90
nrd-1	6 ± 2	104
leo-1	6 ± 2	100
cpf-2	0	82
pcf-11	2 ± 2	52
nab-3	4 ± 2	90
clpf-1	7 ± 3	82
pap-1	2 ± 2	51

Notes: *All RNAi performed in strain containing the *qIs56* reporter transgene to visualize the linker cell; *him-8(e1489)* to increase the incidence of males; and *rrf-3*(*pk1426*), an RNAi-sensitizing mutation. All clones from Ahringer library. †± SEM. ‡Number of animals scored.

Of the catalytic H3K4 methyltransferase subunits, only *set-16*, and not *set-2*, appear to be involved in linker cell death, interesting in light of the tissue-specific roles of MLL-type complexes (**Table 1**). Furthermore, RNAi against *utx-1*, which encodes a UTX-type H3K27 demethylase that can associate with MLL-type complexes, also resulted in linker cell survival, as did RNAi against accessory subunit genes *rbbp-5, wdr-5*, *ash-2*, and *pis-1*/PTIP also resulted in linker cell survival (**Table 1**). However, RNAi against *pap-1*, the gene encoding the catalytic poly-A polymerase in the RNA CPF complex, induced no significant linker cell survival, nor did RNAi against accessory subunits of that complex (**Table 2**). Finally, I confirmed the role of *set-16* in linker cell death using an additional RNAi clone (**Table 1**). Therefore, an H3K4 methyltransferase complex containing SET-16/MLL as its core catalytic subunit likely promotes linker cell death.

To assess whether *set-16* could function in the linker cell, I created a strain in which only the linker cell is competent to perform RNAi. The gene *rde-1* encodes an Argonaute protein acting at the most downstream step in the RNAi machinery, the processing of target mRNAs. RNAi is abrogated in *rde-1* mutants[259], and *set-16*(RNAi) in an *rde-1* mutant causes no linker cell survival. I cloned the *C. elegans rde-1* cDNA and expressed it from the *mig-24* promoter, creating a linker-cell-rescued *rde-1* strain. In this strain, presumably, dsRNA can be taken up from the gut and transferred between cells through the SID-1 transporter[260,261], but can create a functional, RDE-1-containing RNA-induced silencing complex (RISC) only in the linker cell (Figure 8A). In three lines of this strain, *set-16*(RNAi) was again able to induce linker cell survival (Figure 8B), showing that *set-16* functions in the linker cell to promote death.

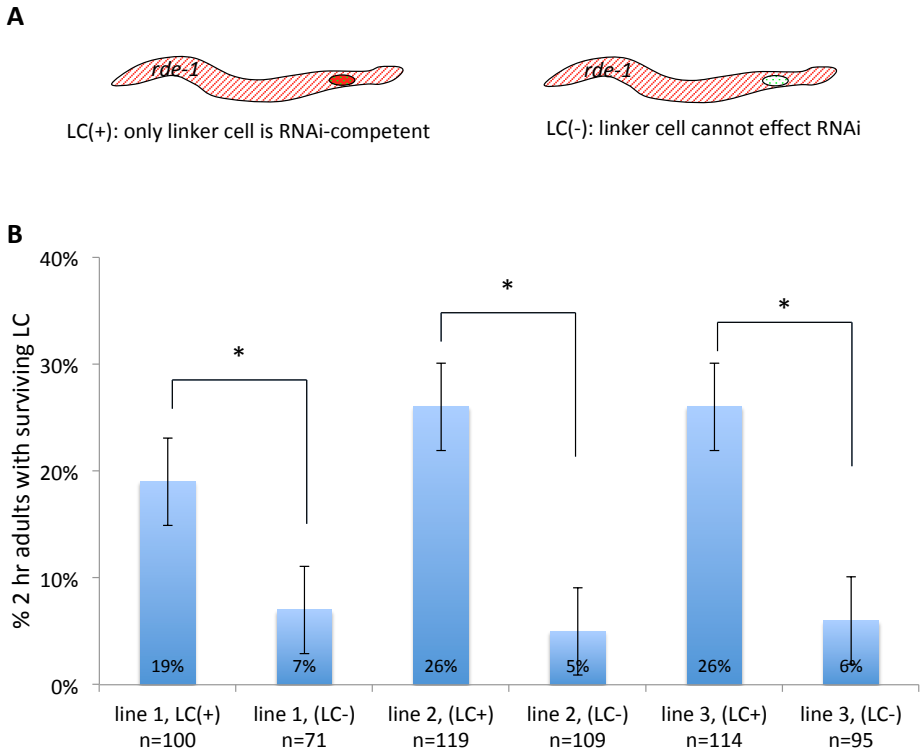

Figure 8: *set-16* functions in the linker cell to promote death. A. Schematic of linker-cell-specific RNAi strain. *him-8(e1489); rde-1(ne219) lag-2*p::GFP animals harboring an extrachromosomal array containing an mCherry-marked *mig-24*p::*rde-1* (3 lines) were fed *set-16* RNAi. L3 males were selected for those containing the array in the linker cell (or not) based on mCherry expression in the linker cell. B. These animals were then scored for surviving linker cells 2 hours after the L4/adult transition, as usual. Error bars, +/- SEM. Asterisk, p<.02, two-tailed T test.

To examine the expression of *set-16*, I engineered a *set-16*-containing fosmid genomic clone, placing GFP in frame at the *set-16* C-terminus. This fosmid showed ubiquitous nuclear expression of SET-16-GFP, including in the linker cell up to its death (Figure 9), consistent with a role in death. Like *swd-2.2*(RNAi), *set-16*(RNAi) does not

affect linker cell migration or expression of *lag-2*, suggesting that *set-16* controls the linker's death specifically, and not its fate.

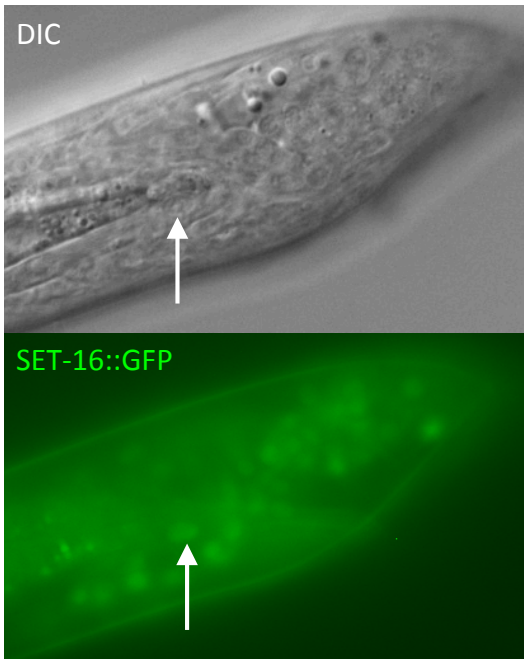

Figure 9: *set-16* is expressed in the linker cell. L4 male harboring a fosmid with GFP engineered in frame with the start codon of the *set-16* genomic locus were examined for GFP expression. Left: DIC channel. Right: GFP channel. White arrow: Linker cell nucleus.

2.4 SET-16 complex: conclusions

Together, my results point to an MLL-type H3K4 methyltransferase complex, centered around the catalytic subunit SET-16, acting cell-autonomously to promote linker cell death. How might *set-16* function to promote linker cell death? Jennifer Zuckerman-Malin in our lab has studied the role of another gene identified in the genome-wide RNAi screen for linker cell death regulators, the E2 ubiquitin ligase gene *let-70.* Jennifer found that *let-70*, as well as other genes encoding members of the ubiquitination and

proteasomal machinery, including *ubq-1*/ubiquitin itself, are transcriptionally induced shortly before linker cell death. Further, she showed that *set-16* is required for the expression of *let-70* and *ubq-1* (Malin *et al.*, unpublished results). Thus, SET-16 H3K4 methyltransferase activity may be required at the promoters of these genes, or of genes controlling them, for efficient expression at the time of linker cell death.

MLL complexes are recruited to promoters through a variety of mechanisms. In mammals, MLL complexes may bind directly to DNA-binding transcription factors, constitutively or upon their modification. In one case, the coactivator Carm1 must methylate an arginine residue on the DNA-binding transcription factor Pax7 to recruit MLL[262]. In another example, a long non-coding RNA, HOTTIP, recruits MLL to the HoxA locus[263]. In yet other instances, MLL, through a number of its N-terminal domains, can directly bind pre-existing histone modifications. Thus, SET-16 could be recruited to the promoters of *let-70* or other target genes through a number of mechanisms.

The study of *set-16*'s role in linker cell death is hampered by methodological obstacles. The *set-16* deletion mutants I examined, *gk438* and *gk445*, are unconditionally embryonic lethal. I could rescue these with my GFP-engineered *set-16* reporter fosmids, but to rescue these lines necessarily transmitted very well and the identification of mosaic animals in sufficient numbers to assess cell-autonomy was extremely laborious, and, ultimately, unsuccessful. Nonetheless, the strategy of expressing tagged SET-16 in a cell-autonomous manner could conceivably be used for cell-specific chromatin immunoprecipitation followed by high throughput sequencing (ChIP-seq) in order to identify relevant SET-16 targets.

3 Two Wnt pathways exert opposing control over linker cell death

To discover additional regulators of linker cell death, I returned to the observation that lesions of the gene *him-4*, which encodes the secreted immunoglobulin superfamily member hemicentin, prevent posterior migration of the linker cell and also result in low-level (~17%) survival of the linker cell[224]. Initially, this result was taken as evidence that linker cell death is largely determined cell-autonomously[224]. However, this result could also suggest that the position of the cell within the animal might dictate the fidelity of cell death execution. To determine whether spatial cues promote linker cell death, I considered the possibility that secreted ligands of the Wnt pathway, which are expressed in restricted domains in the animal[264], contribute to linker cell death.

3.1 Introduction to Wnt signaling

The first Wnt gene was cloned by Nusse and Varmus from mouse breast tumors infected with the oncoretrovirus mouse mammary tumor virus (MMTV). They found that many independent tumors harbored proviral insertions near a common gene, which they named Int1[265]. Because the provirus was not always integrated in the same precise site near the gene, and because Int1 was highly expressed in these tumors, Nusse and Varmus speculated that the presence of the provirus near the gene depressed the Int1 proto-oncogene[265]. Nusse and colleagues later found that Int1 was the mouse homolog of the fly gene *wingless*[266]. This gene had been isolated as a homeotically transformed mutant[267] with seemingly non-autonomous function, as growth of relatively normal tissue could be restored to the defective *wingless* imaginal discs by juxtaposition with wild-type tissue[268].

Nüsslein-Volhard and Wieschaus further showed that *wingless* mutant larvae exhibit segmental polarity defects, deleting the posterior aspects of larval segments and implicating the gene as a broad developmental regulator.

Correspondingly, Nusse and colleages found that both Int1 and *wingless* transcripts encode N-terminal signal sequences, and presciently postulated that the Wingless and Int1 protein products act as secreted glycoprotein growth factors or differentiation factors[266]. Soon thereafter, a similar role for Int1 in patterning was shown in verterbrates. In *Xenopus laevis*, overexpression of Int1 led to duplication of the posterior axis[269], and in mouse, in the first use of homologous recombination to create targeted mutant lines, Int1 was shown to be involved in cerebellar formation[270]. In mice, several Int1-like genes were identified, and the class was renamed Wnt[271]. In fact, Wnt genes appear to be involved in antero-posterior axis specification, or antero-posterior specifications in sub-domains (e.g., the cerebellum is a posterior segment of the vertebrate brain) in most if not all animals, and may therefore have been one of the signaling pathways that allowed the emergence of multicellular animals[272].

Clues to how Wnt/Wingless signaling functions in its target cells emerged from the study of phenotypically similar *Drosophila* mutants[273] as well as from studies of human cancers. Interestingly, while *wingless* appeared to function cell-non-autonomously in *Drosophila*, the gene mutated in *armadillo*, which also exhibits segment polarity defects, was found to function cell-autonomously[274]. Subsequently, further work from Wieschaus and colleagues showed that Armadillo is post-transcriptionally regulated by a number of other segment polarity genes, including *wingless, porcupine* and *disheveled*[275] and to function in the same genetic pathway[276]. In particular, Wingless was shown, as

expected, to be a secreted protein that could act in a soluble, extracellular form[277], whereas Armadillo is surprisingly similar to cytoskeletal proteins involved in cell-cell adhesion[278,279], but acts in a manner that is distinct from cell adhesion to promote cell fate changes[280]. The identity of the Wnt receptor remained elusive for a number of years until work from Nusse and colleagues showed that the *frizzled* gene, previously shown to encode a 7-pass transmembrane protein[281] involved in setting tissue polarity throughout the adult fly cuticle[282] and acting in the, could transmit the Wg signal to Armadillo[283] and required the function of the gene *disheveled*[284]. Interestingly, early evidence showed that Frizzleds did not necessarily act monomolecular receptors but as complexes, with other Frizzled molecules[285,286] and/or low-density-lipoprotein receptor-related proteins (LRPs)[287,288].

Crucial additional insights into Wnt signaling began, as did the identification of Wnts themselves, with human cancer biology. In 1991, two groups reported the molecular cloning of the gene mutated in a familial form of colon cancer, familial adenomatous polyposis coli, in which patients develop innumerable polyps in the colon at a young age, some of which inevitably transform into cancer. In these families, the gene, APC, was found to harbor predicted loss-of-function mutations[289,290]. Amazingly, two years later, the APC protein product was shown to physically associate with the Armadillo homolog ß-catenin[291,292], and to regulate its abundance *in vivo* along with glycogen synthase kinase 3ß (GSK3ß)[293,294] and Axin[295-297]. The role of ß-catenin as the *bona fide* transducer of Wnt signaling in vertebrates awaited the demonstration that ß-catenin bound TCF/Lef family transcription factors in *Xenopus*[298,299] and that a complex of these two proteins could translocate to the nucleus to activate a transcriptional program

that phenocopied the posterior axis duplication found in the early Int1 overexpression experiments. Interestingly, TCF/Lef factors were first identified as transcription factors necessary for the expression of T cell receptor α chains[300], suggesting that Wnts could be active in a number of cellular contexts beyond early development. These results were then recapitulated in *Drosophila*, providing the conclusive evidence that Armadillo and ß-catenin function as transcriptional coactivators of TCF/Lef in response to Wnt signalling[301,302].

Based on these pioneering studies and subsequent confirmatory studies, a canonical Wnt signaling pathway could be proposed (Figure 10). In the absence of Wnt ligand, a complex of Axin, APC, GSK3ß, and casein kinase[303] phosphorylate ß-catenin, leading to its ubiquitination and degradation by the proteasome[304-307]. Upon ligation by Wnts, Frizzled receptors recruit Dishevelled. Through still incompletely understood mechanisms, this event leads to the inhibition of the ß-catenin phosphorylation complex, the resulting cytoplasmic accumulation of ß-catenin, and its nuclear translocation, displacement of Groucho transcriptional repressors[308], and transactivation of TCF/Lef transcription factors[309].

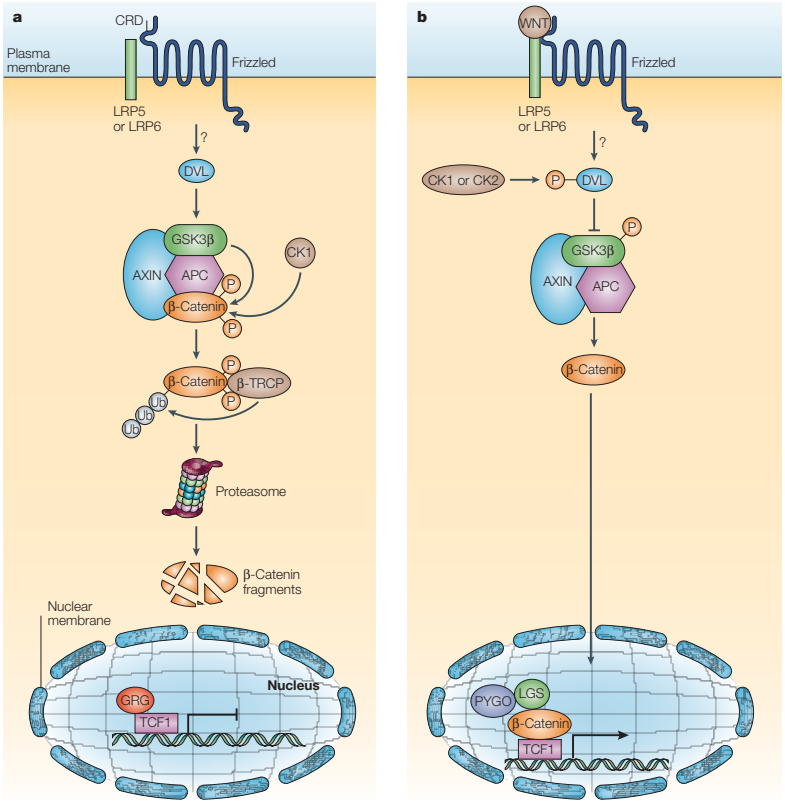

Figure 10: Diagram of the canonical Wnt signaling pathway. A. In the absence of WNT, β-catenin associates with a multiprotein destruction complex that consists of the tumour-suppressor gene products Axin, APC, Casein Kinase 1 (CK1), and GSK3β. β-catenin is phosphorylated by CK1 and GSK3β. This phosphorylation leads to recognition by β-TRCP (β-transducin-repeat-containing protein), leading to the ubiquitination of β-catenin and its degradation by the proteasome. Members of the TCF (T-cell factor)/LEF (lymphocyte- enhancer-binding factor) family are bound in the nucleus by repressors that belong to the GRG (groucho-related gene) family and are therefore inactive. B. WNT proteins bind their receptors, Frizzled proteins, they also bind a co-receptor, LRP5 (low-density-lipoprotein-receptor-related protein 5) or LRP6. The binding of WNT proteins to Frizzled and LRP results in the inactivation of GSK3β by Dishevelled (DVL). β-Catenin migrates to the nucleus, where it binds TCFs to activate target genes. (Figure and legend adapted from Staal and Clever, 2005[310]).

In addition to this canonical Wnt pathway, a number of non-canonical variations have been uncovered in worms, flies, and vertebrates. While the seven-pass Frizzled proteins were the first type of Wnt receptor to be identified, at least two more types have since been uncovered, each single-pass tyrosine-kinase-type receptors. Derailed is required in *Drosophila* for proper axon guidance of a subset of interneurons[311]. However, Derailed does not require kinase activity *in vivo*[312]. Instead, remarkably, Derailed could bind and respond to Wnt ligands, both in flies[312], worms[313], and mammals[314]. Ryk could signal through Dishevelled and TCF and bind to Frizzled proteins[314] in some instances, but act independently of canonical Wnt signaling in others[315], suggesting that whether Ryk/Derailed acts as a Frizzled co-receptor or as a sole receptor may depend on the cellular context.

A third type of Wnt receptor, the ROR-type tyrosine-kinase-like proteins, was found in a screen for genes involved in axial patterning in *Xenopus*[316]. In this study, Xror2 was found to functionally and physically interact with Wnts, again with kinase activity being dispensable. Interestingly, the *C. elegans* ROR protein, CAM-1, functions in a variety of Wnt-dependent contexts, some of which require a functional kinase domain and some of which do not[317]. In some cases, ROR proteins function to antagonize canonical Wnt signaling[318,319], whereas in others they appear to function independently of canonical signaling, acting instead through Jun-N-terminal kinases (JNK)[320] or other mechanisms[321].

The myriad modalities of Wnt signaling frustrate any attempt to concisely present a comprehensive view of this pathway. However, this complexity also testifies to the

pathway's centrality in much of animal biology. Several Wnts exist in every organism where they have been found, and Wnts appear to have the ability to be modified and secreted in different ways. Furthermore, secreted Wnt agonists, such R-spondins[322,323], which act through their own set of LGR4/5/6 receptors[324] can potentiate Wnt signaling or signal to receptive Wnt components on their own. Several types of secreted Wnt antagonists exist. Secreted frizzled-related peptides[325,326] and WIF1[327] directly sequester unbound Wnts, whereas Dickkopfs[328], which inhibit the LRP5/6 coreceptors[329,330] either directly[331] or through their own Kremen receptors[332], refine the organism's Wnt responses. Similarly, as we have seen, at least three classes of Wnt receptors exist, with, in vertebrates, several Frizzled and several RORs. Each of these receptors appears to have different affinity for different Wnts[333] and can interact with other receptors in various combinations. Downstream of Wnts, signaling can happen canonically through β-catenin or through a number of transcriptional or non-transcriptional β-catenin-independent pathways, with cross-talk possible between these pathways and with additional modes of regulation possible within pathways. Complexity exists at every level of Wnt signaling, and every level appears to have the ability to interact with in any number of ways with the levels above and below it.

In fact, while Wnt signaling was first studied in the context of developmental patterning and cancer biology, Wnts are now known the play roles in a number of facets of biology, including, importantly, the regulation of stem cell maintenance and production of cells for homeostasis and repair in many tissues[334]. This latter aspect, of course, is likely responsible for the involvement of Wnt signaling in many types of cancer[335].

Given the role of Wnts in axial patterning in many organisms, it is not surprising that in *C. elegans* as well, Wnts promote antero-posterior fate events in a number of contexts. For example, at the embryonic four-cell stage, the EMS blastomere divides into the anterior MS cell and the posterior E cell, and the orientation of this division is dependent on the P2 blastomere's posterior location relative to EMS[336]. If P2 is removed entirely, two anterior MS cells are formed from EMS, and if P2 is moved anteriorly, the anterior EMS daughter becomes E and the posterior daughter becomes MS[336]. Thorpe *et al.* showed that P2 is a source of the Wnt MOM-2, which in the unperturbed embryo therefore acts on the EMS cell to posteriorize the surface it contacts[337]. In addition to *mom-2,* the worm genome encodes four more Wnt genes: *lin-44, egl-20, cwn-1* and *cwn-2.* In larvae, although Wnts can promote asymmetric cell divisions in a number of planes, the five *C. elegans* Wnts are mostly expressed in the posterior of the animal; indeed, the anterior of the animal expresses a secreted Wnt antagonist, the secreted frizzled-related peptide SFRP-1[338]. *egl-20* promotes the posterior migration of the Q neuroblasts[339] and refines the polarity of posterior vulval precursor cells[321], while *lin-44* promotes the proper antero-posterior orientation of a number of rectal blast cell divisions[340].

The worm genome encodes homologues of most of the canonical Wnt pathway components, and studies have shown that these worm proteins can act largely in the same way as in flies and vertebrates. In addition to its five Wnt genes, the worm harbors four Frizzled homologues, MIG-1, LIN-17, MOM-5 and CFZ-2; one ROR, CAM-1; one Ryk/Derailed, LIN-18; three Dishevelleds, MIG-5, DSH-1 and DSH-2; two Axins, PRY-1 and AXL-1; the APC-like APR-1; the GSK3ß GSK-3; and a single TCF-like protein, POP-1.

Interestingly, whereas vertebrates harbor one β-catenin, *C. elegans* has four. The worm reserves one β-catenin, HMP-2, for cell-adhesion[341]. The remaining three, BAR-1, WRM-1, and SYS-1, function in Wnt signaling but exhibit distinct modes of regulation. Nonetheless, all four β-catenins can to some extent functionally substitute for the others[342,343]. Canonical Wnt signaling in *C. elegans* can function through essentially any Wnt and any Frizzled receptor, but converges on one β-catenin, BAR-1. BAR-1 associates with POP-1, and the complex activates transcription[341,344,345], much as in flies and vertebrates. In contrast, when allowed to accumulate upon Wnt binding to Frizzled receptors, the β-catenin WRM-1 acts a scaffold that facilitates Nemo-like-kinase LIT-1's phosphorylation of POP-1, causing POP-1 to be exported from the nucleus and relieving repression of POP-1-bound promoters[346-348]. Finally, the divergent β-catenin SYS-1 acts as a limiting co-factor for POP-1, such that the ratio of SYS-1 to POP-1 directs transcriptional output[343,349], a mechanism exploited in the worm to specify asymmetric cell divisions.

3.2 A canonical EGL-20/Wnt signal promotes linker cell death

To determine whether Wnt signaling is involved in linker cell death, I examined animals carrying lesions in each of the five *C. elegans* Wnt genes. In *egl-20*/Wnt mutants, the linker cell survives inappropriately (**Table 3**), and surviving cells are not engulfed (Figure 11). Importantly, migration of the cell and expression of reporter genes within it are unaffected in *egl-20* mutants (Figure 12A), suggesting a specific function in linker cell death control. A previous study reported that cells surrounding the cloaca of the hermaphrodite, the site at which the linker cell dies in the male, express EGL-20[339]. I demonstrated that these epithelial cells, including the U.l/rp cells that engulf the linker

cell, but not the linker cell, express EGL-20 in males at the time of linker cell death (Figure 12B).

To determine whether EGL-20 promotes linker cell death in the context of Wnt signaling, I examined mutants defective in other pathway components (Figure 12; **Table 3**). I found that animals carrying mutations in the *mig-14*/Wntless gene, which is required for Wnt secretion[350], also exhibit surviving linker cells at the cloaca (**Table 3**). Similarly, *mig-5*/Dishevelled and *bar-1*/β-catenin mutants, as well as *lin-17*/Frizzled; *mom-5*/Frizzled double mutants, exhibit linker cell survival without defects in migration or reporter expression (**Table 1**). Other Wnt mutants or mutant combinations I examined do not block linker cell death (**Table 4**, **Table 5**). The kinase GSK3β functions to curtail Wnt signaling by promoting degradation of β-catenin[351-353]. I found that a *gsk-3* mutation restores linker cell death to *egl-20* mutants (**Table 3**). Furthermore, a heat-shock-inducible promoter driving a cDNA encoding a stabilized, N-terminally-truncated BAR-1/β-catenin protein (*hsp-16.2*::ΔN-BAR-1), displays heat-shock-dependent restoration of linker cell death not only to *bar-1*/β-catenin mutants, but also to *mig-5*/Dishevelled mutants (Figure 12D, E). These genetic data support involvement of a canonical Wnt pathway in promoting linker cell death.

Table 3. An EGL-20/Wnt pathway promotes linker cell (LC) death.

Genotype*	% LC survival†	n‡
Wild type	1 ± 1	72
egl-20(*n585*)	58 ± 5	96
mig-14(ga62)	36 ± 5	111
mig-5(*rh147*)	38 ± 5	112
bar-1(*ga80*)	52 ± 5	86
lin-17(*n3091*)	0	31
mom-5(RNAi)	1 ± 1	67
lin-17(*n3091*); *mom-5*(RNAi)	37 ± 5	115
gsk-3(*nr2047*) §	3 ± 2	91
gsk-3(*nr2047*); *egl-20*(*n585*)	18 ± 4	84
lin-29(*n333*)	56 ± 6	75
lin-29(*n333*); *egl-20*(*n585*)	90 ± 3	79
lin-29(*n333*); *bar-1*(*ga80*)	81 ± 3	123
pop-1(*q624*)	0	31
pop-1(*hu9*)	0	61
pop-1(q645)	15 ± 4	75
pop-1(RNAi); *rrf-3*(*pk1426*) ‖	16 ± 4	109
pop-1(*hu9*); *egl-20*(*n585*)	45 ± 9	33
pop-1(RNAi); *egl-20*(*n585*)	49 ± 6	59

*All strains also contain the *qIs56* reporter transgene to visualize the linker cell and *him-5*(*e1490*) to increase the incidence of males. Allele numbers are in parentheses. †± SEM. ‡Number of animals scored. §*gsk-3*(*nr2047*) allele is linked to an *unc-101*(*sy216*) allele. ‖*rrf-3*(*pk1426*) is an RNAi-sensitizing mutation.

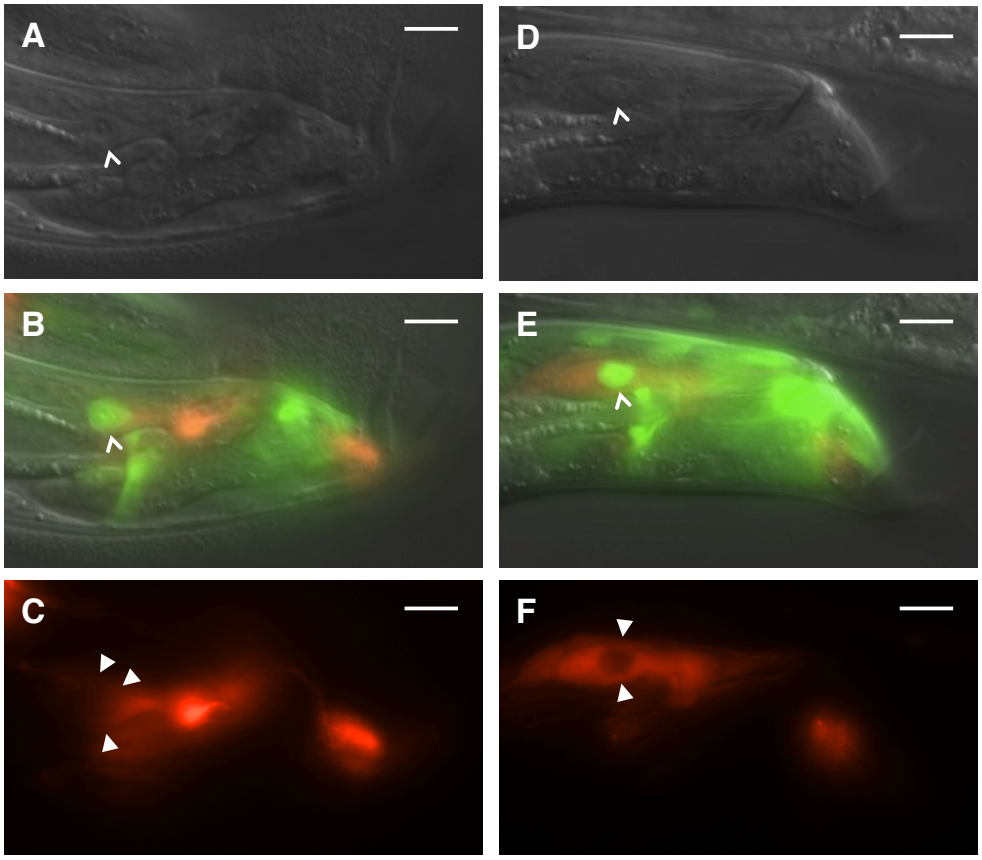

Figure 11: Surviving linker cells in *egl-20* mutants are not engulfed, but dying ones are. A-C, 2-h-old *egl-20*(*n585*) adult male with a surviving linker cell. D-F, 2-h-old *egl-20*(*n585*) adult male with a dying linker cell. A, D, DIC. B, E, DIC/*lag-2*::GFP/*lin-48*::mCherry merge. C, F, *lin-48*::mCherry, marking the U.l/rp cells (arrowheads). Note that in C, the U.l/rp cells abut the surviving linker cell without surrounding it completely, whereas in D, the U.l/rp cells have entirely engulfed the linker cell. White carets in A, B, D, E, linker cell. Scale bars, 10 μm.

Figure 12: Antagonistic Wnt pathways control linker cell death. In (A-C), white caret, linker cell; arrow, Ul/r.p cells; scale bars, 10 μm. (A) Young adult *egl-20(n585)* male expressing a *lag-2*p::GFP reporter. (B) *egl-20*p::EGL-20-GFP expression in an L4 male. (C) *bar-1*p::GFP expression in an L4 male. (D) Linker cell survival in *mig-5*(*rh147)* animals harboring indicated transgenes. *p<.002; **p<10^{-4}; n>50 for each condition. (E) *bar-1*(*ga80*) with and without *hsp-16.2*::ΔN-BAR-1 transgene were heat shocked for 10 min at 34C at the indicated stage and scored as 0-2h adults. *p<10^{-4}; n>60 for all conditions. (F) Electron micrograph of surviving linker cell in a *bar-1*(*ga80*) adult. Representative section from 2 animals examined. Arrows, healthy mitochondria. Arrowheads, healthy nuclear envelope. Carets, healthy endoplasmic reticulum. The imperfectly smooth nuclear contour is an artifact of fixation and is apparent in other cells from these same sections but not on DIC image of the animal prior to fixation. Scale bar, 1 μm. (G) Linker cell survival in *egl-20*(*n585*) and *mig-1*(*e1787*)*; egl-20*(*n585*) animals harboring a *mig-24*p::MIG-1 transgene. *p<.001. n>69 for each condition. (H) Model for Wnt pathway interactions in linker cell death. Electron microscopy performed by Yun Lu.

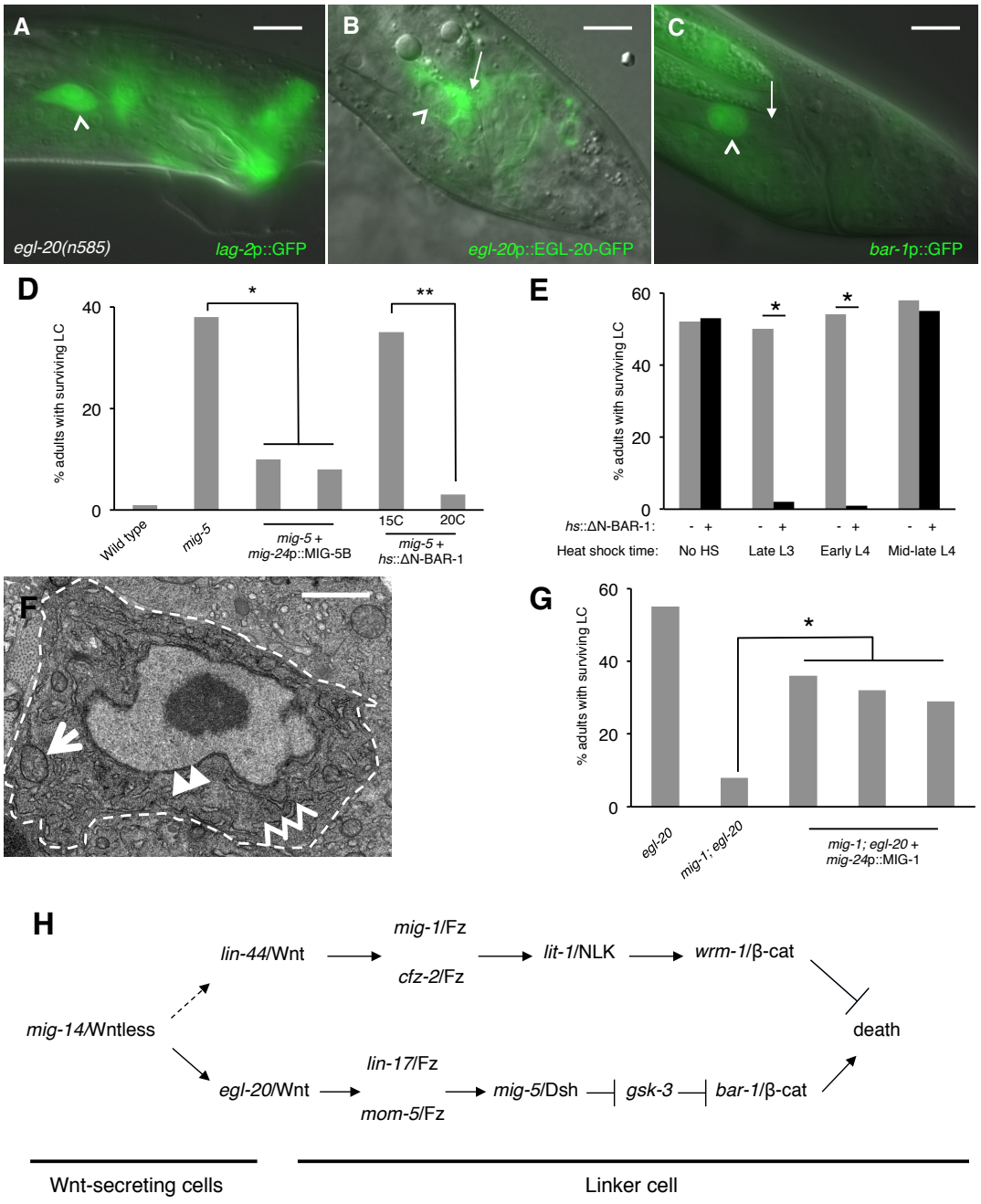
A
egl-20(n585)
lag-2p::GFP
B
egl-20p::EGL-20-GFP
C
bar-1p::GFP
D
% adults with surviving LC
40
20
0
*
**
Wild type
mig-5
mig-5 +
mig-24p::MIG-5B
15C
20C
mig-5 +
hs::ΔN-BAR-1
E
% adults with surviving LC
60
40
20
0
*
*
hs::ΔN-BAR-1:
- +
- +
- +
- +
Heat shock time:
No HS
Late L3
Early L4
Mid-late L4
F
G
% adults with surviving LC
60
40
20
0
*
egl-20
mig-1; egl-20
mig-1; egl-20 +
mig-24p::MIG-1
H
lin-44/Wnt
mig-1/Fz
cfz-2/Fz
lit-1/NLK
wrm-1/β-cat
death
mig-14/Wntless
egl-20/Wnt
lin-17/Fz
mom-5/Fz
mig-5/Dsh
gsk-3
bar-1/β-cat
Wnt-secreting cells
Linker cell

Table 4. Wnt pathway genes not affecting linker cell death

Genotype*	Human homolog	% LC survival†	n‡
cwn-1(*ok546*)	Wnt	3 ± 2	91
cwn-2(*ky756*)	Wnt	0	67
mom-2(*ne834*)	Wnt	0	51
cwn-1(*ok546*); *cwn-2*(*ky756*)	Wnt	2 ± 2	80
egl-20(*n585*) *cwn-2(ok895)*	Wnt	54 ± 6	63
cwn-1(*ok546*); *egl-20*(*n585*)	Wnt	MIG¶	
cam-1(*gm122*)	Ror	7 ± 3	73
lin-18(*e620*)	Ryk	6 ± 3	80
egl-20(*n585*)*; lin-18*(*e620*)		65 ± 5	112
mom-4(*or39*)§	MAPKKK7	0	31
mom-4(*ne1539*)	MAPKKK7	3 ± 2	74
sys-1(RNAi)	β-catenin	0	69
daf-16(*mu86*)	FOXO	1 ± 1	60
daf-21(*p673*)	HSP90	0	48

*All strains also contain the *qIs56* reporter transgene to visualize the linker cell, except for the *mom-2*(*ne834*) and *daf-21*(*p673*) strains which contained the *nsIs64* transgene. Allele numbers are in parentheses. †± SEM. ‡Number of animals scored. ¶This strain had a severe migration defect which precluded accurate scoring of a survival phenotype. §This strain also contained the *unc-13*(*e1091*) allele.

To determine whether receptive Wnt components function in the linker cell to promote its demise, I examined their expression patterns. An 11-kb regulatory region upstream of the *bar-1*/β-catenin gene fused to GFP[354] is not expressed in cloacal cells or in the trailing gonad, but is strongly expressed in the linker cell (Figure 12C). Likewise, *mig-5*/Dishevelled::GFP and *lin-17*/Frizzled::GFP reporters are expressed in the linker cell (Figure 13A-D). Consistent with these data, expression of a *mig-5*/Dishevelled cDNA using a linker-cell-specific promoter restored cell death to *mig-5* mutant males, indicating a cell-autonomous role for this gene (Figure 12D).

To examine when Wnt signaling is required for linker cell death, I expressed *hsp-16.2*::ΔN-BAR-1 in *bar-1*/β-catenin mutants at different time points during larval development, and assessed restoration of cell death. I found that expression as late as the early L4 stage rescues inappropriate linker cell survival (Figure 12E), suggesting that *bar-1* controls linker cell death and not identity. Supporting a role for the Wnt pathway in cell death initiation, surviving linker cells in *bar-1*/β-catenin mutants do not exhibit ultrastructural features of dying linker cells (Figure 12F;[224]), unlike surviving cells in *pqn-41* or *sek-1* mutants, in which organelle changes accompanying cell death initiation are evident in electron micrographs[229]. Taken together, these data suggest that the linker cell responds to an EGL-20/Wnt signal emanating from surrounding cells just prior to its death, and does so using redundant activities of the receptors LIN-17 and MOM-5, and the signal transduction components MIG-5/Dishevelled and BAR-1/β-catenin (Figure 12H).

While null alleles of *egl-20*/Wnt block linker cell death, they do so in only about 60% of animals (**Table 3**), suggesting that another cue likely participates in linker cell death initiation. The linker cell dies at a specific place and time during *C. elegans* male development, and previous studies showed that a developmental timing cue transduced by the Zn-finger transcription factor LIN-29 partially controls linker cell death (**Table 3**; [224]). I found that in *lin-29*; *egl-20*/Wnt and *lin-29*; *bar-1/*β-catenin double mutants most linker cells now survive inappropriately, suggesting that the LIN-29 timing cue and the EGL-20/Wnt positional cue are the main regulators of linker cell death initiation (**Table 3**).

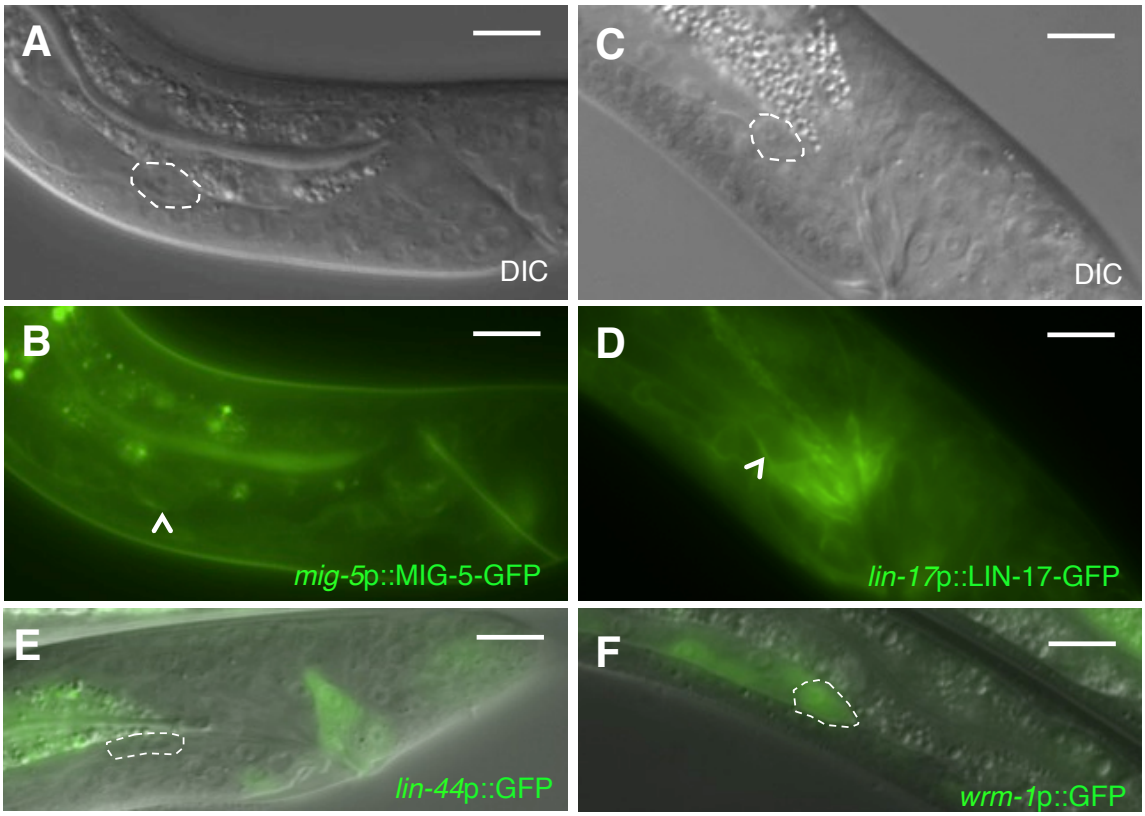

Figure 13: Expression of receptive Wnt components in the linker cell. Shown are typical L4 males harboring reporters for (A, B), *mig-5*; (C, D) *lin-17*. Top panels, DIC. Bottom panels, GFP. (E) Expression of *lin-44*p::GFP reporter in an L4 male. Intestinal expression is an artifact of the vector. (F) Expression of *wrm-1*p::GFP in an L4 male. White carets and dashed circles, linker cell. Scale bars, 10 μm.

3.3 A LIN-44/Wnt pathway promotes linker cell survival

While testing genetic interactions between *egl-20*/Wnt mutants and other *C. elegans* Wnt mutants, I found, surprisingly, that mutations in *lin-44*/Wnt strongly suppressed inappropriate linker cell survival in *egl-20* mutants (**Table 5**). These data suggest that two opposing Wnt pathways control linker cell death: an EGL-20/Wnt pathway promotes, and a LIN-44/Wnt pathway prevents cell death. To test this idea, I examined genetic interactions between EGL-20/Wnt pathway components and other related genes. Linker cell death is restored to *egl-20*/Wnt mutants by mutations in *mig-1*/Frizzled, *cfz-2*/Frizzled, *lit-1*/NLK or *wrm-1*/β-catenin. *lin-44*/Wnt mutations also suppress inappropriate linker cell survival in *bar-1* mutants (**Table 3**, **Table 5**).

lin-44 is expressed in the *C. elegans* male tail (Figure 13E;[355]), consistent with a role in linker cell death. *wrm-1*/β-catenin is expressed in the linker cell, as well as other cells (Figure 13F). Furthermore, expression of a *mig-1*/Frizzled cDNA specifically in the linker cell restores inappropriate linker cell survival to *mig-1*/Frizzled*; egl-20*/Wnt double mutants (Figure 12G). These results therefore suggest that a tail-derived LIN-44/Wnt signal impinges on the MIG-1/Frizzled and CFZ-2/Frizzled receptors. These receptors function together in the linker cell, through *lit-1*/NLK and *wrm-1*/β-catenin, to promote its survival (Figure 12H). While we were unable to score *wrm-1; bar-1* double mutants, as these have a fully penetrant block in linker cell migration (100%, n = many), our results suggest that the EGL-20/Wnt pathway antagonizes the LIN-44/Wnt pathway at or downstream of WRM-1/β-catenin.

Table 5. A LIN-44/Wnt pathway protects against linker cell death

Genotype*	% LC survival†	n‡
lin-44(*n1792*)	2 ± 2	62
lin-44(*n1792*); *egl-20*(*n585*)	16 ± 5	63
lin-44(*n1792*); *bar-1*(*ga80*)	18 ± 5	66
mig-1(*e1787*)	8 ± 2	179
mig-1(*e1787*); *egl-20*(*n585*)	8 ± 3	91
cfz-2(*ok1201*)	2 ± 2	45
egl-20(*n585*); *cfz-2*(*ok1201*)	19 ± 5	52
wrm-1(*ne1982*) *lit-1*(*t512*)	6 ± 3	66
lit-1(*t512*); *egl-20*(*n585*)§	30 ± 4	113
wrm-1(*ne1982*); *egl-20*(*n585*)	19 ± 5	63

*All strains also contain the *qIs56* reporter transgene to visualize the linker cell, except for *cfz-2*(*ok1201*)-containing strains, which contained the *nsIs65* transgene. Allele numbers are in parentheses. †± SEM. ‡Number of animals scored. §*lit-1*(*t512*) allele used in this table is linked to an *unc-32*(*e189*) allele.

Interestingly, while no Wnt gene appears to singly control migration, *cwn-1; egl-20* double mutants have a highly penetrant synthetic migration phenotype (**Table 4**), suggesting that *egl-20* is required, albeit redundantly, for linker cell migration. This *egl-20* synthetic migration phenotype is unique to *cwn-1*, as *lin-44;egl-20* and *egl-20 cwn-2* mutant linker cells migrate correctly (**Table 4**, **Table 5**). *cwn-1* is expressed in a domain just anterior to *egl-20*^{338}, in the final segment of the linker cell's migration, after its final ventral turn. This greater redundancy in Wnt roles for migration is teleologically satisfying; after all, the linker cell's death is functionally and evolutionarily useless if it does not happen at the correct place.

Although *lin-44*/Wnt mutations suppress ectopic linker cell survival in *egl-20*/Wnt and *bar-1*/β-catenin mutants, we found no significant suppression of *lin-29, sek-1,* or *pqn-41* lesions (**Table 6**). Thus, the antagonistic Wnt pathways we uncovered likely act in parallel to these other components. Indeed, double mutants between the null alleles of either *egl-20* or *bar-1* and other known linker cell death factors show dramatic enhancement over each single mutant defect (**Table 3**, **Table 6**). Furthermore, expression of neither ΔN-BAR-1/β-catenin in wild-type animals nor EGL-20/Wnt in *lin-44*/Wnt mutants using a heat-induced promoter causes premature linker cell death or cell death initiation in other cells, suggesting that linker cell death is likely under the control of parallel, partially redundant inputs.

Table 6. Interactions of *lin-44* and *egl-20* with known linker cell death components

Genotype[*]	**% LC survival**[†]	**n**[‡]
lin-29(*n546*)	63 ± 6	77
lin-44(*n1792*); *lin-29*(*n546*)	54 ± 7	52
sek-1(*ag1*)	42 ± 5	83
lin-44(*n1792*)*; sek-1*(*ag1*)	38 ± 6	73
pqn-41(*ns294*)	21 ± 5	63
lin-44(*n1792*); *pqn-41*(*ns294*)	21 ± 4	125
egl-20(*n585*); *sek-1*(*ag1*)	84 ± 4	71
lin-44(*n1792*); *hsf-1*(*sy441*)	43 ± 6	76

[*]All strains also contain the *qIs56* reporter transgene to visualize the linker cell. Allele numbers are in parentheses. [†]± SEM. [‡]Number of animals scored.

3.4 *pop-1*/TCF does not appear to play a role in linker cell death

Unexpectedly, mutations in *pop-1,* the sole *C. elegans* homolog of the canonical Wnt signaling transcription factor Tcf, cause no or weak defects in linker cell death (**Table 3**). Similarly, while RNAi against *pop-1*/Tcf promotes highly penetrant defects in other contexts in *C. elegans*[356,357], only low-level linker cell survival is evident even in RNAi-sensitized backgrounds (**Table 3**). Furthermore, *pop-1* lesions do not enhance or suppress linker cell survival in *egl-20*/Wnt mutants (**Table 3**). Finally, I employed a *pop-1* activity reporter, in which 6 concatenated canonical POP-1 binding sites are placed upstream of a basal promoter driving an mCherry-tagged histone HIS-24. In this strain, cells in which canonical Wnt signaling is active and POP-1 drives gene expression are labeled with a nuclearly localized mCherry-tagged histone[321].

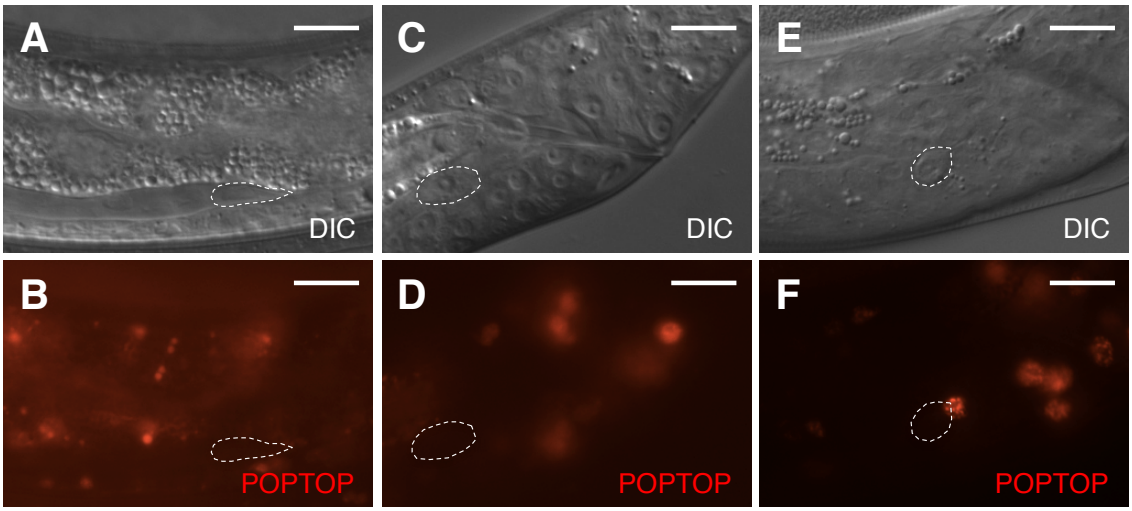

Figure 14: A *pop-1* activity reporter is not expressed in the linker cell early or late. All panels are images of strain *unc-119*(*ed4*); *him-5*(*e1490*); *syIs187*[POPTOP::HIS-24-mCherry]. Linker cell outlined in dashed white. (A, B) Late L3/early L4 male. (C, D) Mid-L4 male. Note the already-apparent linker cell cytoplasmic changes in the DIC image. (E, F) Late L4 male. mCherry-staining nucleus at the top right of the linker cell in (C) belongs to a neighboring overlying cell. Scale bars, 10 μm.

I found that this reporter is not expressed in the linker cell before or during death (Figure 14). While BAR-1/β-catenin has been shown to physically and functionally interact with the transcription factor DAF-16/FOXO[358], I found that a *daf-16* mutation did not block linker cell death (**Table 4**). Therefore, the immediate target/s of Wnt signaling in the linker cell remain unknown.

While β-catenin interaction with TCF/Lef-family transcription factors is the best-studied, if not the dominant mode of Wnt signaling, β-catenin is known to interact, physically and functionally, with transcription factors from a variety of structural families. β-catenin can associate with nuclear hormone receptors, including androgen and estrogen receptors[359-362], and homeodomain transcription factors, including Oct4[363,364] and Prop1[365]. Thus, in the context of the linker cell, BAR-1 may well interact with another, as yet unidentified transcription factor. Such factors might be identified in the future through continued genetic screens, through biochemical screens for BAR-1 interactors, or through direct biochemical tests with existing candidates.

4 The *Abd-B*-like Hox gene *nob-1* controls linker cell death through Wnts

4.1 Background: rationale for Hox gene involvement

Upon discovering that a β-catenin-mediated Wnt pathway is necessary for linker cell death, I wondered whether a Hox gene could be a target of this pathway. Indeed, in *C. elegans*[344,345] and other organisms[366], canonical Wnt pathways can exert their effects through transcriptional control over Hox genes. The name Hox itself is a contraction of the word homeobox, designating a ~180 bp sequence encoding a characteristic and highly conserved helix-turn-helix DNA-binding domain called the homeodomain[367-369] that binds specific DNA sequences[370]. In turn, these domains are named after the homeotic mutant phenotypes found in flies mutant for many of these genes. In these mutants, while the total segment number is unchanged, certain segments or groups of segments adopt the wrong identity. Thus, in *antennapedia* gain-of-function mutants, a cephalic segment adopts a thoracic identity, and ectopic legs grow in place of antennas[371].

While the homeodomain is found in a wide variety of DNA-binding transcription factors, Hox genes proper represent a special set of homeobox-containing genes. Hox genes control antero-posterior identity of segments or regions of animals, and their expression in the animal is reflected in their order on the chromosome that encode them[372-375], a phenomenon known as colinearity. Hox genes typically reside in chromosomal clusters. Flies have two Hox clusters, the Antennapedia complex and the Bithorax complex, encoding 5 anterior and 3 posterior Hox genes, respectively. Humans have four Hox clusters, HoxA-D, each encoding 8-10 Hox genes. The *C. elegans* genome

harbors one Hox cluster with 6 Hox genes. The worm Hox cluster is not quite collinear, as the anterior gene *ceh-13* resides 3' to the central gene *lin-39*, but 5' to the rest of the posterior genes[376], *mab-5, egl-5, nob-1,* and *php-3*.

4.2 *nob-1* promotes linker cell death autonomously

I examined mutants for the five positional Hox genes expressed in the middle and posterior of the animal, reasoning that the linker cell, being born in the mid-body but migrating posteriorly, might express any of these. I observed that 31% of *nob-1(os6)* adult males harbor a surviving linker cell, whereas no other positional Hox gene mutant examined exhibited a significant linker cell death phenotype (**Table 7**). While the relatively strong *egl-5(n486)* allele causes a weak, 10% linker cell survival phenotype, the linker cell is not thought to express *egl-5*[377]. Similar to *pop*-1(RNAi) animals, these *egl-5* mutant males have severely disorganized posterior morphologies, with abnormal division and differentiation of rectal blast cells[378], suggesting that the weak linker cell death phenotype is likely non-cell-autonomous and may result from defects in cells that normally express the linker-cell-death-promoting Wnt gene, *egl-20*.

The allele *nob-1(os6)* is a nonsense allele of *nob-1,* truncating the last 31 amino acids of NOB-1B after N187, including the R-R-M-K-X-K-K motif of the DNA-binding 2nd homeodomain helix, encoded by an alternative fourth exon, that is perfectly conserved among *C. elegans* and *Drosophila* Hox genes. *os6* leaves NOB-1A intact, as this isoform, which is not predicted to encode a homeodomain, does not utilize the fourth exon. Therefore, *os6* is likely a strong loss of function allele for *nob-1B*.

Table 7: *nob-1* is required cell-autonomously for linker cell death and may function upstream of death-controlling Wnt signaling.

Genotype*	% LC survival†	n‡
WT	1 ± 1	72
lin-39(n1880)	1 ± 1	70
egl-5(n486)	10 ± 3	80
mab-5(e1239)	2 ± 2	61
php-3(ok919)	0	73
nob-1(os6)	31 ± 4	131
*nob-1(os6); mig-24*p*::nob-1b* (1)	11 ± 3	106
*nob-1(os6); mig-24*p*::nob-1b* (2)	0	71
*nob-1(os6); mig-24*p*::nob-1b* (3)	2 ± 2	52
lin-44(n1792); nob-1(os6)	1 ± 1	64
gsk-3(*nr2047*)[a]	3 ± 2	91
gsk-3(nr2047)[a]*; nob-1(os6)*	11 ± 4	74

*All strains also contain the *qIs56* reporter transgene to visualize the linker cell. Allele numbers are in parentheses. †± SEM. ‡Number of animals scored. [a]*gsk-3(nr2047)* linked to *unc-101(sy216)*

To ask whether *nob-1* functions in the linker cell to promote its death, I expressed a *nob-1b* cDNA from the *mig-24* promoter. In three independent lines, *mig-24*p::*nob-1b* could rescue the linker cell death phenotype of *nob-1(os6)* (**Table 7**), strongly suggesting that *nob-1* functions cell-autonomously in linker cell death. Consistent with such a cell-autonomous role, a 15-kb genomic fragment of *nob-1* fused to GFP, including about 9 kb of sequence upstream of the common *NOB-1* ATG and generating a GFP-tagged NOB-1^{379}, expressed strongly in the linker cell nucleus as early as the L3 stage and through its death (Fig. 3). As expected, I detected NOB-1-GFP in many cells in the tail of the male, but the linker cell and several cells of the developing *vas deferens* were the only cells not born in the tail that expressed *nob-1* (Fig. 3). Thus, *nob-1* is likely the only positional Hox gene that cell-autonomously controls linker cell death.

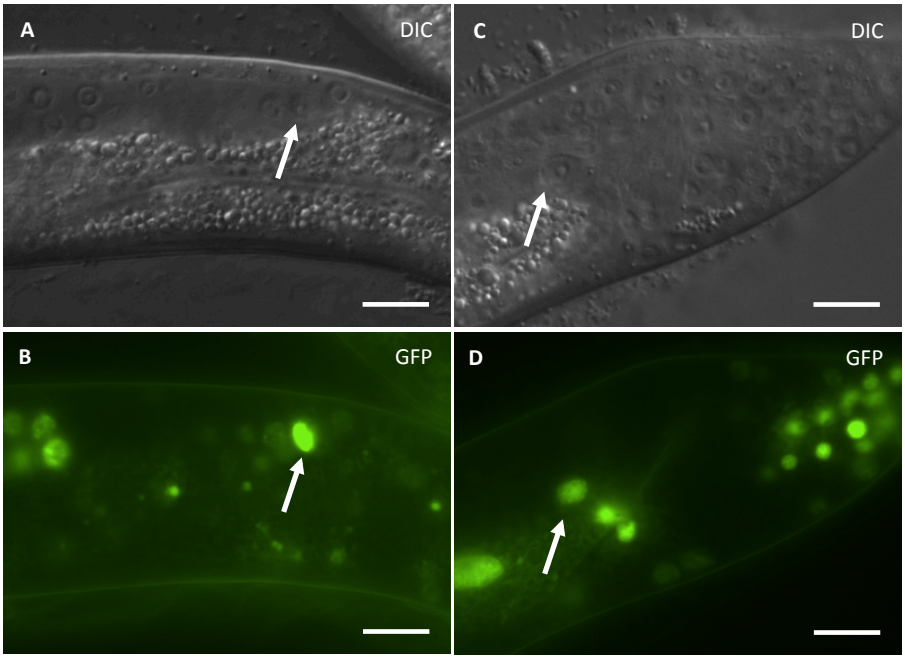

Figure 15: The linker cell expresses *nob-1* for most of its life. A, B. Late L3 male expressing *NOB-1::GFP.* C, D. mid-late L4 male expressing *NOB-1::GFP*. White arrows, linker cell. Top panels, DIC; bottom panels, fluorescence. Scale bars, 10 μm.

4.3 *nob-1* likely functions upstream of Wnts to promote death

Although I previously showed that an EGL-20-BAR-1 Wnt pathway is necessary only just before death to kill the linker cell, these experiments could not address whether this late requirement for BAR-1 activity reflected its physiological time of action. Therefore, it was still possible that this Wnt pathway controlled *nob-1* expression. However, I found that the linker cell's expression of *nob-1* in *egl-20(n585)* and *bar-1(ga80)* animals was unaffected (**Table 8**). Furthermore, *nob-1* was correctly expressed in *sek-1(ag1), lin-29(n333), nhr-67(pf159),* and *set-16(RNAi)* linker cells, as well as in *egl-20; sek-1* double

mutant linker cells (**Table 8**). Together, these data show that *nob-1* expression is not controlled by any known linker cell death genes and that *nob-1* functions upstream or in parallel to all of these genes.

Table 8: NOB-1-GFP expression is not controlled by linker cell death genes.

Genotype (+ *NOB-1::GFP*) ‡	% L4 linker cells expressing NOB-1-GFP*
egl-20(n585)	100
bar-1(ga80)	100
sek-1(ag1)	100
egl-20(n585); sek-1(ag1)	100
lin-29(n333)	100
set-16(RNAi) †	100
nhr-67(pf159)	100

‡All strains also contained the *him-5(e1490)* to increase the incidence of males and a *qIs56*[*lag-2*p::GFP] transgene to visualize the linker cell. *n=40 for all. †Strain contained RNAi-sensitizing *rrf-3(pk1426)*.

As shown in **Table 5**, *lin-44* mutation suppresses the phenotype of *egl-20* and of *bar-1* mutants. I constructed *lin-44(n1792); nob-1(os6)* double mutants, and found that *lin-44(n1792)* efficiently suppresses the *nob-1* phenotype (**Table 7**), suggesting that *nob-1* functions upstream of the Wnt pathway. Furthermore, *gsk-3(nr2047)*, an allele of the Wnt-antagonizing kinase Gsk3β[353], could also suppress the *nob-1* phenotype (**Table 7**). Taken together, the suppression of the *nob-1* phenotype by alleles of *lin-44* and *gsk-3* and the fact that *nob-1* expression is not regulated by *egl-20* or *bar-1* suggest that *nob-1* functions upstream, not downstream, of Wnt signaling to promote the death of the linker cell.

4.4 *nob-1* and Wnts: a conserved circuit?

In fact, such a pathway would not be without precedent, in flies[380] or in worms. Ji *et al.* have described regulation of Wnt receptor expression by the Wnt-induced Hox gene *mab-5*[381]. These positive and negative feedback loops help confer robustness on the expression level of *mab-5* and thus on the migration of QL neuroblast progeny. In contrast, we have found that *nob-1* likely functions primarily upstream of Wnt signals. By extension of the model in Ji *et al,* it is not hard to imagine that Wnt-Hox regulatory loops may exist on a continuum, from the more classical model where Wnts primarily function upstream of Hox genes and control their expression, to the situation in the linker cell, where the Hox gene primarily functions upstream of Wnt signaling components. In the Ji *et al.* study, the Frizzled-regulating activity of the Hox gene *mab-5* in QL descendants is regulated cell-non-autonomously, by Wnts. Work from the same group has shown that the QR.pa neuroblast uses a cell-intrinsic timing mechanism to regulate expression of MIG-1/Fz and terminate its migration[382]. However, this study did not identify the timing mechanism in this cell.

One might speculate that in the linker cell, a similar cell-intrinsic timing mechanism might terminate the expression of the pro-survival Wnt receptors, or upregulate the expression of pro-death receptors. Indeed, *lin-29* might be a *prima facie* good candidate for this timing mechanism, given the known roles of *lin-29* in cell-autonomous timing activities. However, the fact that *lin-44(n1792)* cannot suppress *lin-29* mutations suggests that *lin-29* does not function upstream of the linker cell's Wnt response. Rather, in light of my data showing that *nob-1* functions upstream of Wnt pathway components, and in parallel to all known linker cell death transcriptional

regulators, *nob-1* may be responsible for tuning the linker cell's levels of Frizzleds, in a cell-autonomous way. This hypothesis awaits experimental query, and if confirmed would of course only raise the question of what, in turn, times the activity of *nob-1*.

The linker cell's expression of a posterior Hox gene is interesting in regards to its position. The linker cell spends most of its life outside of the domain of *nob-1* expression, reaching it only at the end of its life. In other *C. elegans* cells with relatively long migrations, cells also express the Hox gene typical of cells at their destination rather than their origin[383,384]. However, in these cases, the Hox gene is required for migration to that domain[385]. Unlike these other migrating cells, the linker cell's migration does not seem to be singularly controlled by *nob-1,* as *nob-1(os6)* does not cause a migration defect as a single mutant. *nob-1* may still be required for some aspects of migration, as we have observed that *nob-1(os6)* enhances the migration defect of other mutants, notably that of *sek-1(ag1)* and *lin-29(n333)* (data not shown), but the linker cell is certainly more dependent on *nob-1* for its death than for its migration.

While the study of *nob-1* might provide insight into how the linker cell responds to the various Wnt signals around it, the targets of the Wnt pathway in the linker cell remained elusive.

5 HSF-1 promotes linker cell death

While exploring possible roles for stress response genes in linker cell death, I found that a weak loss-of-function allele of the *C. elegans* heat shock factor gene, *hsf-1*(*sy441*), which lacks part of a region encoding the transcriptional transactivation domain, causes linker cell survival (**Table 9**). Compromised stress responses do not generally block linker cell death, as neither unfolded protein response mutants[229], nor *daf-16*/FOXO or *daf-21/*HSP90 mutants (**Table 4**) show linker cell death defects. A single-copy *hsf-1* promoter*::hsf-1*(R145A) transgene, expressing a DNA-binding-defective HSF-1 protein[386], further increases linker cell survival in *hsf-1*(*sy441*) mutants (**Table 9**), revealing a major role for this gene and its DNA-binding activity in promoting linker cell death. A single copy *hsf-1* promoter::*hsf-1*-GFP transgene[386] restores linker cell death to *hsf-1*(*sy441*) mutants, as does expression of an *hsf-1* cDNA using the *mig-24* linker-cell-specific promoter (**Table 9**), suggesting a cell-autonomous role in promoting linker cell death. Indeed, a rescuing HSF-1::GFP protein is expressed in the linker cell nucleus (Figure 16). Thus, HSF-1 functions in the linker cell to promote death.

Table 9. HSF-1 promotes linker cell death.

Genotype[*]	% LC survival[†]	n[‡]
Wild type, 20C	1 ± 1	72
Wild type, 25C	17 ± 4	71
Wild type +heat shock, -4h[§]	17 ± 4	70
Wild type +heat shock, -6h[§]	5 ± 2	105
hsf-1(*sy441*), 20C	29 ± 5	87
hsf-1(*sy441*); *hsf-1* promoter::*hsf-1*[¥]	13 ± 3	129
hsf-1(*sy441*); *mig-24* promoter::*hsf-1 cDNA* line 1	5 ± 2	86
hsf-1(*sy441*); *mig-24* promoter::*hsf-1 cDNA* line 2	6 ± 3	80
hsf-1(*sy441*); *mig-24* promoter::*hsf-1 cDNA* line 3	3 ± 2	60
hsf-1 promoter::*hsf-1*(R145A)(1)[¶, ¥], 20C	2 ± 1	95
hsf-1 promoter::*hsf-1*(R145A)(1), 25C	3 ± 2	105
hsf-1(*sy441*); *hsf*-1 promoter::*hsf-1*(R145A)(1), 20C	67 ± 6	67
hsf-1(sy441); hsf-1 promoter::*hsf-1*(R145A)(2), 20C	54 ± 5	81

[*]All strains also contain the *qIs56* reporter transgene to visualize the linker cell. Allele numbers are in parentheses. Unless otherwise noted, *hsf-1*(R145A) refers to *drSi28* transgene. [†]± SEM. [‡]Number of animals scored. [§]Heat shock was performed 4 or 6 hours before scoring by exposing worms to 37C for 10 minutes. See Chapter 9, Methods and Materials, for details. [¥]In these transgenes, *hsf-1* cDNA is fused to GFP.

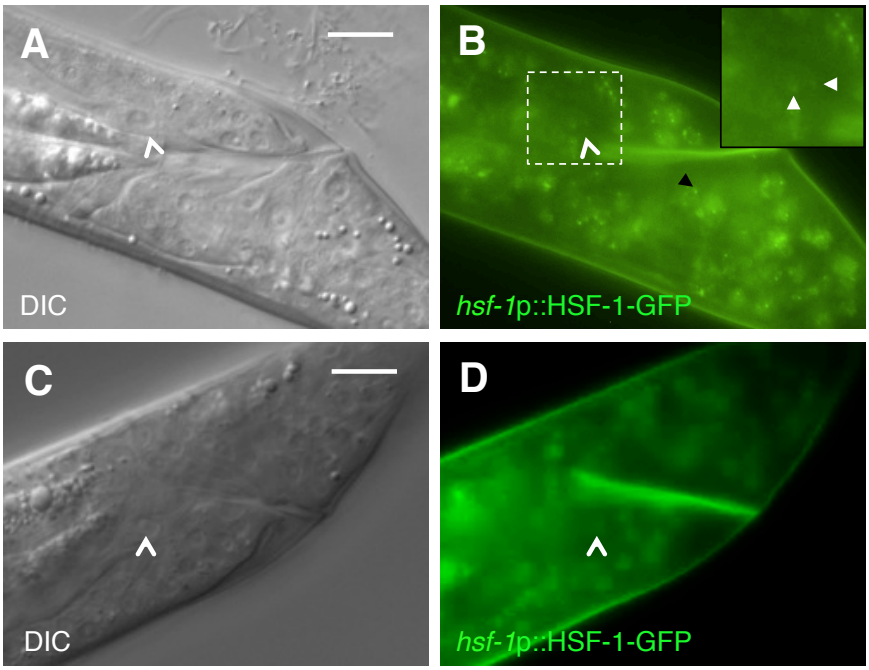

Figure 16: HSF-1-GFP is present in the LC, can form nuclear stress granules in the LC, but does not normally do so. (A, B) L4 male imaged in NaN_3 to induce HSF-1 nuclear stress granules (A) DIC (B) GFP. Dashed square magnified 1.5x in inset. (C, D) L4 male imaged in tetramisole to maintain unstressed HSF-1 (C) DIC (D) GFP. Inset in (B), close-up of LC region. White carets, LC. White arrowheads in (B) inset, nuclear stress granules in the LC. Black arrowhead, stress granule in another cell. Scale bars, 10 μm.

5.1 Introduction to heat shock factors and the heat shock response

The heat shock response was first observed in *Drosophila* as short-lived puffs in the salivary gland polytene chromosomes upon exposure to elevated temperatures, whose appearance was closely followed by the synthesis of large amounts of a number of specific proteins[387]. Many of these proteins where named heat shock proteins (HSP) of a certain size according to their migration on acrylamide gel electrophoresis, so HSP70 and HSP90 migrate at 70 kDa and 90kDa, respectively. While the function of HSPs remained

elusive from quite some time, clues came from observations that polypeptides likely need to unfold to be transported into organelles [388-390], and that HSPs bind to these proteins, are required for their transport, and consume ATP[389,391,392]. Further, HSP70 was found to bind unfolded proteins independently of their transport[393]. Thus, HSPs and their homologs help in folding nascent proteins and in refolding proteins that were denatured, by heat or other noxious treatments[394-396], acting as molecular chaperones.

Indeed, a chaperone production response similar to the heat shock response was found to be induced by a wide variety of cellular stressors, including various mitochondrial uncoupling agents and other oxidizers, and the appearance of the heat shock RNAs was not dependent on new protein synthesis, suggesting that the relevant transcription factor is constitutively present in cells but inactive[397,398]. Promoters for the genes encoding various heat shock proteins were found to contain similar motifs, termed heat shock elements (HSEs), consisting of inverted GAA repeats separated by two or more nucleotides, that were sufficient to drive expression of irrelevant genes in response to heat[399-401]. These sequences were then used to identify the heat shock transcription factor by affinity chromatography and cDNA expression screening[402,403], and individual heat shock factor molecules were found to bind individual GAA binding sites[404].

Upon heat shock, the *Saccharomyces cerevisiae* heat shock factor (HSF1) was found to be phosphorylated[403], and the amount of phosphorylation correlated with an early and a late phase of heat shock factor activation[405]. Further, yeast HSF binds DNA constitutively in a trimeric state[406,407], suggesting that phosphorylation may be the primary mode of HSF regulation in yeast. In contrast, HSF1 in *Drosophila* and humans was found to be monomeric at rest, and heat shock to induce HSF1 trimerization in

addition to phosphorylation[408-411]. Indeed, HSF1 is thought to be kept in a monomeric state by HSP90[412,413] until the presence of unfolded competes HSP90 away from HSF1, allowing its trimerization. Subsequently, HSP70 may play a role in reducing HSF1 activity back to baseline[414], although this process may require many additional regulatory events[415].

Still, in multicellular eukaryotes, HSF1 trimerization alone appears insufficient to promote transcription[416] and phosphorylation, following trimerization, remains crucial for transcriptional activity[417,418]. Furthermore, not all stresses induce HSF1 phosphorylation to the same extent[410], and different stressors may induce phosphorylation of different sites[419,420]. Interestingly, however, phosphorylation, presumably of different sites or of different combinations of sites than those induced by stress, is also able to repress heat shock factor activity[421-424]. Indeed, HSF1 can be a substrate for number of kinase families, including ERK, JNK, p38, GSK, PKC, and CamKII[423,425-427]. Therefore, the precise combination of phosphorylation sites, in response to an array of different inputs, may play a crucial role in tuning HSF1 activity[428,429].

Interestingly, in *Drosophila*, HSF trimers were found to bind not just loci encoding genes induced in response to heat shock, but also of genes known to be induced during specific developmental events[408], suggesting that HSF1 is either able to act as a repressor of these genes or that non-heat-shock protein genes are induced in response to heat shock.

In both *Drosophila* and *C. elegans*, HSF1 is required for early larval development; however, induction of HSPs does not appear to mediate this requirement[386,430]. Similarly, mice deficient for HSF1 exhibit unaltered levels of basal

HSP expression and a variety of developmental defects[431]. These results raise the tantalizing possibility that HSF1 regulates developmental transcription independently of its role in the stress response.

Conversely, the heat shock response can vary with development. Even though they express HSF1, early *Drosophila* and mouse embryos are refractory to heat shock protein induction[432,433], and mouse testes have a lower threshold for heat shock factor induction than mouse liver[434]. One explanation for these results is that proteins from different tissues have different propensities to unfold and trigger a heat shock response; however, it seems more likely that the HSF1 set point is developmentally regulated. Indeed, the basal nuclear localization of embryonic *Drosophila* HSF1 is developmentally regulated[433], and the temporary loss of a heat shock response in *Xenopus* embryos correlates not with a loss of trimerization and DNA binding capacity, which are unaffected, but with a loss of transcriptional transactivation[435]. Concordantly, genome-wide studies of HSF1 promoter occupancy before and after heat shock suggest that enhancer binding by HSF1 is not sufficient to induce transcription[436,437]. Further, these studies found a number of genes occupied by HSF1 not known to be involved in the heat shock response, suggesting that HSF1 might be able to induce a broader set of targets than previously appreciated, developmentally or otherwise. Indeed, an examination of HSF1 targets in several types of cancer suggests that HSF1 can drive transcriptional programs distinct from the heat shock response[438].

5.2 HSF-1 functions independently of the heat shock response to promote linker cell death

HSF-1 is thought to function primarily in a cytoprotective role; therefore, the observation that HSF-1 instead promotes linker cell death is surprising. I examined whether HSF-1 functions in linker cell death in the context of a stress response. While nuclear-cytoplasmic shuttling does not appear to control HSF-1 activity in *C. elegans* [386], HSF-1 forms nuclear aggregates in all cells, including the dying linker cell, following exposure to certain stressors (Figure 16A,B; [386]). However, no such aggregates are evident in the dying linker cell, or the surrounding cells, of unstressed animals (Figure 16C,D). Furthermore, I find that HSF-1-dependent target genes of the heat-shock response are not induced in the linker cell as it dies (Figure 17A-D). Finally, as shown in Figure 12E, *hsp-16.2*::ΔN-BAR-1 rescued *bar-1*/β-catenin mutants only after heat-shock, again suggesting that this heat shock promoter is not active in the linker cell in unstressed animals. I conclude, therefore, that HSF-1 likely functions independently of the stress response in linker cell death.

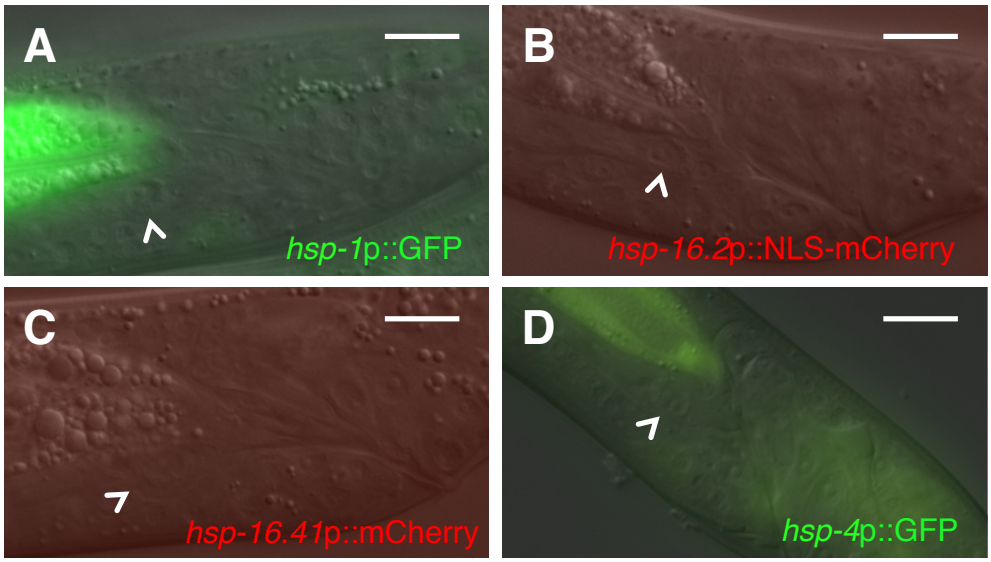

Figure 17: Induction of typical and atypical heat-shock-inducible promoters is not seen in dying linker cells. Shown are L4 males harboring reporters for (A) *hsp-1*; (B) *hsp-16.2*; (C) *hsp-16.41*; (D) *hsp-4*. At least 20 animals were examined for each reporter. *hsp-4* is not a typical heat shock *hsf-1* target but harbors cryptic heat shock elements in its proximal promoter.

I wondered whether the linker-cell-death and stress-response functions of HSF-1 might compete with each other. Indeed, I found that while the linker cell of wild-type males raised at 20C always dies, some wild-type adult males raised at 25C harbor a surviving linker cell (**Table 9**). Likewise, males subjected to a 37C heat shock four hours prior to linker cell death also exhibit a surviving linker cell, whereas males heat-shocked just two hours earlier, or six hours prior to death, exhibit fewer surviving linker cells (**Table 9**). These results suggest that heat shock may functionally sequester HSF-1 away from its linker cell death role, and that activity of HSF-1 just before the cell dies is required to promote linker cell death.

Previous studies described developmental activities for HSF proteins that are independent of the stress response. Some of these activities may be mediated by monomeric forms of the protein[386,439] or by complexes of HSF with other transcription factors[440,441]. My initial attempts to test this idea in the context of linker cell death using mutant trimerization domain transgenes suggested that this domain may be important for protein expression (8/8 lines). As an alternative, I reasoned that expression of an HSF-1 protein containing a DNA-binding-domain mutation might preferentially disrupt the stability or function of higher order HSF-1 complexes, as trimer binding to DNA heat shock elements is cooperative and promotes trimer stability[442]. Indeed, I found that unlike the wild type, animals carrying a single-copy *hsf-1* promoter::*hsf-1*(R145A) transgene exhibit no linker cell survival at 25C (**Table 9**). This transgene, therefore, behaves as a gain of HSF-1 linker-cell-death function, and allowed me to explore the relationship between HSF-1 and Wnt signaling.

5.3 HSF-1 functions downstream of known linker cell death regulators

Strikingly, I found that HSF-1(R145A) expression could restore linker cell death to *egl-20*/Wnt and *bar-1*/β-catenin mutants (**Table 10**). Importantly, a *lin-44*/Wnt mutation could not restore cell death to *hsf-1*(*sy441*) animals (**Table 6**). While I was not able to demonstrate direct physical interactions of BAR-1/β-catenin or WRM-1/β-catenin proteins with HSF-1, my results nonetheless provide strong support for the notion that HSF-1, or an HSF-1 target, function downstream of or in parallel to the Wnt cell death initiation signal to promote linker cell death.

Table 10. HSF-1 acts downstream of known linker cell death genes.

Genotype*	% LC survival†	n‡
Wild type, 20C	1 ± 1	72
egl-20(*n585*); *hsf*-1 promoter::*hsf-1*(R145A)(1)	31 ± 6	70
hsf-1(*sy441*); *bar-1*(*ga80*)	74 ± 5	85
hsf-1 promoter::*hsf-1*(R145A)(1); *bar-1*(*ga80*)	22 ± 4	92
hsf-1 promoter::*hsf-1*(R145A)(2); *bar-1*(*ga80*)	33 ± 5	91
hsf-1 promoter::*hsf-1*(R145A)(3); *bar-1*(*ga80*)	29 ± 5	79
pqn-41(*ns294*), 20C	21 ± 5	63
pqn-41(ns294), 25C	34 ± 5	88
pqn-41(*ns294*), 15C	45 ± 6	60
hsf-1(*sy441*); *pqn-41*(*ns294*) 20C	82 ± 4	96
pqn-41(*ns294*); *hsf*-1 promoter::*hsf-1*(R145A)(1), 20C	9 ± 3	75
pqn-41(*ns294*); *hsf*-1 promoter::*hsf-1*(R145A)(1), 15C	16 ± 3	149
sek-1(*ag1*), 20C	42 ± 5	83
sek-1(*ag1*), 25C	46 ± 5	86
hsf-1(*sy441*); *sek-1*(*ag1*)	86 ± 3	174
sek-1(*ag1*); *hsf*-1 promoter::*hsf-1*(R145A)(1)	18 ± 4	111
lin-29(RNAi)	53 ± 5	96
hsf-1(*sy441*); *lin-29*(RNAi)	70 ± 4	138
lin-29(RNAi); *hsf*-1 promoter::*hsf-1*(R145A)(1)	28 ± 5	71

*All strains also contain the *qIs56* reporter transgene to visualize the linker cell. Allele numbers are in parentheses. Unless otherwise noted, *hsf-1*(R145A) refers to *drSi28* transgene. †± SEM. ‡Number of animals scored. ¥In these transgenes, *hsf-1* cDNA is fused to GFP. ¶Three independent R145 transgenic lines were tested. These are labeled (1), (2), (3) after the transgene name.

I also examined the interactions of *hsf-1* mutations with other known linker cell death mutations. *sek-1*/MAPKK and *pqn-41*/Q-rich are thought to act in the same pathway to promote linker cell death[229]. I found synergistic interactions between mutations in these genes and the *hsf-1*(*sy441*) mutation (**Table 10**). Importantly, I demonstrated that HSF-1(R145A) expression restores linker cell death to *sek-1* and *pqn-41* mutants (**Table 10**). These interactions are interesting in light of the known central role of MAPK pathways in regulating HSF-1 function[443,444]. Intriguingly, cultivation of at 25C enhances the linker cell death defect of *pqn-41* mutants, but not of *sek-1* mutants (**Table 10**), suggesting that *sek-1* may have a specific role in restricting HSF-1 function in the linker cell. Finally, restoration of linker cell death was also observed in *lin-29* mutants expressing HSF-1(R145A) (**Table 10**). Taken together, our results demonstrate that HSF-1 or its targets function downstream of, or in parallel to, all known linker cell death genes. Intriguingly, MLL/Trx has been shown to function as an HSF-1 coactivator in both flies[445] and mammals[446], suggesting that *set-16* might also function through *hsf-1* in linker cell death.

The studies presented here demonstrate for the first time that cell death during *C. elegans* development can be regulated cell non-autonomously. The data allows the construction of a model framework for the initiation and execution of linker cell death. Linker cell death is controlled by spatial and temporal cues, provided by Wnt and LIN-29 genes, respectively. These activities, together with the functions of SEK-1/MAPKK and PQN-41/Q-rich, impinge on HSF-1, or key HSF-1 targets, to promote linker cell death. Importantly, HSF-1 functions in a capacity distinct from its role in the stress response to

promote cell death, a novel role for a protein previously thought to be primarily protective.

5.4 HSF-1's pro-death role: discussion and relevance to other contexts

Such a model places HSF-1's linker cell death function under both cell-autonomous and cell-non-autonomous control. Several recent studies have shown that HSF-1's role in the *C. elegans* heat shock response is also coordinated cell-non-autonomously, through the AFD thermosensory neuron[447,448] and through insulin receptor signaling[449]. However, these studies do not ascribe an active role to the heat-shock-inactive HSF-1. Instead, these authors regard inactive HSF-1 as a reservoir on which to draw to enhance the capacity of the heat shock response. Our evidence suggests that this – or another - "reservoir" pool may have active developmental roles. A non-heat-shock-response HSF1-driven program has been described in aggressive cancers[438], although we believe that the role of *hsf-1* in linker cell death represents the first instance of a precise developmental function of *hsf-1* function.

How might HSF-1 promote linker cell death? As mentioned previously, Jennifer Malin-Zuckerman in our lab has characterized a set of ubiquitin-proteasome system components, including the E2 ligase LET-70 and ubiquitin UBQ-1 itself, which required for linker cell death and are transcriptionally induced shortly before death (Malin *et al,* unpublished data). Intriguingly, ubiquitin was previously known to be inducible by heat shock in a number of organisms[450,451], though not in *C. elegans*, and both *let-70* and *ubq-1* contain candidate HSE in their proximal promoter region that are conserved in sequence and location relative to the translational start site in related nematodes (Malin *et al*, unpublished data). Therefore, it is possible that HSF-1 directly induces the

transcription of ubiquitin-proteasome machinery genes in the linker cell to promote its ordered destruction. If chaperones are involved in linker cell death, they are likely a set distinct from those induced by heat shock, as inducing a heat shock response prevents death. However, chaperones have been implicated in dismantling certain macromolecular structures in cells. Notably, the constitutively expressed HSC70, an HSP70 homolog, is required for the uncoating of clathrin from exocytic vesicles[452,453], acting in an enzymatic manner rather than by sequestering clathrin monomers[454]. Characterizing the HSF-1-dependent linker cell transcriptome should uncover additional mechanisms that promote linker cell death.

Disruptions in proteostasis play a central role in a number of diseases, including cancer and neurodegeneration[438,455,456]. Given that in patients and murine models of polyglutamine expansion diseases, some dying cells exhibit morphology similar to linker cell death[229], my identification of a novel, pro-death role of a key proteostatic regulator, HSF-1, that competes with its protective role, is intriguing. In addition, these results suggest an additional explanation for the frequent activation of stress response pathways in tumors[438,457-459]. Specifically, these pathways may not only relieve genotypic and environmental stress that accompany the tumor state, but may also directly sequester pro-death HSF-1 activity.

6 The nuclear hormone receptor NHR-67 promotes linker cell death

In the genome-wide RNAi screen for genes required for linker cell death[229], Blum *et al.* recovered the *Tailless*/Tlx-like nuclear hormone receptor gene *nhr-67*. *Tailless* was discovered as an essential gene encoding an orphan nuclear hormone receptor required for early anterior and posterior ectodermal patterning in the *Drosophla* embryo as well as in central nervous system patterning[460-462]. In the fly, *Tailless* appears to act in a fairly upstream role, controlling expression of gap and pair-end homeotic genes[463]. In contrast, in mammals, the homolog Tlx/NR2E1 appears to have more restricted functions, in nervous system patterning[464] and neurogenesis[465]. Previously, *C. elegans nhr-67* has been implicated in neuronal, uterine, and vulval development[466-468], some of which roles are reminiscent of its worm and mammalian functions. *nhr-67* is also a key regulator of linker cell migration, required for progression through various morphological stages during the cell's migration and the expression of many migration-associated genes[469,470]. I found that RNAi against *nhr-67* induces 72% of linker cells to survive (**Table 11**), and that, as previously reported[469], 100% of *nhr-67(RNAi)* linker cells also prematurely arrested their migration.

Table 11: *nhr-67* is required cell-autonomously for linker cell death

Genotype*	% LC survival†	n‡
WT	1 ± 1	72
Empty vector RNAi	4 ± 2	122
nhr-67(RNAi), full postembryonic	72 ± 5	76
nhr-67(pf159)	67 ± 3	202
nhr-67(pf159); *mig-24*p::*nhr-67* (1)	25 ± 4	96
nhr-67(pf159); *mig-24*p::*nhr-67* (2)	16 ± 4	74
nhr-67(pf159); *mig-24*p::*nhr-67* (3)	10 ± 4	58
nhr-67(RNAi), 7h postembryonic§	20 ± 6	50
lin-29(n333) §	56 ± 6	75
lin-29(n333); *nhr-67*(RNAi), 7h postembryonic§	81± 6	42
egl-20(n585) §	58 ± 5	96
egl-20(n585); *nhr-67*(RNAi), 7h postembryonic§	91± 4	43
lin-44(*n1792*); *nhr-67*(RNAi)	57± 5	87

*All strains also contain the *qIs56* reporter transgene to visualize the linker cell. Allele numbers are in parentheses. †± SEM. ‡Number of animals scored. §Only fully migrated cells were scored in these experiments.

I then examined *nhr-67(pf159)*, an allele which deletes 484 bp from a region of the *nhr-67* promoter that may be required for *nhr-67* expression in the anchor cell[468], the linker cell's lineal homolog in hermaphrodites. I found that this allele causes 67% of linker cells to survive until 2 hours past the L4 to adult transition (**Table 11**), along with a fully penetrant migration defect (Figure 18A,B). Furthermore, 40% of 24-h-old *nhr-67(pf159)* males exhibited healthy-appearing surviving linker cells (n=82) (Figure 18C, D), showing that *nhr-67* lesions can fully block linker cell death rather than merely delay the process.

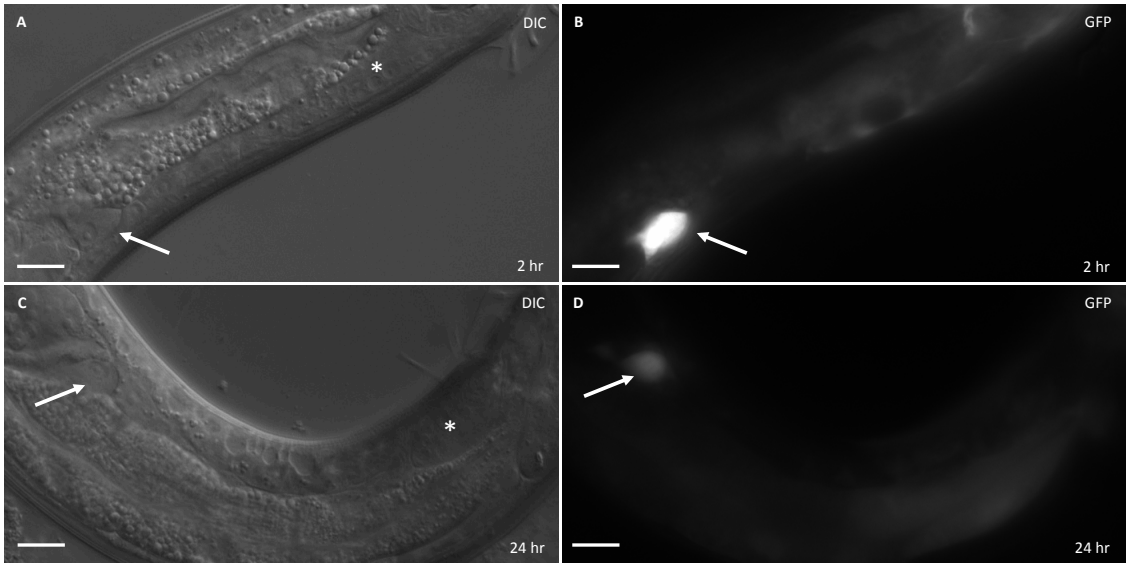

Figure 18: The linker cell survives in *nhr-67* mutants. A, B. Two-hour-old male of genotype *nhr-67(pf159); qIs56[lag-2*p*::GFP] him-5(e1490).* C, D. Day-old male of the same genotype. White arrows, linker cell. Asterisks, approximate final destination of the linker cell in wild type. Left panels, DIC; right panels, GFP. *lag-2*p*::GFP* marks the linker cell. White arrows, linker cell. Scale bars, 10 μm.

While *nhr-67* has been shown to act cell-autonomously for linker cell migration[469], I wondered whether this was the case for linker cell death. Re-expressing NHR-67 specifically in the linker cell efficiently rescued the death defect in 3 independent lines (**Table 11**). Thus, *nhr-67* acts specifically in the linker cell to promote its death. Surprisingly, the *mig-24*p::*nhr-67* transgene entirely failed to rescue the migration defect of *pf159* in all 3 lines. I favor a technical explanation for this apparent discrepancy between this result and those of Kato and Sternberg[469], which I discuss below. This discrepancy notwithstanding, my results show that the inappropriate linker cell survival seen in *nhr-67* mutants can be decoupled from arrested migration and is

therefore not simply a consequence of this earlier defect. Consequently, *nhr-67*'s role in linker cell death is functionally distinct from its role in migration. This conclusion is in keeping with Kato and Sternberg's analysis of *nhr-67*'s role in migration, in which they show that enactment of later *nhr-67* migratory functions is not contingent upon completion of earlier ones[469]. To further buttress a migration-independent role of *nhr-67* in linker cell death, I released synchronized, arrested L1 larvae on *nhr-67* RNAi *E. coli* and fed them this treatment for 7h, before switching them to non-RNAi-expressing OP50 *E. coli* for the remainder of their development. I found that this treatment allowed about half of linker cells to complete their migration, of which 20% inappropriately survived (**Table 11**), clearly showing that *nhr-67* promotes linker cell death independently of its function in linker cell migration.

Consistently with a cell-autonomous role of *nhr-67* in linker cell death, I confirmed that the linker cell expresses *nhr-67* through its death, using a 2 kb upstream promoter region, which includes the sequence deleted from *pf159* mutants, fused to mCherry (Figure 19A,B). This promoter expressed quite specifically in the linker cell, although other *nhr-67* regulatory regions drive expression in other tissues[467]. I then fused just the 484 bp sequence deleted in the *pf159* allele to a *pes-10* minimal promoter driving GFP and observed robust linker cell expression using this construct up to the time of death (Figure 19C,D). Thus, the *pf159* sequence likely contains a DNA element required for linker cell expression of *nhr-67*.

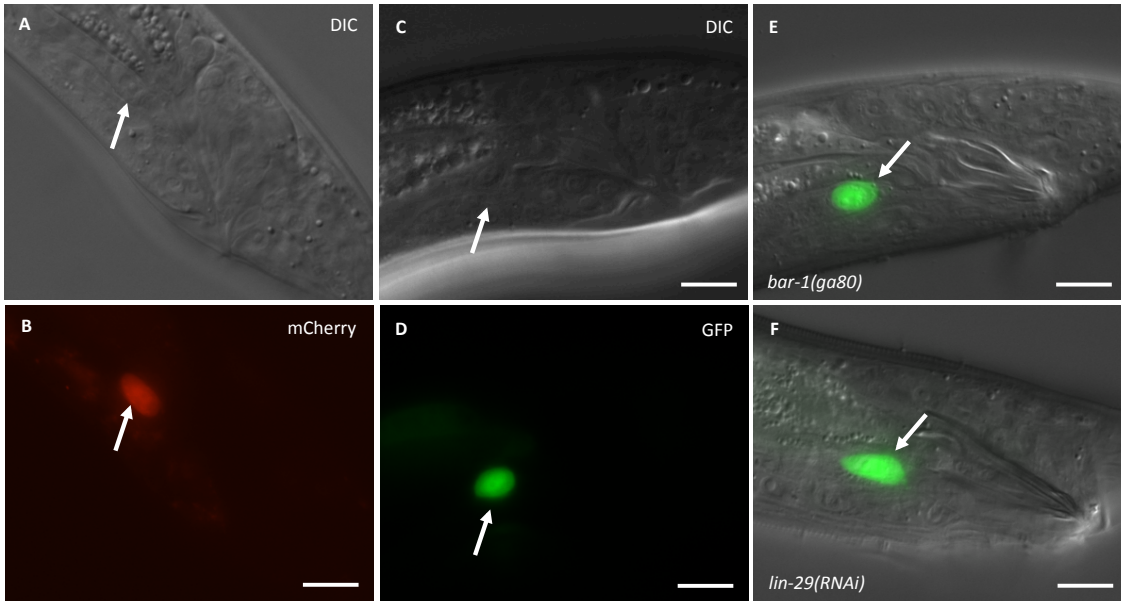

Figure 19: The linker cell expresses *nhr-67* until its death. A, B. L4 male expressing a 2 kb *nhr-67*p::*mCherry.* C, D. L4 male expressing the 484 bp *pf159-pes-10min::GFP* construct. E. *bar-1(ga80)* and F. *lin-29(RNAi)* adult males expressing 484 bp *pf159-pes-10min::GFP* construct in their surviving linker cells. White arrows, linker cell. Scale bars, 10 μm.

None of our other strong linker cell death mutants shows the same robust migration phenotype as *nhr-67* loss of function, suggesting that they do not control the linker cell's expression of *nhr-67.* To confirm this, I placed the 484 bp *nhr-67-pes-10-*minimal*::GFP* construct in a *bar-1(ga80)* background and observed unabated expression (Figure 19E), nor did *lin-29(RNAi)* prevent expression from this construct (Figure 19F).

How then might *nhr-67* promote linker cell death? Linker cell death is controlled by *lin-29*[224]) and the Wnt *egl-20* (**Table 11**). To examine *nhr-67*'s genetic interactions with these genes independently of the confounding effect of *nhr-67*'s migration phenotype, I performed the 7h *nhr-67*(RNAi) treatment on the strong or null *lin-29(n333)*

and *egl-20(n585)* mutants. Counting only cells which completed their migration, I found that *nhr-67*(RNAi) strongly enhanced the phenotype of both of these mutants (**Table 11**), suggesting that *nhr-67* acts in parallel to both *lin-29* and *egl-20* to promote linker cell death. Mammalian beta-catenin is known to associate with nuclear receptors (see section 3.4), suggesting that NHR-67 might associate with BAR-1 in linker cell death. However, *lin-44* mutation fails to appreciably suppress the *nhr-67* death phenotype (**Table 11**), corroborating the idea that the Wnt pathways and *nhr-67* function in parallel to each other.

How might *nhr-67* function to promote linker cell death? Interestingly, Jennifer Zuckerman-Malin has found that *nhr-67*(RNAi) induces transcriptional *let-70*::GFP and *ubq-1*::GFP reporters earlier, and the *let-70* reporter to higher levels, than seen in the wild type or in control RNAi, suggesting that *nhr-67* works to limit these genes' expression (Malin *et al*, unpublished results). In *Drosophila*, Tailless is known to function in both activating and repressive capacities[463], a duality which is probably conserved[471]. As a master regulator of linker cell migration, *nhr-67* could be responsible for repressing death effectors during migration. Additionally, it is possible that NHR-67 functions at least in part to tune the levels of LET-70 and other proteasomal degradation machinery components, perhaps to ensure proper stoichiometry of components or to prevent induction of compensatory responses that would promote linker cell survival.

7 Discussion and concluding remarks

The work I have presented here significantly advances our understanding of the regulatory mechanisms governing the death of the linker cell. Linker cell death appears to require several parallel instigating lines of input. The heterochronic transcription factor LIN-29 may provide temporal information. The EGL-20/Wnt and LIN-44/Wnt pathways provide spatial input, and the Hox protein NOB-1 regulates the linker cell's responsiveness to these Wnt signals. These temporal and spatial inputs converge onto the activity of the heat shock factor HSF-1, which induces the transcription of a set of genes, possibly including components of the ubiquitin-proteasome machinery, necessary to kill the linker cell. This developmental function of HSF-1 exists in competition with its heat shock role, and the MAPKK SEK-1 functions upstream of HSF-1 to promote its developmental function, possibly by curtailing its heat shock role. A histone H3K4 methyltransferase complex structured around the catalytic SET-16/MLL subunit also promotes the transcription of ubiquitin-proteasome genes and possibly others. In parallel, the nuclear hormone receptor NHR-67 promotes linker cell death through less clear mechanisms. These pathways are summarized in Figure 20.

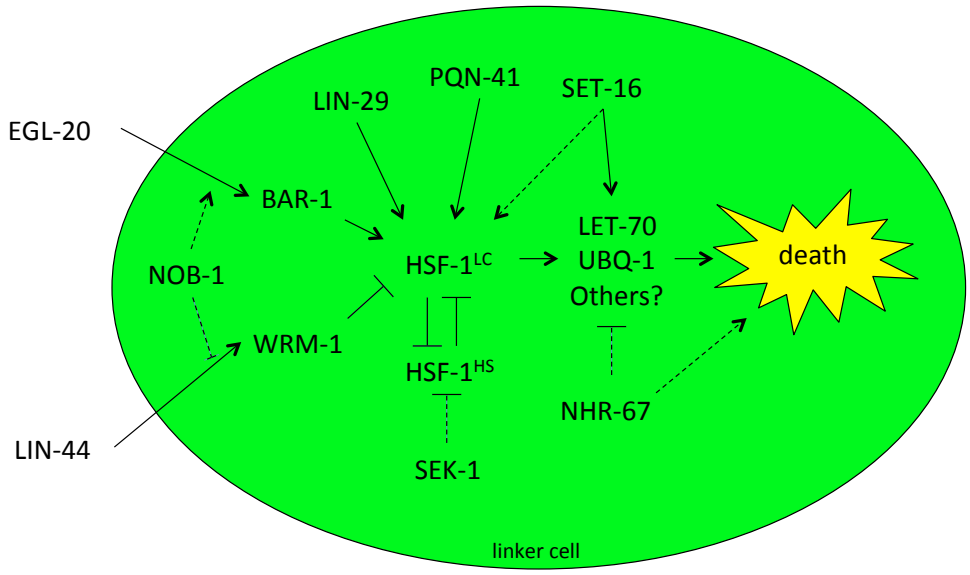

Figure 20: Current model of linker cell death regulatory mechanisms. Dashed arrows represent less clear interactions. See text for details.

Clearly, my work raises many questions concerning how these players interact with each other to promote linker cell death. Below I will summarize a few of the major questions remaining and outline possibilities and prospects for addressing them.

7.1 How does *nob-1* regulate Wnt signaling from within the linker cell?

As mentioned previously, *nob-1* functions genetically upstream of Wnt signaling to promote linker cell death. Because *nob-1* functions in the linker cell, the most likely possibility is that *nob-1* controls the expression of receptive Wnt components. Knowing which Wnt pathway, EGL-20 or LIN-44, *nob-1* primarily regulates would facilitate this task. Preliminary data suggests that induction of *hsp-16.2*::ΔN-BAR-1 cannot rescue the *nob-1* mutant phenotype, and that *nob-1* therefore likely does not function to allow BAR-

1 accumulation. First, I will attempt to confirm this result. If correct, this conclusion would suggest that *nob-1* functions instead to curtail the linker cell's responsiveness to WRM-1. Since Hox genes have previously been implicated in regulating the expression of Frizzled Wnt receptors[381], I will test whether *nob-1* controls the expression of *mig-1* or *cfz-2* using the same single molecule fluorescent *in situ* hybridization (smFISH) that was previously used to investigate expression of Frizzled genes in *C. elegans*[381,382]. In parallel, I will also test whether *nob-1* controls the expression of *lin-17* or *mom-5*, as it is formally possible that *nob-1* acts on both arms of the linker cell death Wnt pathway. *nob-1* may also control the expression or activity of receptive Wnt components downstream of Wnt receptors, although such a role has not yet been described in *C. elegans*. If the studies of *nob-1* control of Frizzled expression are not instructive, however, finding other possible targets of *nob-1* will be challenging.

Finally, it may be possible to identify NOB-1 binding regions or motifs within the Frizzled genes, using promoter deletion studies and electrophoretic mobility shift assays (EMSA). Candidate sequences similar to the canonical *Drosophila* Abd-B binding site[472], TTTATGGC, are present only a few times in each *C. elegans* Frizzled gene, although the actual NOB-1 binding site may differ from that of its fly cousin. If *nob-1* does directly control expression of Frizzled genes, the temporal dynamics of its control will be interesting to observe, and may raise the question of what, in turn, controls the action of *nob-1*, as no other linker cell death genes whose phenotypes can be suppressed by *lin-44* mutation are known.

7.2 What is the role of kinases in regulating HSF-1 in the linker cell?

Phosphorylation represents one of the main modes of HSF-1 regulation in multicellular eukaryotes (see section 5.1). Therefore, the involvement of both *sek-1* and *hsf-1* in linker cell death, as well as their striking genetic interactions, raises the possibility that a MAPK cascade involving SEK-1 phosphorylates HSF-1, either to promote its linker cell death role or to repress its heat shock role. Because the HSF-1 C-terminus is much less conserved at the primary sequence level than its N-terminus, mapping potential phosphorylation sites by homology to known *Drosophila* and mammalian sites is difficult. Furthermore, the HSF-1 C-terminus, depending on how it is defined, can harbor as many as 20 serine and threonine residues, as well as 3 tyrosine residues, making a systematic mutagenic study of potential phosphorylation sites laborious. One avenue for narrowing the range of possibilities would be to immunoprecipitate the rescuing GFP-tagged HSF-1 protein from wild-type and *sek-1* mutants and to identify differentially phosphorylated sites by mass spectrometry of tryptic fragments[473]. A possible drawback of this method is that obtaining enough material would likely require starting with whole worms, which may obscure the relevant modification sites if they are rarely used outside of the linker cell. Still, if a manageable number of such sites is identified, one might envision then studying the effect of phosphomimetic or unphosphorylatable HSF-1 mutants on both linker cell death and on the heat shock response in wild-type, *sek-1*, and *hsf-1* mutants.

A second question regarding SEK-1's action is what kinases it works through, or with, if any. Blum *et al*., in a candidate screen of single genetic mutants, did not identify any other kinases involved in linker cell death[229]. I have begun to examine the possibility

of redundancy at other levels of the MAPK cascade. In other contexts, SEK-1 is known to function directly through the p38-like MAPK PMK-1[474,475], which is transcribed in an operon along with two neighboring p38-like paralogs, *pmk-2* and *pmk-3*. I have found that *pmk-2(qd279qd171)pmk-1(km25)* double mutants have a weak linker cell death defect (15%, n=72), which can be enhanced by RNAi against the third *C. elegans* p38 homolog, *pmk-3* (25%, n=88). Thus, in the linker cell, SEK-1 may function partially redundantly through the three p38 homologs.

In preliminary studies using *hsf-1(sy441)* and a weak *sek-1* allele as sensitizing backgrounds for the identification of other kinase genes, I found that a double *dlk-1(tm4024); sek-1(km4)* mutant exhibits a dramatic enhancement (67%, n=66) over the single *sek-1(km4)* mutant phenotype (21%, n>87). In the worm, *dlk-1* encodes a dual leucine zipper kinase, which is thought to act as a MAPKKK. DLK-1 has never been shown to work through SEK-1; rather, it is thought to work through the MAPKK MKK-4[476,477]. Intriguingly, however, DLK-1 and MKK-4 appear to work through the MAPK PMK-3, which may itself have a role in the linker cell death (see above). Further, DLK-type kinases have been implicated in axonal degeneration mediated by the TIR-1 homolog Sarm1[186]. These results show that additional kinases, which may function with SEK-1 or act in parallel MAPK cascades to promote linker cell death, remain to be found, and may also function through HSF-1. Additionally, given that HSF-1 can be both positively and negatively regulated by phosphorylation, kinase pathways that inhibit linker cell death may exist. Given the centrality of phosphorylation in regulating HSF-1, characterizing the complete set of involved kinases may prove crucial in understanding how HSF-1's role in linker cell death is specified.

7.3 What transcriptional programs kill the linker cell?

The pathways known to control linker cell death are largely transcriptional. LIN-29, HSF-1, NOB-1, and NHR-67 are all DNA-binding transcription factors. MAPK pathways, of which SEK-1 is a member, often function to regulate the activity of transcription factors, and β-catenin and MLL are known transcriptional co-activators. At least one isoform of the protein of unknown function, PQN-41, is an ubiquitously expressed, nuclear polyglutamine protein, making it, too, a good candidate for being a transcriptional regulator[478-480]. In fact, the only genes we know to be transcriptionally induced in the linker cell before death are those encoding members of the ubiquitin proteasome machinery, which may be controlled by Wnts, HSF-1, the SET-16 complex, NHR-67, and minorly by LIN-29 (Jennifer Zuckerman-Malin, unpublished data). However, precocious linker-cell expression of even several members of the ubiquitin-proteasome machinery fails to induce an early death, nor does ectopic expression of these components in other cells induce death (Jennifer Zuckerman-Malin, unpublished data). Therefore, other induced genes remain to be discovered.

To identify genes that are transcriptionally induced in the linker at the time of death, I have developed a method to isolate intact linker cells from large numbers of worms (Appendix I). This method should allow a temporally resolved characterization of the linker cell transcriptome in any desired genetic background using high throughput sequencing of cDNA (RNAseq). At a minimum, the transcriptomes of wild-type linker cells from much before and just before death can be compared, and one can imagine sequencing the transcriptomes of linker cells from *bar-1, lin-29,* and *hsf-1* mutants, at a minimum.

To fully elucidate which genes *set-16* controls to promote linker cell death, one would have to consider two parallel approaches. Firstly, one might want to sort linker cells (Appendix 1) from wild-type animals and from animals that have been fed *set-16* RNAi, and perform RNA-seq transcriptome characterization. Secondly, using an analogous method, one might want to perform chromatin immunoprecipitation followed by high throughput sequencing (ChIP-seq) against SET-16::GFP on sorted linker cells or linker cell nuclei. While the techniques available are likely be a major hurdle in the latter experiment, recent advances on performing ChIP-seq on genetically labeled, cross-linked, and sorted nuclei might be a fruitful starting point[481], because one could use an arbitrarily large number of worms and collect material over the course of several preparations to obtain enough for ChIP-seq.

7.4 Why linker cell death?

Why would animals have evolved what seems to be an entirely separate cell death program in addition to apoptosis? The precise lineage of the worm tells us that the linker cell is the longest-lived cell to die, living almost two full days before dying. The linker cell is also one of very few fully differentiated cells to die a natural death, and one of the largest. Most other cells die shortly after their birth as relatively small, undifferentiated daughters of blast cells. Perhaps, therefore, cells that have accumulated enough functional machinery or are simply larger require other mechanisms for efficient death. Indeed, as discussed previously, inducing caspase-dependent death in the very large body wall muscle of hatched *C. elegans* larvae resulted in a necrotic, vacuolated morphology, whereas inducing death in these cells in embryos, where they are smaller, resulted in a more classical refractile death[216]. Alternatively, engulfing cells may have different

requirements for the kinds of corpses they are able to process. Supporting this idea is the fact that linker cell death seems to be accompanied by an entirely novel engulfment pathway. Indeed, doubly mutating both engulfment pathways has very little effect on linker cell death, and the cloacal linker cell corpse is not ringed by CED-1::GFP, as are corpses of any other apoptotic cells. Further, when linker cells migrated incorrectly and die, corpse ringing with CED-1 can be observed but is often slower than for apoptotic corpses and incomplete[224]. In contrast, apoptotic corpses almost always exhibit fully encircling CED-1[482]. The difference suggests some incompatibility between linker cell death and classical engulfment. How effective the linker cell engulfment pathway would be at engulfing an apoptotic corpse is unknown. These questions might be answered in the worm by examining the consequences of inducing apoptosis in the linker cell. Would it be killed efficiently? Would it be engulfed properly, and by the correct cells? Would the male be fertile? Answers to these questions might provide some guidance as to where to look for linker-cell-death-like processes in vertebrates.

7.5 Closing remarks

Although we likely still know little regarding what actually kills the linker cell, mechanisms governing death initiation are arguably of equal pathological importance than the details of the execution. Indeed, Apaf1 and caspases are seldom directly mutated in cancer, and Bcl-2 lesions promote only a small subset of all cancers. Rather, most cancers seem to dysregulate the mechanisms that initiate apoptosis. One of the many physiological functions of p53, the most commonly mutated gene in cancer, is to induce the transcription of a variety of pro-apoptotic BH3-only-domain proteins, much as most *C. elegans* cells induce *egl-1* transcription to die. In another example, one physiological

function of EGF signaling in normal breast tissue is to upregulate the anti-apoptotic Bcl-2-like protein Mcl-1. While Mcl-1 was identified in a myeloid cell leukemia, Mcl-1 mutations are typically not found in breast cancer. Rather, activating EGFR mutations define a subset of breast cancer, which inhibit apoptosis through inappropriate upregulation of Mcl-1. In a similar way, if a linker-cell-death-like program is to be relevant in human pathology, its regulatory mechanisms may provide crucial therapeutic insights that may be hard to glean from the execution machinery alone.

8 Appendix – A method for collecting rare cell populations in *C. elegans*

In mammalian systems, and especially in the hematopoietic lineage, obtaining differential transcriptomics data is, if not straightforward, then at least fairly common. One obtains the cell population of interest, extracts RNA, and then characterizes that RNA using microarrays of RNA-seq. Two classes of methods have been developed to obtain RNA from defined cell populations. In the first, one obtains the desired amount of tissue, dissociates the tissue into a single-cell suspension, and then sorts the desired cell population based on its expression of certain markers, through magnetic (MACS) and/or fluorescence-assisted cell sorting (FACS) methods. In the second, RNAs from a genetically defined cell population are obtained using genetically-encoded affinity-tagging of RNA or RNA-binding proteins. The latter method has been adapted in *C. elegans* with varying degrees of success, but the linker cell presents a unique challenge: to date, no reporter exists that uniquely labels the linker cell in a mixed population of hermaphrodites and males, which would be necessary to harvest cells in sufficient quantities. Our best reporter, the *mig-24* promoter, also labels the hermaphrodite distal tip cells[234], and although a temperature-sensitive strain doubly mutant for two sex-determination genes, *tra-2(ar221)*; *xol-1(y9)*, grows as a nearly 100% XX male population at 25C, I found that this strain grows too slowly and is too sick to be of use, especially if I wanted to cross linker-cell-death mutants into this background. Therefore, I chose to explore the possibility of adapting a cell sorting method to isolate large numbers of linker cells for transcriptional profiling.

I began by creating a strain in which the linker cell would be uniquely labeled in a mixed population of hermaphrodites and males. I integrated an array harboring two reporter constructs: 1.2-kb-*mig-24*p::Venus, which, as discussed previously, labels the linker cell and the hermaphrodite distal tip cells, and 2-kb-*nhr-67*p::mCherry, which strongly labels the linker cell and weakly labels a few neurons in the head of post-embryonic animals of both sexes [467]. These fluorescent proteins' excitation and emission spectra are well separated, which enables excitation using different lasers on the FACS machine and minimizes bleed-through from one channel to the other. Further, both are bright and stable *in vivo*. I obtained two stably integrated strains with the array integrated on different chromosomes, which will enable crossing this set of markers into any single mutant genetic background. I backcrossed each integrant five times to the parent *unc-119(ed3); him-5(e1490)* and observed that the linker cell was indeed the only cell in the mixed population that was doubly labeled with Venus and mCherry, whereas the distal tip cells are strongly labeled with only Venus (Figure 21).

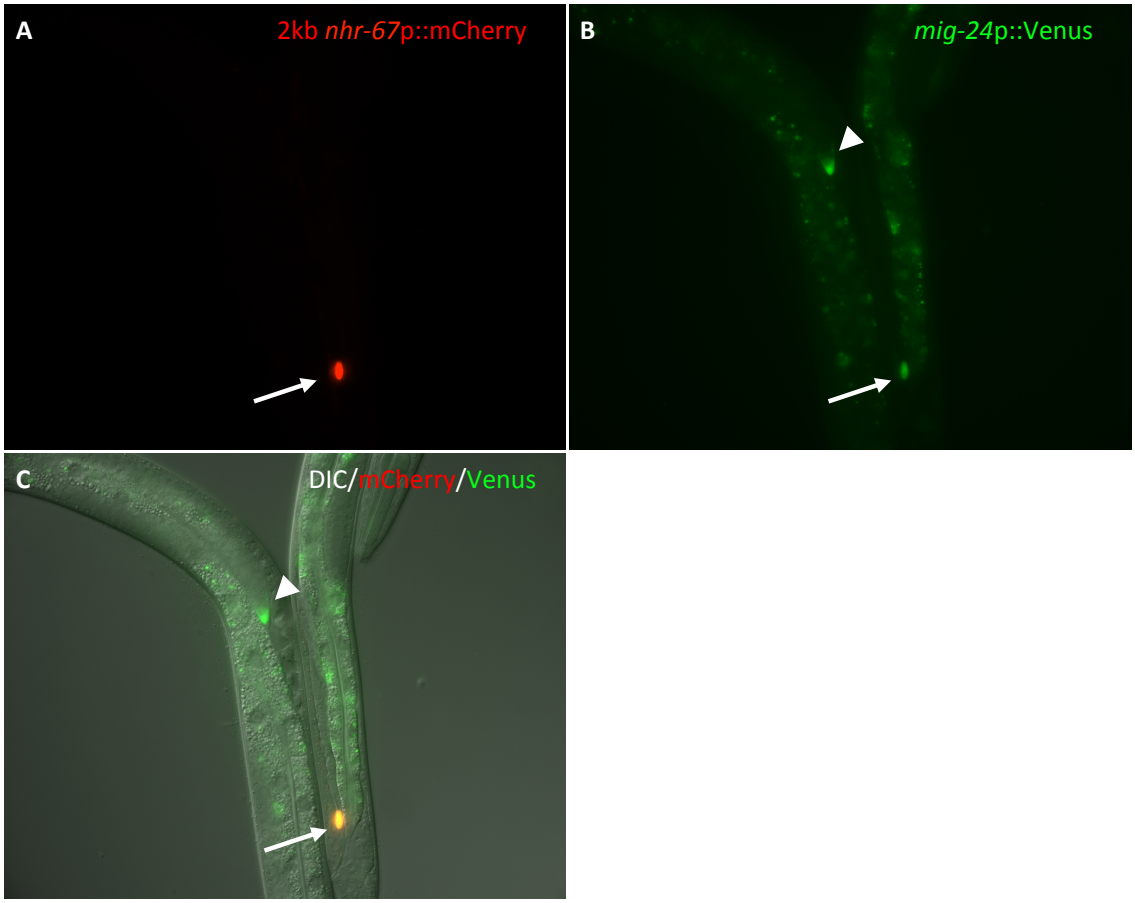

Figure 21: L4 male and hermaphrodite expressing linker cell sorting marker. Animals harboring an integrated *nhr-67*p::mCherry + *mig-24*p::Venus transgene. A. mCherry. B. Venus . C. DIC/mCherry/Venus overlay. Note that linker cell is only cell in the population that is double-labeled. Arrow, linker cell. Arrowhead, distal tip cell. Note B, the gut granule autofluorescent granules are not cells.

This expression pattern turns out to be ideal for the broader experimental design. We are interested in death-specific genes, which should be upregulated near or at the end of the linker cell's migration. However, it is possible that the linker cell would still contain migration-related transcripts at the time of its death. Distal tip cells are the close hermaphrodite functional homolog of the male linker cell, acting as the migrating leader cell for the hermaphrodite gonad and also as a germ line nurse cell, a function which the

linker cell does not perform[483]. Importantly, the distal tip cells do not die. Therefore, comparing linker cell transcripts to distal tip cell transcripts and unlabeled cell transcripts should distinguish housekeeping genes, general leader-cell-migration genes, and linker-cell-specific genes. However, as evidenced by the fact that *nhr-67* controls linker cell but not distal tip cell migration[469], the linker cell's migration program is not identical to the distal tip cell's, and the linker cell will express migration-specific genes not found in the distal tip cells. Furthermore, death-specific genes may not be present at all times within the linker cell. I will therefore include a temporal component to the experiment, by comparing linker cells collected well before death, in the early L4 period, to linker cells in the mid-late L4 period, where most linker cells have at least reached the cloaca. In this way, I will be able to distinguish genes that are upregulated in the linker cell at the time of death. Additionally, by comparing linker cells from a number of our death-mutant backgrounds, I can identify genes controlled by the transcriptional pathways I have studied. Importantly, the linker cell is constantly performing active functions requiring a number of transcriptional programs and on EM contains numerous ribosomes. The cell should therefore be amenable to gene expression profiling.

Working with Dr. Menachem Katz, a postdoctoral fellow in the lab, who wanted to isolate and transcriptionally profile his own cell population of interest, I optimized existing *C. elegans* dissociation protocols to allow for the isolation and immediate *ex vivo* sorting of a rare cell from a large number of L4 larvae. Existing methods rely, briefly, on treating the worms with a solution of SDS and 200 mM DTT to reduce the extensive cuticle crosslinks, then triturating worms in a solution containing the non-specific protease Pronase, then filtering the resulting cell soup through a 5 μm filter to obtain a

single cell suspension[484]. However, applying these methods to our cells did not yield sufficient cells for RNAseq, and we had to improve the protocol. Compared to previous methods, the key improvements have been: to extend the time of SDS-DTT treatment of the cuticle; to use two, instead of one, protease treatment steps, separated by a step where broken worm body fragments are washed with EDTA to remove Ca^{2+} from within the body, thereby loosening cadherin and integrin interactions, then washing Ca^{2+} back in to permit protease activity in the second protease treatment step; to further include EDTA in all wash steps in an effort to progressively loosen intercellular junctions; to include collagenase and elastase alongside pronase in the protease cocktail in order to better attack the different layers of the cuticle[485] and elements of the extracellular matrix; to optimize the composition of the buffers used in order to maximize protease activity[486]; to use a glass Dounce homogenizer with very slow strokes instead of trituration through a needle, which allowed starting with an arbitrarily large number of worms, as Dounce homogenizers come in a wide range of sizes, and better preservation of cellular integrity, as Dounce homogenizers have a fixed clearance between the mortar and pestle; to use slower centrifugation spins in the wash steps to allow progressive removal of subcellular debris without affecting cell yield; to use a sequence of 40, 20, and 10 μm filters after the dissociation to obtain a single cell fraction that includes large cells; and to further purify the cells on a Percoll gradient prior to sorting, removing much of the subcellular debris and allowing for enrichment of linker cells in the target fraction.

To sort the cells, I include the cell-impermeable, near-UV chromatin dye DAPI, to label damaged cells, and the cell-permeable, far-red DNA dye DRAQ5 to distinguish singly nucleated cells from large cellular aggregates as well as non-nucleated debris. I

gate first on singly nucleated, live cells on the DRAQ5 vs. DAPI plot, then, examining these events on an mCherry vs. Venus plot, I gate for linker cells and distal tip cells, and for each I then perform forward- and side-scatter-based singlet selection to ensure that a pure population is obtained. Importantly, after the first DRAQ5 vs DAPI gate, all gated populations are obvious, well-circumscribed populations of cells (Figure 22). To obtain a negatively labeled cell population, I gate on the unlabeled cells in the mCherry vs. Venus plot, then select a population with roughly the same forward-to-side-scatter ratio as distal tip cells and linker cells.

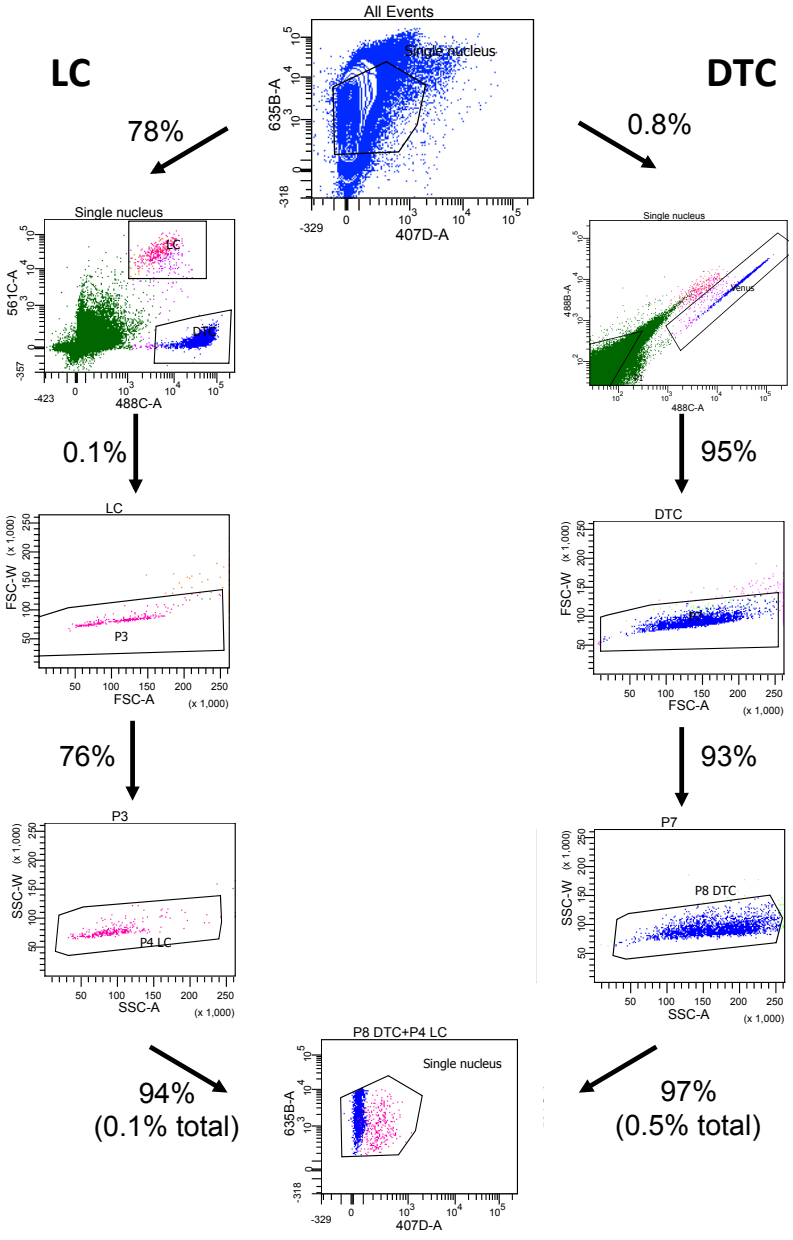

Figure 22: Gating strategy for obtaining linker cells and distal tip cells. From common DRAQ5 vs. DAPI plot, linker cell (LC) gating strategy goes to the left column, and distal tip cell (DTC) gating strategy goes to the right. Percentages are expressed as percentage of parent gate, except for last step where percentage in parentheses is percentage of initial total population. Bottom plot shows purified distal tip cells and linker cells on the same axes as original population, showing that the selected populations are uniform.

The linker cell comprises at most approximately 1 in 2500 somatic cells in a mixed *him-5(e1490)* population, where males comprise about 40% of animals. This is not counting the many germ line nuclei that are born in the L4 stage and begin to cellularize by the end of the L4 stage. Therefore, despite these protocol improvements, the sortable linker cell population remains at most 0.2% of the total cell population, still a marked improvement over the expected number. Over 5 hours of sorting, I can collect 10,000-50,000 linker cells, as well as, usually, twice to three times that number of distal tip cells, and an arbitrarily large number of non-fluorescent-protein-labeled cells. Previous methods used the Trizol reagent to collect cells for RNA extraction, but Menachem and I found that Trizol is not ideally suited to the preparation of high-quality RNA from this number of cells. Therefore, I sort my cells into the extraction buffer of a kit designed for isolating RNA from small numbers of cells (Arcturus PicoPure kit). Using this method, I am able to reliably extract low-nanogram amounts of un-degraded, high-quality RNA from this number of cells.

9 Materials and methods

Strains and alleles

C. elegans were cultured using standard methods[14], at 20C unless otherwise indicated. Temperature-sensitive mutants were hatched and synchronized as starved L1s at 15C before being transferred to plates seeded with *E. coli* OP50 and raised to adulthood at 20C, except where indicated. Most strains harbor one of two mutations that generate a high percentage of male progeny, *him-8*(*e1489*) IV or *him-5*(*e1490*) V, as well as one of two integrated linker cell markers, *qIs56*[*lag-2*::GFP] V or *nsIs65*[*mig-24*::Venus] X. Other alleles and transgenes used are as follows:

LG I: *hsf-1*(*sy441*), *lin-44*(*n1792*), *mig-1*(*e1787*), *lin-17*(*n3091*), *unc-101*(*sy216*), *gsk-3*(*nr2047*), *pop-1*(*q624*), *pop-1(q645), pop-1*(*hu9*), *daf-16*(*mu86*), *unc-13(e1091), hlh-2(bx115)*

LG II: *mig-14(ga62), lin-29*(*n333*), *lin-29*(*n546*), *mig-5*(*rh147*), *cam-1*(*gm122*), *cwn-1*(*ok546*), *rrf-3*(*pk1426*), *drSi13*[*hsf-1*p::*hsf-1*-gfp], *drSi28*[*hsf-1*p:: *hsf-1*(R145A)-GFP], *nsSi2*[*hsf-1*(R145A)-GFP], *nsSi3*[*hsf-1*(R145A)-GFP].

LG III: *pqn-41*(*ns294*), *wrm-1*(*ne1982*), *lit-1*(*t512*), *unc-32*(*e189*), *mom-4*(*ne1539*), *mom-4*(*or39*), *unc-119*(*ed4*), *nob-1(os6), egl-5(n486), lin-39(n1880), mab-5(e1239), php-3(ok919)*

LG IV: *egl-20*(*n585*), *cwn-2*(*ky756*), *cwn-2*(*ok895*), *nhr-67(pf159)*

LG V: *cfz-2*(*ok1201*), *mom-2*(*ne834*), *daf-21*(*p673*).

LG X: *bar-1*(*ga80*), *sek-1*(*ag1*), *lin-18*(*e620*).

Sequencing of *nob-1(os6)*

The *nob-1* exonic regions of *nob-1(os6)* animals were amplified by PCR in fragments and subjected to Sanger sequencing. The sequences obtained were compared to the reference genome on Wormbase. A single C to T mutation was found, which is predicted to change Arg188 to an opal stop.

Transgenic strains

Transgene	Constructs
syIs187	POPTOP::HIS-24-mCherry
mhIs9	*lin-17*::GFP
wyEx806	*lin-44*::GFP + *odr-1*p::GFP
huIs7	*hsp-16.2*::ΔN-BAR-1*, dpy-20*(+)*, mec-7*::GFP
muIs49	*egl-20*::GFP*, unc-22*(+)
sEx10067	*hsp-1*::GFP
otIs198	*hsp-16.2*::NLS-mCherry
nsIs230	*hsp-16.41*::mCherry
deIs12	10.8kb-*bar-1*p::GFP
muIs53	*hsp-16.2*::*egl-20* + *unc-22*(*as*)
nsEx2779-80	pMJK03[*swd-2.2*p::GFP] (50 ng/uL) + unc-119(+) (50 ng/uL)
nsEx3060, nsEx3061, and *nsEx3149*	pMJK15[*mig-24*pro::*C.brenn. swd-2.2::SL2-mCherry*] (25ng/uL) + *lag-2*p::YFP (25 ng/uL) + pSL1180 (50 ng/uL)

nsEx3081, 3148	pMJK13[*mig-24*p::*rde-1*::SL2-mCherry] (50 ng/uL) + pEB30[*lag-2*::mCherry] (25 ng/uL) + pSL1180 (25 ng/uL)
nsEx3269-71	GFP-SET-16 fosmid (30 ng/μL) + *unc-119*(+) (50 ng/μL)
nsEx4592	pGO80[2.5kb *wrm*-1p::GFP], 25 ng/μL + *unc-119*(+), 75 ng/μL
nsEx4584-5	pMJK61[*mig-24*::*mig-5*B] (10 ng/μL) + pEB30[*lag-2*::mCherry] (25 ng/μL) + *odr-1*::rfp (25 ng/μL) + L4440, 40 ng/μL
nsEx4589-90	pMJK62[*mig-24*::*mig-1*B] (50 ng/μL) + pEB30[*lag-2*::mCherry] (25 ng/μL) + *odr-1*::rfp (25 ng/μL)
nsEx4591	pMJK62[*mig-24*::*mig-1*B] (25 ng/μL) + pEB30[*lag-2*::mCherry] (25 ng/μL) + *odr-1*::rfp (25 ng/μL)
nsEx4586-8	pMJK60[*mig-24*::HSF-1] (1 ng/μL) + pEB30[*lag-2*::mCherry] (25 ng/μL) + *odr-1*::rfp (25 ng/μL) + pBluescript, 49 ng/μL
nsSi2-3	MosSCI integrants of pOG124[*hsf-1*::HSF-1(R145A)-GFP*]*
nsIs346	UV/TMP integration of *mhEx127*[5kb *mig-5*p::*mig-5*A-gfp + *unc-119*], a gift of M. Herman.
nsIs495	*lin-48*p::*mCherry* (25 ng/μL) + pBluescript (75 ng/μL), a gift of L. Kutscher.
ctIs57	*nob-1*p::*nob-1::GFP* + pRF4[*rol-6(d)*]
nsEx3433, nsEx3577	*mig-24*p::*nhr-67* (10 ng/μL) + *lag-2::mCherry* (25 ng/μL) + pSL1180 (65 ng/μL).
nsEx3726,	pMJK33[*mig-24*p::*nob-1B*] (20 ng/μL) + *lag-2::mCherry* (20 ng/μL) +

3735, 3736	pSL1180 (60 ng/μL)
nsIs497	pMJK62[2kb *nhr-67::SL2-mCherry*] (25 ng/μL) + *mig-24::Venus* (20 ng/μL) + *unc-119(+)* (25 ng/μL)+ pSL1180 (30 ng/μL), integrated with UV/TMP

Scoring linker cell survival and imaging

Linker cell death was scored as previously described[229]. Briefly, worms were synchronized by treating gravid hermaphrodites with alkaline bleach and allowing the eggs to hatch in M9 medium overnight. Synchronized L1s were released onto fresh NGM plates seeded with OP50 or HT115 *E. coli* containing the RNAi clone of interest, and maintained at 20C. Animals were picked to a new plate as late L4s with a fully retracted tail tip with rays visible under the unshed L4 cuticle. Two hours later, newly molted adults were mounted on slides on 2% agarose-water pads, anaesthetized in 30 mM sodium azide or 5 mM tetramisole, and examined on a Zeiss Axioplan 2 or AxioScope A1 under Nomarski optics and widefield fluorescence at 40x or 63x. Images were acquired through a Zeiss AxioCam and the Axiovision software. The linker cell was identified by green fluorescence (from reporter transgenes) as well as by its location and morphology. A linker cell was scored as surviving if its nucleus was circular with an intact nucleolus, if the cell shape was not rounded, and if the cell had not shed any large blebs. All other cells were scored as dead or dying. Rescuing extrachromosomal arrays contained a *lag-2*p::mCherry construct, and, in an effort to prevent selection bias towards survival, males with Cherry-expressing linker cells were picked as L3s for scoring the following day as young adults, as above. Some Wnt pathway mutants exhibited two

linker cells. For these strains, animals with only one visible linker cell were picked as L3s to score the following day. Only correctly migrated cells that had reached the cloaca were used in determining survival percentages.

RNA interference

Standard feeding RNAi methods[233] were used. All RNAi clone was from the Ahringer library except *pop-1* clone, which was from the Vidal library (both libraries Source BioScience). For scoring, late L4 animals were picked from an RNAi plate, seeded with HT115 bacteria containing the clone of interest, to a fresh OP50 plate as above.

Germline transformation

Germline transformation was performed as previously described[487]. Rescuing transgenes were injected into strain OS238[*qIs56 him-5*(*e1490*)] and crossed into the relevant mutant backgrounds.

MosSCI

Two additional lines of *hsf-1*p*::*HSF-1(R145A)-GFP were generated from pOG124 (a gift of T. Lamitina), by the 'direct' method, as previously described[488]. One line failed to exhibit *bar-1* mutant suppression, but also did not enhance *hsf-1*(*sy441*) survival, suggesting it was inactive, and was therefore not used in analysis. Inserts were verified by PCR and expression of HSF-1::GFP.

Fosmid recombineering

Fosmid WRM066cA03 (containing *set-16*) was recombineered using pBALU1 according to the method of Tursun *et al*.[489].

Plasmid construction

All cDNAs amplified from mixed staged cDNA (*C. brenneri* cDNA prepared from liquid culture of *C. brenneri*).

swd-2.2 (2) RNAi clone: *swd-2.2* cDNA fragment was amplified from mixed stage cDNA using oligos 5'-TATGGATCCAACGAAGACAACGTGGAATG-3' and 5'-GAGGGATCCCAAGTGATTACGATTGTTGTGC-3', and ligated into L4440 as BamHI and KpnI fragment.

pMJK03: *swd-2.2*p:: GFP. A ~4 kb *swd-2.2* promoter fragment was amplified from genomic DNA using oligos 5'-CAGGCATGCTCTGCTTTTCTCTCGGCTTC-3' and 5'-CAGGTCGACGTTGTGTCATTTGGTTGCTG-3' and subcloned into pPD95.75 as an SphI/SalI fragment.

set-16 (2) RNAi clone: *set-16* cDNA fragment was amplified from mixed stage cDNA using oligos 5'-ACTAGTAAGAAGCAGAAAGAGCCGCGAC-3' and 5'-ACTAGTCTGGTGCTGCTCTTGTAGTAACAAC-3', cloned into L4440 SpeI site.

pMJK15: *mig-24*pro::*C.brenn. swd-2.2::SL2-mCherry.* First cloned 1.2kb *mig-24* promoter into pSM-SL2-mCherry (gift of C. Bargmann) as BamHI/KpnI fragment. Then amplified *C. brenneri swd-2.2* cDNA using oligos 5'-GGTACCCATGAATGCATCAAAAGAG-3' and 5'-GGTACCTTATTGATGCGCTTGTGCTT-3', and cloned this fragment into this vector as KpnI/KpnI fragment to make pMJK15.

pMJK13: *mig-24*pro::*rde-1::SL2-mCherry. rde-1* cDNA was amplified from phage clone yk296b10 (a gift of Y. Kohara) using oligos 5'- AGTACCCATGTCCTCGAATTTTCC-3' and 5'- CGGTACCTTATGCGAACGACATTC-3' and subcloned into pMJK15 as a KpnI/KpnI fragment, replacing the *swd-2.2* fragment in pMJK15.

pMJK33: *mig-24*p::*nob-1b.* A 1.2 kb *mig-24* promoter was amplified as an *Fse*I/*Asc*I fragment using oligos 5'- ACTGGGCCGGCCTTTATCAGTTATCAGCAAG-3' and 5'-CCATGGCGCGCCTCATTTTAATAAAATTGTGTAAG-3' and subcloned into pSM-SL2-mCherry, a gift of C. Bargmann. *NOB-1B* cDNA, a gift of W. Wood, was amplified using oligos 5'-CAAGGCGCGCCATGATTTCGGTGATGCAACAAATG-3' and 5'-CAAGTCGACTCAGTTGATCAATCGCTCGATG-3' and cloned into this vector as an *Asc*I/*Sal*I fragment to create pMJK33, in which the *NOB-1B* ATG is in frame with the endogenous *mig-24* ATG.

pMJK60: *mig-24*::*hsf-1.* A ~1.2kb *mig-24* promoter, a gift of E. Blum, was amplified as a *Pst*I/*Xma*I fragment using oligos 5'-

ACACTGCAGTTTATCAGTTATCAGCAAGCAGAGAAATG -3' and 5'-ACACCCGGGCGCCATTTTAATAAAATTGTGTAAGATG -3' and subcloned into pTB4[*vap-1*::*hsf-1*::*unc-54* 3'UTR] to generate pMJK60.

pMJK61: *mig-24*::*mig-5*B. *mig-5*B cDNA, a gift of H. Korswagen, was amplified as an *Xma*I/*Sal*I fragment using oligos 5'-AGTCCCGGGATGGAGCCGCCATGCAC-3' and 5'-ATCGTCGACCTACTGTTCTCCCCGTCGAAATC-3' and subcloned into pMJK60, to generate pMJK61.

pMJK62: *mig-24*::*mig-1*B. The *mig-24* promoter was amplified as an *Fse*I/*Asc*I fragment using oligos 5'- ACTGGGCCGGCCTTTATCAGTTATCAGCAAG-3' and 5'-CCATGGCGCGCCTCATTTTAATAAAATTGTGTAAG-3' and subcloned into pSM-SL2-mCherry, a gift of C. Bargmann. *mig-1*B cDNA, on pJRK135, also a gift from C. Bargmann, was amplified as an *Asc*I/*Eco*RI fragment using oligos 5'-TGAGGCGCGCCATGGGACCATTTCGTGGTTAC-3' and 5'-ACTGAATTCTCAAATCATATTATTAGTTCGAAACGTC-3' and subcloned into this plasmid to generate *mig-24*::*mig-1*B.

pMJK62: 2 kb *nhr-67::SL2-mCherry.* A ~2 kb *nhr-67* upstream promoter just upstream of the *nhr-67* ATG was amplified from a mixture of fosmids WRM0623aD02 and WRM0631bG05 using oligos 5'-TGTGGCCGGCCAGAAGTTAATGCCTACGTGATG-3' and 5'-

TGTGGTACCTCTTGGCGCCAGATTC-3' and cloned into pSM-SL2-mCherry, a gift of C. Bargmann, as an *Fse*I/*Kpn*I fragment, to create pMJK62.

pMJK63: 484 bp *nhr-67- pes-10 minimal::GFP:* A 192 bp "basal" *pes-10* promoter was amplified from N2 genomic DNA using oligos 5'-ACACCTGCAGGAATCGATTTTTTGCAAATTACG -3' and 5'-TGTGGATCCAATCAATGCCTGAAAGTTAAAAATTACAGTATAAAG -3' and cloned into pPD95.75 as a *Sbf*I/*Bam*HI fragment to create pMJK44. A 484 bp sequence of the *nhr-67* promoter, corresponding to the sequence deleted in *nhr-67(pf159)* [468], was amplified from pMJK62 using oligos 5'-ACTAAGCTTTGTCTATCTCTCTTCAACGAC-3' and 5'-ACTCTGCAGAAATCGAACCAAAAAACCAATATC -3' and cloned into pMJK44 as a *Hin*DIII/*Pst*I fragment to create pMJK63.

pGO80 a gift from G. Oikonomou

*mig-24*p::*nhr-67* and *lag*-2p::YFP a gift of E. Blum

mig-24::Venus a gift of K. Nishikawi

Heat shock assays

Animals were cultured on 4 cm NGM agar plates seeded with *E. coli* OP50. These plates were sealed with parafilm, placed in a water bath at the indicated temperature for the indicated time, agar face down, and subsequently returned to the 20C incubator, until animals were picked for scoring as above.

Electron microscopy

Just-molted (0-2h) *qIs56 him-5*(*e1490*)*; bar-1*(*ga80*) adult males with surviving linker cells were imaged using a Zeiss Axioplan 2 compound microscope to measure the relative location of the linker cell within the worm. Animals were then fixed, stained, embedded in resin, and sectioned using standard methods[229]. Images were acquired on a FEI TECNAI G2 Spirit BioTwin Transmission Electron Microscope with a Gatan 4K x 4K digital camera.

Protocol for linker cell isolation for FACS – one day's sorting experiment.

Preparation

Make ~30 10 cm 6x peptone plates with 1.2 g NaCl + 20 g peptone + 25 g agar per liter of medium. Seed each plate with 1.5 mL an overnight culture of NEP NA22 *E. coli* in LB, spread culture around plate so that it covers most of the plate, and incubate to dry overnight at 37C.

7d before sort

Collect worms from 4-5 6x peptone plates full of gravid hermaphrodites and eggs in M9. *C. elegans* tends to burrow into 6x peptone plates when cultured at too high density, so a strain-dependent titration of the approximate number of worms per plate should be done.

-Treat worms with alkaline bleach. All bleach treatments are as follows:

Wash worms off plates in M9 medium and into one or several 15 mL conical tubes, as needed. To obtain the maximum number of eggs, use a plastic cell lifter (Corning), with the edge flamed briefly and melted to prevent cutting into the agar, to gently scrape eggs off the plate. Wash worms once with M9. For each tube of worms collected, make up 10 mL of fresh bleaching solution as follows:

7 mL ddH_2O + 0.4 mL 10N NaOH + 2.5 mL 5% NaOCl. Resuspend worms in this solution and immediately vortex on full speed for 5 min. Then wash eggs 3 times in M9 and hatch in M9 on a rotator in a 20C environment overnight.

6 days before sort

-Seed synchronized L1s on 20-25 6x peptone plates.

3 days before sort

-Bleach synchronized gravids and eggs again. The resulting animals will form the population that will be dissociated and sorted. To date, I have sorted from a maximum of ~1.5 million mixed males and hermaphrodites in a full 5-6h day of sorting, with left over cell suspension by the end of the day. The number of animals to grow up in each two-step synchronization and expansion step will be strain-dependent.

-Preferably in the early afternoon, seed 1 to 2 2L flasks with 1L LB each and inoculate with NEP NA22.

2 days before sort

-Pour saturated overnight culture of NEP NA22 into centrifuge bottles, spin 15 min, 5000g, 4C on a pre-cooled SLA-3000-type rotor. Pour off LB supernatant.

-Place a 40 μm cup filter over a 50 mL conical tube. Gently pour the synchronized L1 population over filter and allow to drain into the tube. Rinse 15 mL tubes with M9 and pour over filter again. Add M9 to filter until the surface of the M9 just touches the bottom of the filter, and cover top of filter with the cap of the tube. Incubate for at least 15 min to allow as many L1s as possible to swim through the filter.

-Make up complete S medium. I grow ~200,000 worms in 35-40 mL of S medium in one 250 mL flask, with several flasks depending on the size of the experiment.

-For 4 flasks' worth of S medium, use a spatula to spoon 1.5L's worth (~3 centrifuge bottles) of packed NEP NA22 into the S medium, and break up into large chunks with the spatula. Then use a 25 mL serological pipette to triturate medium until no more chunks of *E. coli* settle to the bottom. This process also helps oxygenate the medium.

-Take L1 population in the 50 mL conical and split into 15 mL conicals again, spin 1 min 500g to collect. Combine L1s into one 15 mL conical and bring volume to 4 mL.

-Using a marker, draw a 5x5 grid on a 18-22 mm square coverslip. Take 5 μL of well-mixed L1 worm suspension, apply to a glass slide, cover with gridded coverslip, and

count the number of worms under a dissecting microscope. Repeat twice and average to obtain an estimate of the concentration of L1s.

-Transfer ~200,000 L1s per flask of S medium with NEP NA22. Place on a horizontal shaker at 20C and rotate at 150 rpm to keep culture aerated.

-Thaw frozen bottle of AccuMax protease solution at 4C.

1 day before sort

-Monitor culture in afternoon or evening to ensure that it does not starve. If necessary, add drops of concentrated NEP NA22 in S basal.

-Prepare SDS-DTT solution as described[484], freeze at -20C in 5 mL aliquots.

-Prepare 8L of sterile-filtered (CN high flow filters) egg buffer as described[484], but omit Ca and Mg salts. This will be the sheath fluid for sorting; bring to sorting facility for overnight degassing.

-Prepare the three dissection buffers, adjust each to ~330 mmol/kg (320-340 should be fine) on a vapor pressure osmometer.

-Buffer 1: 130 mM NaCl, 5 mM KCl, 5 mM $CaCl_2$, 50 mM HEPES pH 7.5

-Buffer 2: 130 mM NaCl, 5 mM KCl, 5 mM NaEDTA, 50 mM HEPES pH 7.5

-Buffer 3: 140 mM NaCl, 5 mM KCl, 50 mM HEPES pH 7.5

-Prepare “100%” Percoll. Mix 9 vol Percoll to 1 vol 10x PBS. Adjust osmolarity using Percoll to 330 mmol/kg. This is the “100%” Percoll.

-Prepare 65%, 35%, and 10% Percoll dilutions with Buffer 3. Mix well and store at 4C.
-Adjust osmolarity of AccuMax (Stem cell technologies) to 330 mmol/kg, return to 4C.

Day of sort

-Take 10 μL worm culture out of a flask, drop onto a plate and examine under dissecting microscope to make sure worms are at the right stage.

-Thaw aliquots of SDS-DTT solution to room temperature. Do not thaw on ice, SDS will not re-dissolve well.

-Find a P1000 pipette with very smooth action. In a 50 mL conical, taking care not to splash, add 5 mL 65% Percoll, and mark the level. Then, tilt the tube to ~45° angle, and very gently layer 5 mL of 35% Percoll on top of the 65% layer, 1 mL at a time. Using a P1000 pipette, touch the pipette tip to the side of the tube a few cm above the meniscus and depress pipette very slowly and smoothly so that the 35% Percoll trickles out at a constant rate. Aim for dispensing 1 mL in about 30s. Mark the level of the 35% Percoll. Repeat with another 5 mL of 10% Percoll. Cap the tube and gently place gradient at 4C. This takes practice – do not try for the first time on an actual sort.

-Make 10 mL protease cocktail. Bring protease powders to scale on ice. In a 15 mL conical, measure out 150 mg collagenase type 1 (Sigma), 100 mg Pronase E (Sigma), 25 mg lyophilized Elastase (Worthington). Gently add 10 mL buffer 1, cap, vortex a few times, put on ice. Vortex occasionally to break up chunks. Enzymes will go into solution over time even on ice.

-Turn on refrigerated microcentrifuge and refrigerated clinical centrifuge to cool to 4C.

-Take worm cultures and distribute into 15 mL conicals. Spin all conicals at 500g, 30s. Aspirate supernatant, combine worms into one or two conicals. Wash with ddH_2O 7-8x, spinning at 500 g for 20 s after each new wash. Combine worms into one conical, wash once again, spin 1000 g for 30 s, and take off as much supernatant as possible. Estimate pellet volume.

-Take protease cocktail off ice and onto a rotator to warm to room temp. To worm pellet, add 2x pellet volume room-temperature SDS-DTT solution, mix well, start 5 min timer. Split worm suspension into as many 2 mL microfuge tubes as needed and set on a rotator. When timer is up, quickly place tubes into the refrigerated microfuge and spin for 30 s, 1000 g. Place tubes on ice, pipette off supernatant, resuspend in ice-cold buffer 2, spin again. Wash for a total of 4 times in cold buffer 2, then wash once in cold buffer 1. Complete wash steps as quickly as possible to maximize cell viability.

-Take buffer 1 supernatant off, split 2x original pellet volume of room-temperature protease cocktail into the microfuge tubes, resuspend worms, and transfer to a 7 mL Dounce homogenizer. Rinse microfuge tubes with 1 mL protease cocktail and add to Dounce homogenizer. Pipette up and down with P1000 to mix well.

-Dounce very slowly with B-type (tight) pestle for 20 min, taking ~15 s for each downstroke and ~15 s for each upstroke, taking care not to introduce bubbles. Every 5 min, pipette up and down 10x with P1000, taking care not to introduce bubbles

-If doing for first time, monitor dissociation by briefly pipetting up and down with P1000, placing 5 μL of just-mixed worm suspension on slide, and examining under 10x brightfield.

-After 20 min, mix with P1000 and split worms into 2 mL microfuge tubes. Spin 3 min 3000g 4C, take off supernatant, wash with 1 mL cold buffer 2 per tube. To wash, disrupt pellet with tip of pipette first, then triturate gently to break apart clumps. Completely resuspending pellet is not essential. Wash a total of twice with cold buffer 2 and once with cold buffer 1.

-Add 2x original pellet volume between microfuge tubes, resuspend worms, and return to Dounce homogenizer. Dounce gently with B pestle for 20 more min with pipetting up and down with P1000 every 5 min. The length of this homogenization can vary a little bit more. Monitor as before.

-After 20 min, mix with P1000 and split worms into 2 mL microfuge tubes. Spin 3 min 3000g 4C, take off supernatant, wash with 1 mL cold buffer 2 per tube. To wash, disrupt pellet with tip of pipette first, then triturate gently to break apart clumps. Completely resuspending pellet is not essential. Wash a total of twice with cold buffer 2 and once with cold buffer 3.

-Completely resuspend in 3 mL cold AccuMax, combine in a 15 mL conical.

- Stack adapter ring, 10 μm, 20 μm, and 40 μm filters (all Pluristrainer) on top of a 50 mL conical and place on ice. Prewet filters with 0.5 mL buffer 3. Apply AccuMax cell suspension to top filter and allow to drain through, applying suction by affixing a 5 mL syringe on the adapter ring if necessary. Wash tubes with 1 mL buffer 3, apply this wash to the top filter and allow drain. Wash filters again with 1 mL buffer 3.

- Take filtered cell suspension and gently apply it to cold gradient as before.

-Spin on a refrigerated swinging-bucket clinical centrifuge with precooled tube adapters for 20 min at 400 g. Set to lowest possible acceleration and deceleration settings. Removing the brake adds 10-15 min to spin time.

- Gently remove gradient from centrifuge, collect 35%-65% interface with P1000 and place into a new 15 mL conical. I usually collect this fraction in 3-4 mL, as well as the

65% pellet and the 10%-35% interface, each into separate tubes, in case there is left over time on the sorter, although the 35%-65% interface is most enriched in linker cells and many more linker cells will be sorted if this fraction can be sorted for the entire duration of the sort.

-Add cold buffer 3 to all tubes up to 15 mL, spin in cold swinging-bucket centrifuge for 8 min, 2000 g, with acceleration and break on.

-During spin, prepare a few FACS tubes of 600-900 μL Trizol LS (Invitrogen) and a few siliconized microfuge tubes of 135 μL Extraction Buffer from Arcturus PicoPure RNA extraction kit. Number of tubes depends on number of cells expected; I usually bring around 9 of each.

-Remove most of supernatant, resuspend cell pellet in 1-2 mL cold buffer 3.

-Add DRAQ5 (Thermo) to 5 μM and DAPI to 0.5 μg/mL, mix gently, place in ice and cover. Bring stained cell suspension to sorting facility in ice.

-Establish gates to sort single live cells (DRAQ5 med/DAPI-). From these, gate on linker cells (Cherry+/Venus+ in *nsIs497*), distal tip cells (Cherry-/Venus+ in *nsIs497*), and negative controls (Cherry-/Venus-). Use doublet discrimination gates on forward scatter and side scatter plots.

-Linker cells are usually rare enough that 1-3 tubes of 135 μL Arcturus picopure extraction buffer can each be filled with 10,000 linker cells. I collect an equivalent number of tubes of distal tip cells and negative control cells, which are more abundant, and once those are exhausted, I collect the more abundant populations in Trizol. Every 10-15 min, vortex and spin down collection tubes.

-After sort, process RNA using Arcturus kit. Incubate tubes at 42C for 30 min, then spin 3000g 2min, transfer supernatant to new tube, and freeze at -80C. Freeze Trizol tubes at -80C.

-Follow directions for Arcturus Picopure extraction kit. Perform on-column DNase digestion with Qiagen RNase-free DNase set. Freeze RNA or submit directly for high throughput sequencing.

10 Bibliography

1. Maghsoudi, N., Zakeri, Z. & Lockshin, R. A. Programmed cell death and apoptosis--where it came from and where it is going: from Elie Metchnikoff to the control of caspases. *Exp. Oncol.* **34,** 146–152 (2012).

2. Clarke, P. G. H. & Clarke, S. Nineteenth century research on cell death. *Exp. Oncol.* **34,** 139–145 (2012).

3. Lockshin, R. A. & WILLIAMS, C. M. PROGRAMMED CELL DEATH--I. CYTOLOGY OF DEGENERATION IN THE INTERSEGMENTAL MUSCLES OF THE PERNYI SILKMOTH. *J. Insect Physiol.* **11,** 123–133 (1965).

4. Tata, J. R. Requirement for RNA and protein synthesis for induced regression of the tadpole tail in organ culture. *Dev Biol* **13,** 77–94 (1966).

5. Kerr, J. F., Wyllie, A. H. & Currie, A. R. Apoptosis: a basic biological phenomenon with wide-ranging implications in tissue kinetics. *Br. J. Cancer* **26,** 239–257 (1972).

6. Schweichel, J. U. & Merker, H. J. The morphology of various types of cell death in prenatal tissues. *Teratology* **7,** 253–266 (1973).

7. Ameisen, J. C. On the origin, evolution, and nature of programmed cell death: a timeline of four billion years. *Cell Death Diff.* **9,** 367–393 (2002).

8. Cowan, W. M., Fawcett, J. W., O'Leary, D. D. & Stanfield, B. B. Regressive events in neurogenesis. *Science* **225,** 1258–1265 (1984).

9. Rubel, E. W., Smith, D. J. & Miller, L. C. Organization and development of brain stem auditory nuclei of the chicken: ontogeny of n. magnocellularis and n. laminaris. *J. Comp. Neurol.* **166,** 469–489 (1976).

10. Kappler, J. W., Roehm, N. & Marrack, P. T cell tolerance by clonal elimination in the thymus. *Cell* **49,** 273–280 (1987).

11. Krammer, P. H. CD95's deadly mission in the immune system. *Nature* **407,** 789–795 (2000).

12. Fuchs, Y. & Steller, H. Programmed cell death in animal development and disease. *Cell* **147,** 742–758 (2011).

13. Sulston, J. E. & Horvitz, H. R. Post-embryonic cell lineages of the nematode, Caenorhabditis elegans. *Dev Biol* **56,** 110–156 (1977).

14. Brenner, S. The genetics of Caenorhabditis elegans. *Genetics* **77,** 71–94 (1974).

15. C. elegans Sequencing Consortium. Genome sequence of the nematode C. elegans: a platform for investigating biology. *Science* **282,** 2012–2018 (1998).

16. Ellis, H. M. & Horvitz, H. R. Genetic control of programmed cell death in the nematode C. elegans. *Cell* **44,** 817–829 (1986).

17. Nehme, R. & Conradt, B. egl-1: a key activator of apoptotic cell death in C. elegans. *Oncogene* **27 Suppl 1,** S30–40 (2008).

18. Conradt, B. & Horvitz, H. R. The C. elegans protein EGL-1 is required for programmed cell death and interacts with the Bcl-2-like protein CED-9. *Cell* **93,** 519–529 (1998).

19. Yang, X., Chang, H. Y. & Baltimore, D. Essential role of CED-4 oligomerization in CED-3 activation and apoptosis. *Science* **281,** 1355–1357 (1998).

20. Yan, N. *et al.* Structure of the CED-4-CED-9 complex provides insights into programmed cell death in Caenorhabditis elegans. *Nature* **437,** 831–837 (2005).

21. Qi, S. *et al.* Crystal structure of the Caenorhabditis elegans apoptosome reveals an octameric assembly of CED-4. *Cell* **141,** 446–457 (2010).

22. Xue, D., Shaham, S. & Horvitz, H. R. The Caenorhabditis elegans cell-death protein CED-3 is a cysteine protease with substrate specificities similar to those of the human CPP32 protease. *Genes Dev* **10,** 1073–1083 (1996).

23. Hirose, T., Galvin, B. D. & Horvitz, H. R. Six and Eya promote apoptosis through direct transcriptional activation of the proapoptotic BH3-only gene egl-1 in Caenorhabditis elegans. *Proc Natl Acad Sci USA* **107,** 15479–15484 (2010).

24. Hirose, T. & Horvitz, H. R. An Sp1 transcription factor coordinates caspase-dependent and -independent apoptotic pathways. *Nature* **500,** 354–358 (2013).

25. Peden, E., Kimberly, E., Gengyo-Ando, K., Mitani, S. & Xue, D. Control of sex-specific apoptosis in C. elegans by the BarH homeodomain protein CEH-30 and the transcriptional repressor UNC-37/Groucho. *Genes Dev* **21,** 3195–3207 (2007).

26. Nehme, R. *et al.* Transcriptional upregulation of both egl-1 BH3-only and ced-3 caspase is required for the death of the male-specific CEM neurons. *Cell Death Diff.* **17,** 1266–1276 (2010).

27. Maurer, C. W., Chiorazzi, M. & Shaham, S. Timing of the onset of a developmental cell death is controlled by transcriptional induction of the C. elegans ced-3 caspase-encoding gene. *Development* **134,** 1357–1368 (2007).

28. Chiorazzi, M. *et al.* Related F-box proteins control cell death in Caenorhabditis elegans and human lymphoma. *Proc Natl Acad Sci USA* **110,** 3943–3948 (2013).

29. Barros, R., Freund, J.-N., David, L. & Almeida, R. Gastric intestinal metaplasia revisited: function and regulation of CDX2. *Trends Mol. Med.* **18,** 555–563 (2012).

30. White, J. Q. *et al.* The sensory circuitry for sexual attraction in C. elegans males. *Curr. Biol.* **17,** 1847–1857 (2007).

31. Schwartz, H. T. & Horvitz, H. R. The C. elegans protein CEH-30 protects male-

specific neurons from apoptosis independently of the Bcl-2 homolog CED-9. *Genes Dev* **21,** 3181–3194 (2007).

32. Hodgkin, J. A genetic analysis of the sex-determining gene, tra-1, in the nematode Caenorhabditis elegans. *Genes Dev* **1,** 731–745 (1987).

33. Zarkower, D. & Hodgkin, J. Molecular analysis of the C. elegans sex-determining gene tra-1: a gene encoding two zinc finger proteins. *Cell* **70,** 237–249 (1992).

34. Shaham, S., Reddien, P. W., Davies, B. & Horvitz, H. R. Mutational analysis of the Caenorhabditis elegans cell-death gene ced-3. *Genetics* **153,** 1655–1671 (1999).

35. Shaham, S. Identification of multiple Caenorhabditis elegans caspases and their potential roles in proteolytic cascades. *J. Biol. Chem.* **273,** 35109–35117 (1998).

36. Denning, D. P., Hatch, V. & Horvitz, H. R. Both the caspase CSP-1 and a caspase-independent pathway promote programmed cell death in parallel to the canonical pathway for apoptosis in Caenorhabditis elegans. *PLoS Genet* **9,** e1003341 (2013).

37. Geng, X. *et al.* Caenorhabditis elegans caspase homolog CSP-2 inhibits CED-3 autoactivation and apoptosis in germ cells. *Cell Death Diff.* **16,** 1385–1394 (2009).

38. Geng, X. *et al.* Inhibition of CED-3 zymogen activation and apoptosis in Caenorhabditis elegans by caspase homolog CSP-3. *Nat Struct Mol Biol* **15,** 1094–1101 (2008).

39. Li, X., Johnson, R. W., Park, D., Chin-Sang, I. & Chamberlin, H. M. Somatic gonad sheath cells and Eph receptor signaling promote germ-cell death in C. elegans. *Cell Death Diff.* **19,** 1080–1089 (2012).

40. Perrin, A. J. *et al.* Noncanonical control of C. elegans germline apoptosis by the insulin/IGF-1 and Ras/MAPK signaling pathways. *Cell Death Diff.* **20,** 97–107 (2013).

41. Church, D. L., Guan, K. L. & Lambie, E. J. Three genes of the MAP kinase cascade, mek-2, mpk-1/sur-1 and let-60 ras, are required for meiotic cell cycle progression in Caenorhabditis elegans. *Development* **121,** 2525–2535 (1995).

42. Rutkowski, R. *et al.* Regulation of Caenorhabditis elegans p53/CEP-1-dependent germ cell apoptosis by Ras/MAPK signaling. *PLoS Genet* **7,** e1002238 (2011).

43. Gumienny, T. L., Lambie, E., Hartwieg, E., Horvitz, H. R. & Hengartner, M. O. Genetic control of programmed cell death in the Caenorhabditis elegans hermaphrodite germline. *Development* **126,** 1011–1022 (1999).

44. Park, D., Jia, H., Rajakumar, V. & Chamberlin, H. M. Pax2/5/8 proteins promote cell survival in C. elegans. *Development* **133,** 4193–4202 (2006).

45. Fu, N. Y. *et al.* EGF-mediated induction of Mcl-1 at the switch to lactation is essential for alveolar cell survival. *Nat Cell Biol* **17,** 365–375 (2015).

46. Hall, D. H. *et al.* Neuropathology of degenerative cell death in Caenorhabditis elegans. *J. Neurosci.* **17,** 1033–1045 (1997).

47. Aballay, A. & Ausubel, F. M. Programmed cell death mediated by ced-3 and ced-4 protects Caenorhabditis elegans from Salmonella typhimurium-mediated killing. *Proc. Natl. Acad. Sci. U.S.A.* **98,** 2735–2739 (2001).

48. Salinas, L. S., Maldonado, E. & Navarro, R. E. Stress-induced germ cell apoptosis by a p53 independent pathway in Caenorhabditis elegans. *Cell Death Diff.* **13,** 2129–2139 (2006).

49. Andux, S. & Ellis, R. E. Apoptosis maintains oocyte quality in aging Caenorhabditis elegans females. *PLoS Genet* **4,** e1000295 (2008).

50. Sendoel, A., Kohler, I., Fellmann, C., Lowe, S. W. & Hengartner, M. O. HIF-1 antagonizes p53-mediated apoptosis through a secreted neuronal tyrosinase. *Nature* **465,** 577–583 (2010).

51. Schumacher, B. *et al.* C. elegans ced-13 can promote apoptosis and is induced in response to DNA damage. *Cell Death Diff.* **12,** 153–161 (2005).

52. Ye, A. L., Ragle, J. M., Conradt, B. & Bhalla, N. Differential regulation of germline apoptosis in response to meiotic checkpoint activation. *Genetics* **198,** 995–1000 (2014).

53. Ito, S., Greiss, S., Gartner, A. & Derry, W. B. Cell-nonautonomous regulation of C. elegans germ cell death by kri-1. *Curr. Biol.* **20,** 333–338 (2010).

54. Morthorst, T. H. & Olsen, A. Cell-nonautonomous inhibition of radiation-induced apoptosis by dynein light chain 1 in Caenorhabditis elegans. *Cell Death Dis* **4,** e799 (2013).

55. Syntichaki, P., Xu, K., Driscoll, M. & Tavernarakis, N. Specific aspartyl and calpain proteases are required for neurodegeneration in C. elegans. *Nature* **419,** 939–944 (2002).

56. Ellis, R. E., Jacobson, D. M. & Horvitz, H. R. Genes required for the engulfment of cell corpses during programmed cell death in Caenorhabditis elegans. *Genetics* **129,** 79–94 (1991).

57. Suzuki, J., Denning, D. P., Imanishi, E., Horvitz, H. R. & Nagata, S. Xk-related protein 8 and CED-8 promote phosphatidylserine exposure in apoptotic cells. *Science* **341,** 403–406 (2013).

58. Chen, Y.-Z., Mapes, J., Lee, E.-S., Robert Skeen-Gaar, R. & Xue, D. Caspase-mediated activation of Caenorhabditis elegans CED-8 promotes apoptosis and phosphatidylserine externalization. *Nat Commun* **4,** 2726 (2013).

59. Jagasia, R., Grote, P., Westermann, B. & Conradt, B. DRP-1-mediated

mitochondrial fragmentation during EGL-1-induced cell death in C. elegans. *Nature* **433,** 754–760 (2005).

60. Irmler, M., Hofmann, K., Vaux, D. & Tschopp, J. Direct physical interaction between the Caenorhabditis elegans 'death proteins' CED-3 and CED-4. *FEBS Letters* **406,** 189–190 (1997).

61. Huang, W. *et al.* Mechanistic insights into CED-4-mediated activation of CED-3. *Genes Dev* **27,** 2039–2048 (2013).

62. Chen, P., Rodriguez, A., Erskine, R., Thach, T. & Abrams, J. M. Dredd, a novel effector of the apoptosis activators reaper, grim, and hid in Drosophila. *Dev Biol* **201,** 202–216 (1998).

63. Muzio, M. *et al.* FLICE, a novel FADD-homologous ICE/CED-3-like protease, is recruited to the CD95 (Fas/APO-1) death--inducing signaling complex. *Cell* **85,** 817–827 (1996).

64. Boldin, M. P., Goncharov, T. M., Goltsev, Y. V. & Wallach, D. Involvement of MACH, a novel MORT1/FADD-interacting protease, in Fas/APO-1- and TNF receptor-induced cell death. *Cell* **85,** 803–815 (1996).

65. Kischkel, F. C. *et al.* Cytotoxicity-dependent APO-1 (Fas/CD95)-associated proteins form a death-inducing signaling complex (DISC) with the receptor. *EMBO J* **14,** 5579–5588 (1995).

66. Chinnaiyan, A. M., O'Rourke, K., Tewari, M. & Dixit, V. M. FADD, a novel death domain-containing protein, interacts with the death domain of Fas and initiates apoptosis. *Cell* **81,** 505–512 (1995).

67. Moreno, E., Yan, M. & Basler, K. Evolution of TNF signaling mechanisms: JNK-dependent apoptosis triggered by Eiger, the Drosophila homolog of the TNF superfamily. *Curr. Biol.* **12,** 1263–1268 (2002).

68. Dorstyn, L., Colussi, P. A., Quinn, L. M., Richardson, H. & Kumar, S. DRONC, an ecdysone-inducible Drosophila caspase. *Proc. Natl. Acad. Sci. U.S.A.* **96,** 4307–4312 (1999).

69. Quinn, L. M. *et al.* An essential role for the caspase dronc in developmentally programmed cell death in Drosophila. *J. Biol. Chem.* **275,** 40416–40424 (2000).

70. Fraser, A. G., McCarthy, N. J. & Evan, G. I. drICE is an essential caspase required for apoptotic activity in Drosophila cells. *EMBO J* **16,** 6192–6199 (1997).

71. Song, Z., McCall, K. & Steller, H. DCP-1, a Drosophila cell death protease essential for development. *Science* **275,** 536–540 (1997).

72. Rodriguez, A. *et al.* Dark is a Drosophila homologue of Apaf-1/CED-4 and functions in an evolutionarily conserved death pathway. *Nat Cell Biol* **1,** 272–279 (1999).

73. Pang, Y. *et al.* Structure of the apoptosome: mechanistic insights into activation of an initiator caspase from Drosophila. *Genes Dev* **29,** 277–287 (2015).

74. Sevrioukov, E. A. *et al.* Drosophila Bcl-2 proteins participate in stress-induced apoptosis, but are not required for normal development. - PubMed - NCBI. *Genesis* **45,** 184–193 (2007).

75. Galindo, K. A., Lu, W.-J., Park, J. H. & Abrams, J. M. The Bax/Bak ortholog in Drosophila, Debcl, exerts limited control over programmed cell death. *Development* **136,** 275–283 (2009).

76. White, K. *et al.* Genetic control of programmed cell death in Drosophila. *Science* **264,** 677–683 (1994).

77. Hay, B. A., Wassarman, D. A. & Rubin, G. M. Drosophila homologs of baculovirus inhibitor of apoptosis proteins function to block cell death. *Cell* **83,** 1253–1262 (1995).

78. Rothe, M., Pan, M. G., Henzel, W. J., Ayres, T. M. & Goeddel, D. V. The TNFR2-TRAF signaling complex contains two novel proteins related to baculoviral inhibitor of apoptosis proteins. *Cell* **83,** 1243–1252 (1995).

79. Liston, P. *et al.* Suppression of apoptosis in mammalian cells by NAIP and a related family of IAP genes. *Nature* **379,** 349–353 (1996).

80. Uren, A. G., Pakusch, M., Hawkins, C. J., Puls, K. L. & Vaux, D. L. Cloning and expression of apoptosis inhibitory protein homologs that function to inhibit apoptosis and/or bind tumor necrosis factor receptor-associated factors. *Proc. Natl. Acad. Sci. U.S.A.* **93,** 4974–4978 (1996).

81. Kaiser, W. J., Vucic, D. & Miller, L. K. The Drosophila inhibitor of apoptosis D-IAP1 suppresses cell death induced by the caspase drICE. *FEBS Letters* **440,** 243–248 (1998).

82. Hawkins, C. J., Wang, S. L. & Hay, B. A. A cloning method to identify caspases and their regulators in yeast: identification of Drosophila IAP1 as an inhibitor of the Drosophila caspase DCP-1. *Proc. Natl. Acad. Sci. U.S.A.* **96,** 2885–2890 (1999).

83. Wang, S. L., Hawkins, C. J., Yoo, S. J., Müller, H. A. & Hay, B. A. The Drosophila caspase inhibitor DIAP1 is essential for cell survival and is negatively regulated by HID. *Cell* **98,** 453–463 (1999).

84. Ryoo, H. D., Bergmann, A., Gonen, H., Ciechanover, A. & Steller, H. Regulation of Drosophila IAP1 degradation and apoptosis by reaper and ubcD1. *Nat Cell Biol* **4,** 432–438 (2002).

85. Vucic, D., Kaiser, W. J., Harvey, A. J. & Miller, L. K. Inhibition of reaper-induced apoptosis by interaction with inhibitor of apoptosis proteins (IAPs). *Proc. Natl. Acad. Sci. U.S.A.* **94,** 10183–10188 (1997).

86. Vucic, D., Kaiser, W. J. & Miller, L. K. Inhibitor of apoptosis proteins physically

interact with and block apoptosis induced by Drosophila proteins HID and GRIM. *Molecular and Cellular Biology* **18,** 3300–3309 (1998).

87. Goyal, L., McCall, K., Agapite, J., Hartwieg, E. & Steller, H. Induction of apoptosis by Drosophila reaper, hid and grim through inhibition of IAP function. *EMBO J* **19,** 589–597 (2000).

88. Clem, R. J. Baculoviruses and apoptosis: the good, the bad, and the ugly. *Cell Death Diff.* **8,** 137–143 (2001).

89. Clem, R. J., Fechheimer, M. & Miller, L. K. Prevention of apoptosis by a baculovirus gene during infection of insect cells. *Science* **254,** 1388–1390 (1991).

90. Martinou, I. *et al.* Viral proteins E1B19K and p35 protect sympathetic neurons from cell death induced by NGF deprivation. *J. Cell Biol* **128,** 201–208 (1995).

91. Sugimoto, A., Friesen, P. D. & Rothman, J. H. Baculovirus p35 prevents developmentally programmed cell death and rescues a ced-9 mutant in the nematode Caenorhabditis elegans. *EMBO J* **13,** 2023–2028 (1994).

92. Xue, D. & Horvitz, H. R. Inhibition of the Caenorhabditis elegans cell-death protease CED-3 by a CED-3 cleavage site in baculovirus p35 protein. *Nature* **377,** 248–251 (1995).

93. Zhou, Q. *et al.* Interaction of the Baculovirus Anti-apoptotic Protein p35 with Caspases. Specificity, Kinetics, and Characterization of the Caspase/p35 Complex. *Biochemistry* **37,** 10757–10765 (1998).

94. Fisher, A. J., Cruz, W. D., Zoog, S. J., Schneider, C. L. & Friesen, P. D. Crystal structure of baculovirus P35: role of a novel reactive site loop in apoptotic caspase inhibition. *EMBO J* **18,** 2031–2039 (1999).

95. Lohmann, I., McGinnis, N., Bodmer, M. & McGinnis, W. The Drosophila Hox gene deformed sculpts head morphology via direct regulation of the apoptosis activator reaper. *Cell* **110,** 457–466 (2002).

96. Robinow, S., Draizen, T. A. & Truman, J. W. Genes that induce apoptosis: transcriptional regulation in identified, doomed neurons of the Drosophila CNS. *Dev Biol* **190,** 206–213 (1997).

97. Arya, R., Sarkissian, T., Tan, Y. & White, K. Neural stem cell progeny regulate stem cell death in a Notch and Hox dependent manner. *Cell Death Diff.* (2015).

98. Bergmann, A., Agapite, J., McCall, K. & Steller, H. The Drosophila gene hid is a direct molecular target of Ras-dependent survival signaling. *Cell* **95,** 331–341 (1998).

99. Shklover, J., Levy-Adam, F. & Kurant, E. The role of Drosophila TNF Eiger in developmental and damage-induced neuronal apoptosis. *FEBS Letters* **589,** 871–879 (2015).

100. Perez-Garijo, A., Fuchs, Y. & Steller, H. Apoptotic cells can induce non-

autonomous apoptosis through the TNF pathway. *Elife* **2,** e01004 (2013).

101. Yang, Y., Hou, L., Li, Y., Ni, J. & Liu, L. Neuronal necrosis and spreading death in a Drosophila genetic model. *Cell Death Dis* **4,** e723 (2013).

102. Stennicke, H. R. & Salvesen, G. S. Caspases - controlling intracellular signals by protease zymogen activation. *Biochim. Biophys. Acta* **1477,** 299–306 (2000).

103. Yuan, J., Shaham, S., Ledoux, S., Ellis, H. M. & Horvitz, H. R. The C. elegans cell death gene ced-3 encodes a protein similar to mammalian interleukin-1 beta-converting enzyme. *Cell* **75,** 641–652 (1993).

104. Li, P. *et al.* Cytochrome c and dATP-dependent formation of Apaf-1/caspase-9 complex initiates an apoptotic protease cascade. *Cell* **91,** 479–489 (1997).

105. Fernandes-Alnemri, T., Litwack, G. & Alnemri, E. S. CPP32, a novel human apoptotic protein with homology to Caenorhabditis elegans cell death protein Ced-3 and mammalian interleukin-1 beta-converting enzyme. *J. Biol. Chem.* **269,** 30761–30764 (1994).

106. Srinivasula, S. M., Ahmad, M., Fernandes-Alnemri, T. & Alnemri, E. S. Autoactivation of procaspase-9 by Apaf-1-mediated oligomerization. *Mol Cell* **1,** 949–957 (1998).

107. Yu, X. *et al.* A structure of the human apoptosome at 12.8 A resolution provides insights into this cell death platform. *Structure* **13,** 1725–1735 (2005).

108. Sentman, C. L., Shutter, J. R., Hockenbery, D., Kanagawa, O. & Korsmeyer, S. J. bcl-2 inhibits multiple forms of apoptosis but not negative selection in thymocytes. *Cell* **67,** 879–888 (1991).

109. Tsujimoto, Y. & Croce, C. M. Analysis of the structure, transcripts, and protein products of bcl-2, the gene involved in human follicular lymphoma. *Proc. Natl. Acad. Sci. U.S.A.* **83,** 5214–5218 (1986).

110. Boise, L. H. *et al.* bcl-x, a bcl-2-related gene that functions as a dominant regulator of apoptotic cell death. *Cell* **74,** 597–608 (1993).

111. Kozopas, K. M., Yang, T., Buchan, H. L., Zhou, P. & Craig, R. W. MCL1, a gene expressed in programmed myeloid cell differentiation, has sequence similarity to BCL2. *Proc. Natl. Acad. Sci. U.S.A.* **90,** 3516–3520 (1993).

112. Yin, X. M., Oltvai, Z. N. & Korsmeyer, S. J. BH1 and BH2 domains of Bcl-2 are required for inhibition of apoptosis and heterodimerization with Bax. *Nature* **369,** 321–323 (1994).

113. Chittenden, T. *et al.* A conserved domain in Bak, distinct from BH1 and BH2, mediates cell death and protein binding functions. *EMBO J* **14,** 5589–5596 (1995).

114. Zha, H., Aimé-Sempé, C., Sato, T. & Reed, J. C. Proapoptotic protein Bax heterodimerizes with Bcl-2 and homodimerizes with Bax via a novel domain

(BH3) distinct from BH1 and BH2. *J. Biol. Chem.* **271,** 7440–7444 (1996).

115. Huang, D. C. S., Adams, J. M. & Cory, S. The conserved N-terminal BH4 domain of Bcl-2 homologues is essential for inhibition of apoptosis and interaction with CED-4. *EMBO J* **17,** 1029–1039 (1998).

116. Vaux, D. L., Weissman, I. L. & Kim, S. K. Prevention of programmed cell death in Caenorhabditis elegans by human bcl-2. *Science* **258,** 1955–1957 (1992).

117. Garcia, I., Martinou, I., Tsujimoto, Y. & Martinou, J. C. Prevention of programmed cell death of sympathetic neurons by the bcl-2 proto-oncogene. *Science* **258,** 302–304 (1992).

118. Hengartner, M. O. & Horvitz, H. R. C. elegans cell survival gene ced-9 encodes a functional homolog of the mammalian proto-oncogene bcl-2. *Cell* **76,** 665–676 (1994).

119. Oltvai, Z. N., Milliman, C. L. & Korsmeyer, S. J. Bcl-2 heterodimerizes in vivo with a conserved homolog, Bax, that accelerates programmed cell death. *Cell* **74,** 609–619 (1993).

120. Chittenden, T. *et al.* Induction of apoptosis by the Bcl-2 homologue Bak. *Nature* **374,** 733–736 (1995).

121. Vander Heiden, M. G., Chandel, N. S., Williamson, E. K., Schumacker, P. T. & Thompson, C. B. Bcl-xL regulates the membrane potential and volume homeostasis of mitochondria. *Cell* **91,** 627–637 (1997).

122. Narita, M. *et al.* Bax interacts with the permeability transition pore to induce permeability transition and cytochrome c release in isolated mitochondria. *Proc. Natl. Acad. Sci. U.S.A.* **95,** 14681–14686 (1998).

123. Du, C., Fang, M., Li, Y., Li, L. & Wang, X. Smac, a mitochondrial protein that promotes cytochrome c-dependent caspase activation by eliminating IAP inhibition. *Cell* **102,** 33–42 (2000).

124. Verhagen, A. M. *et al.* Identification of DIABLO, a mammalian protein that promotes apoptosis by binding to and antagonizing IAP proteins. *Cell* **102,** 43–53 (2000).

125. Chai, J. *et al.* Structural and biochemical basis of apoptotic activation by Smac/DIABLO. *Nature* **406,** 855–862 (2000).

126. Suzuki, Y. *et al.* A serine protease, HtrA2, is released from the mitochondria and interacts with XIAP, inducing cell death. *Mol Cell* **8,** 613–621 (2001).

127. Martins, L. M. *et al.* The serine protease Omi/HtrA2 regulates apoptosis by binding XIAP through a reaper-like motif. *J. Biol. Chem.* **277,** 439–444 (2002).

128. Verhagen, A. M. *et al.* HtrA2 promotes cell death through its serine protease activity and its ability to antagonize inhibitor of apoptosis proteins. *J. Biol. Chem.* **277,** 445–454 (2002).

129. Susin, S. A. *et al.* Bcl-2 inhibits the mitochondrial release of an apoptogenic protease. *J. Exp. Med.* **184,** 1331–1341 (1996).

130. Susin, S. A. *et al.* Molecular characterization of mitochondrial apoptosis-inducing factor. *Nature* **397,** 441–446 (1999).

131. Kluck, R. M., Bossy-Wetzel, E., Green, D. R. & Newmeyer, D. D. The release of cytochrome c from mitochondria: a primary site for Bcl-2 regulation of apoptosis. *Science* **275,** 1132–1136 (1997).

132. Liu, X., Kim, C. N., Yang, J., Jemmerson, R. & Wang, X. Induction of apoptotic program in cell-free extracts: requirement for dATP and cytochrome c. *Cell* **86,** 147–157 (1996).

133. Wang, K., Yin, X. M., Chao, D. T., Milliman, C. L. & Korsmeyer, S. J. BID: a novel BH3 domain-only death agonist. *Genes Dev* **10,** 2859–2869 (1996).

134. O'Connor, L. *et al.* Bim: a novel member of the Bcl-2 family that promotes apoptosis. *EMBO J* **17,** 384–395 (1998).

135. Wei, M. C. *et al.* tBID, a membrane-targeted death ligand, oligomerizes BAK to release cytochrome c. *Genes Dev* **14,** 2060–2071 (2000).

136. Kuwana, T. *et al.* Bid, Bax, and lipids cooperate to form supramolecular openings in the outer mitochondrial membrane. *Cell* **111,** 331–342 (2002).

137. Yu, J., Zhang, L., Hwang, P. M., Kinzler, K. W. & Vogelstein, B. PUMA induces the rapid apoptosis of colorectal cancer cells. *Mol Cell* **7,** 673–682 (2001).

138. Nakano, K. & Vousden, K. H. PUMA, a novel proapoptotic gene, is induced by p53. *Mol Cell* **7,** 683–694 (2001).

139. Oda, E. *et al.* Noxa, a BH3-only member of the Bcl-2 family and candidate mediator of p53-induced apoptosis. *Science* **288,** 1053–1058 (2000).

140. Han, J., Sabbatini, P. & White, E. Induction of apoptosis by human Nbk/Bik, a BH3-containing protein that interacts with E1B 19K. *Molecular and Cellular Biology* **16,** 5857–5864 (1996).

141. Inohara, N., Ding, L., Chen, S. & Nuñez, G. harakiri, a novel regulator of cell death, encodes a protein that activates apoptosis and interacts selectively with survival-promoting proteins Bcl-2 and Bcl-X(L). *EMBO J* **16,** 1686–1694 (1997).

142. Cheng, E. H. *et al.* BCL-2, BCL-X(L) sequester BH3 domain-only molecules preventing BAX- and BAK-mediated mitochondrial apoptosis. *Mol Cell* **8,** 705–711 (2001).

143. Llambi, F. *et al.* A unified model of mammalian BCL-2 protein family interactions at the mitochondria. *Mol Cell* **44,** 517–531 (2011).

144. Chipuk, J. E., Moldoveanu, T., Llambi, F., Parsons, M. J. & Green, D. R. The BCL-2 family reunion. *Mol Cell* **37,** 299–310 (2010).

145. Sax, J. K. *et al.* BID regulation by p53 contributes to chemosensitivity. *Nat Cell Biol* **4,** 842–849 (2002).

146. Matsuda, M. *et al.* Protective activity of adult T cell leukemia-derived factor (ADF) against tumor necrosis factor-dependent cytotoxicity on U937 cells. *J. Immunol.* **147,** 3837–3841 (1991).

147. Hsu, H., Xiong, J. & Goeddel, D. V. The TNF receptor 1-associated protein TRADD signals cell death and NF-kappa B activation. *Cell* **81,** 495–504 (1995).

148. Micheau, O. & Tschopp, J. Induction of TNF receptor I-mediated apoptosis via two sequential signaling complexes. *Cell* **114,** 181–190 (2003).

149. Lindsten, T. *et al.* The combined functions of proapoptotic Bcl-2 family members bak and bax are essential for normal development of multiple tissues. *Mol Cell* **6,** 1389–1399 (2000).

150. Hughes, M. A. *et al.* Reconstitution of the death-inducing signaling complex reveals a substrate switch that determines CD95-mediated death or survival. *Mol Cell* **35,** 265–279 (2009).

151. Jost, P. J. *et al.* XIAP discriminates between type I and type II FAS-induced apoptosis. *Nature* **460,** 1035–1039 (2009).

152. Chávez-Galán, L., Arenas-Del Angel, M. C., Zenteno, E., Chávez, R. & Lascurain, R. Cell death mechanisms induced by cytotoxic lymphocytes. *Cell. Mol. Immunol.* **6,** 15–25 (2009).

153. Masson, D. & Tschopp, J. Isolation of a lytic, pore-forming protein (perforin) from cytolytic T-lymphocytes. *J. Biol. Chem.* **260,** 9069–9072 (1985).

154. Masson, D., Zamai, M. & Tschopp, J. Identification of granzyme A isolated from cytotoxic T-lymphocyte-granules as one of the proteases encoded by CTL-specific genes. *FEBS Letters* **208,** 84–88 (1986).

155. Masson, D. & Tschopp, J. A family of serine esterases in lytic granules of cytolytic T lymphocytes. *Cell* **49,** 679–685 (1987).

156. Darmon, A. J., Nicholson, D. W. & Bleackley, R. C. Activation of the apoptotic protease CPP32 by cytotoxic T-cell-derived granzyme B. *Nature* **377,** 446–448 (1995).

157. Yoshida, H. *et al.* Apaf1 Is Required for Mitochondrial Pathways of Apoptosis and Brain Development. *Cell* **94,** 739–750 (1998).

158. Honarpour, N. *et al.* Adult Apaf-1-deficient mice exhibit male infertility. *Dev Biol* **218,** 248–258 (2000).

159. Oppenheim, R. W. *et al.* Developing postmitotic mammalian neurons in vivo lacking Apaf-1 undergo programmed cell death by a caspase-independent, nonapoptotic pathway involving autophagy. *J Neurosci* **28,** 1490–1497 (2008).

160. Zou, H. & Niswander, L. Requirement for BMP signaling in interdigital

apoptosis and scale formation. *Science* **272,** 738–741 (1996).

161. MacDonald, B. T., Adamska, M. & Meisler, M. H. Hypomorphic expression of Dkk1 in the doubleridge mouse: dose dependence and compensatory interactions with Lrp6. *Development* **131,** 2543–2552 (2004).

162. Zuzarte-Luis, V. & Hurle, J. M. Programmed cell death in the embryonic vertebrate limb. *Semin. Cell Dev. Biol.* **16,** 261–269 (2005).

163. Fernández Terán, M. A., Hinchliffe, J. R. & Ros, M. A. Birth and death of cells in limb development: a mapping study. *Dev. Dyn.* **235,** 2521–2537 (2006).

164. Chautan, M., Chazal, G., Cecconi, F., Gruss, P. & Golstein, P. Interdigital cell death can occur through a necrotic and caspase-independent pathway. *Curr. Biol.* **9,** 967–970 (1999).

165. Oppenheim, R. W. *et al.* Programmed cell death of developing mammalian neurons after genetic deletion of caspases. *J Neurosci* **21,** 4752–4760 (2001).

166. Landmesser, L. & Pilar, G. Synapse formation during embryogenesis on ganglion cells lacking a periphery. *J. Physiol. (Lond.)* **241,** 715–736 (1974).

167. Pilar, G. & Landmesser, L. Ultrastructural differences during embryonic cell death in normal and peripherally deprived ciliary ganglia. *J. Cell Biol* **68,** 339–356 (1976).

168. McCarthy, N. J., Whyte, M. K., Gilbert, C. S. & Evan, G. I. Inhibition of Ced-3/ICE-related proteases does not prevent cell death induced by oncogenes, DNA damage, or the Bcl-2 homologue Bak. *J. Cell Biol* **136,** 215–227 (1997).

169. Ekert, P. G. *et al.* Apaf-1 and caspase-9 accelerate apoptosis, but do not determine whether factor-deprived or drug-treated cells die. *J. Cell Biol* **165,** 835–842 (2004).

170. Avery, L. & Horvitz, H. R. A cell that dies during wild-type C. elegans development can function as a neuron in a ced-3 mutant. *Cell* **51,** 1071–1078 (1987).

171. Southwell, D. G. *et al.* Intrinsically determined cell death of developing cortical interneurons. *Nature* **491,** 109–113 (2012).

172. VARFOLOMEEV, E. Targeted Disruption of the Mouse Caspase 8 Gene Ablates Cell Death Induction by the TNF Receptors, Fas/Apo1, and DR3 and Is Lethal Prenatally. *Immunity* **9,** 267–276 (1998).

173. Holler, N. *et al.* Fas triggers an alternative, caspase-8-independent cell death pathway using the kinase RIP as effector molecule. *Nat Immunol* **1,** 489–495 (2000).

174. Degterev, A. *et al.* Chemical inhibitor of nonapoptotic cell death with therapeutic potential for ischemic brain injury. *Nat Chem Biol* **1,** 112–119 (2005).

175. He, S. *et al.* Receptor interacting protein kinase-3 determines cellular necrotic

response to TNF-alpha. *Cell* **137,** 1100–1111 (2009).

176. Sun, L. *et al.* Mixed lineage kinase domain-like protein mediates necrosis signaling downstream of RIP3 kinase. *Cell* **148,** 213–227 (2012).

177. Wang, H. *et al.* Mixed Lineage Kinase Domain-like Protein MLKL Causes Necrotic Membrane Disruption upon Phosphorylation by RIP3. *Mol Cell* **54,** 133–146 (2014).

178. Pasparakis, M. & Vandenabeele, P. Necroptosis and its role in inflammation. *Nature* **517,** 311–320 (2015).

179. Mariño, G., Niso-Santano, M., Baehrecke, E. H. & Kroemer, G. Self-consumption: the interplay of autophagy and apoptosis. *Nat Rev Mol Cell Biol* **15,** 81–94 (2014).

180. Berry, D. L. & Baehrecke, E. H. Growth arrest and autophagy are required for salivary gland cell degradation in Drosophila. *Cell* **131,** 1137–1148 (2007).

181. Martin, D. N. & Baehrecke, E. H. Caspases function in autophagic programmed cell death in Drosophila. *Development* **131,** 275–284 (2004).

182. Qu, X. *et al.* Autophagy gene-dependent clearance of apoptotic cells during embryonic development. *Cell* **128,** 931–946 (2007).

183. Takács-Vellai, K. *et al.* Inactivation of the autophagy gene bec-1 triggers apoptotic cell death in C. elegans. *Curr. Biol.* **15,** 1513–1517 (2005).

184. Kroemer, G. & Levine, B. Autophagic cell death: the story of a misnomer. *Nat Rev Mol Cell Biol* **9,** 1004–1010 (2008).

185. Kanda, H., Igaki, T., Okano, H. & Miura, M. Conserved metabolic energy production pathways govern Eiger/TNF-induced nonapoptotic cell death. *Proc Natl Acad Sci USA* **108,** 18977–18982 (2011).

186. Yang, J. *et al.* Pathological Axonal Death through a MAPK Cascade that Triggers a Local Energy Deficit. *Cell* **160,** 161–176 (2015).

187. Yacobi-Sharon, K., Namdar, Y. & Arama, E. Alternative germ cell death pathway in Drosophila involves HtrA2/Omi, lysosomes, and a caspase-9 counterpart. *Dev Cell* **25,** 29–42 (2013).

188. Bloss, T. A., Witze, E. S. & Rothman, J. H. Suppression of CED-3-independent apoptosis by mitochondrial betaNAC in Caenorhabditis elegans. *Nature* **424,** 1066–1071 (2003).

189. Galvin, B. D., Kim, S. & Horvitz, H. R. Caenorhabditis elegans genes required for the engulfment of apoptotic corpses function in the cytotoxic cell deaths induced by mutations in lin-24 and lin-33. *Genetics* **179,** 403–417 (2008).

190. Clandinin, T. R., Katz, W. S. & Sternberg, P. W. Caenorhabditis elegans HOM-C genes regulate the response of vulval precursor cells to inductive signal. *Dev Biol* **182,** 150–161 (1997).

191. Anderluh, G. & Lakey, J. H. Disparate proteins use similar architectures to damage membranes. *Trends Biochem. Sci.* **33,** 482–490 (2008).

192. Reddien, P. W., Cameron, S. & Horvitz, H. R. Phagocytosis promotes programmed cell death in C. elegans. *Nature* **412,** 198–202 (2001).

193. Joshi, P. & Eisenmann, D. M. The Caenorhabditis elegans pvl-5 gene protects hypodermal cells from ced-3-dependent, ced-4-independent cell death. *Genetics* **167,** 673–685 (2004).

194. Ditzel, M. *et al.* Inactivation of effector caspases through nondegradative polyubiquitylation. *Mol Cell* **32,** 540–553 (2008).

195. Xue, D. & Horvitz, H. R. Caenorhabditis elegans CED-9 protein is a bifunctional cell-death inhibitor. *Nature* **390,** 305–308 (1997).

196. Sommer, R. J. & Sternberg, P. W. Apoptosis and change of competence limit the size of the vulva equivalence group in Pristionchus pacificus: a genetic analysis. *Curr. Biol.* **6,** 52–59 (1996).

197. Sommer, R. J. *et al.* The Pristionchus HOX gene Ppa-lin-39 inhibits programmed cell death to specify the vulva equivalence group and is not required during vulval induction. *Development* **125,** 3865–3873 (1998).

198. Driscoll, M. & Chalfie, M. The mec-4 gene is a member of a family of Caenorhabditis elegans genes that can mutate to induce neuronal degeneration. *Nature* **349,** 588–593 (1991).

199. Chalfie, M. & Wolinsky, E. The identification and suppression of inherited neurodegeneration in Caenorhabditis elegans. *Nature* **345,** 410–416 (1990).

200. Shreffler, W., Magardino, T., Shekdar, K. & Wolinsky, E. The unc-8 and sup-40 genes regulate ion channel function in Caenorhabditis elegans motorneurons. *Genetics* **139,** 1261–1272 (1995).

201. Hong, K. & Driscoll, M. A transmembrane domain of the putative channel subunit MEC-4 influences mechanotransduction and neurodegeneration in C. elegans. *Nature* **367,** 470–473 (1994).

202. Bianchi, L. *et al.* The neurotoxic MEC-4(d) DEG/ENaC sodium channel conducts calcium: implications for necrosis initiation. *Nat Neurosci* **7,** 1337–1344 (2004).

203. Wang, Y. *et al.* Neurotoxic unc-8 mutants encode constitutively active DEG/ENaC channels that are blocked by divalent cations. *J. Gen. Physiol.* **142,** 157–169 (2013).

204. Treinin, M. & Chalfie, M. A mutated acetylcholine receptor subunit causes neuronal degeneration in C. elegans. *Neuron* **14,** 871–877 (1995).

205. Xu, K., Tavernarakis, N. & Driscoll, M. Necrotic cell death in C. elegans requires the function of calreticulin and regulators of Ca(2+) release from the

endoplasmic reticulum. *Neuron* **31,** 957–971 (2001).

206. Syntichaki, P., Samara, C. & Tavernarakis, N. The vacuolar H+ -ATPase mediates intracellular acidification required for neurodegeneration in C. elegans. *Curr. Biol.* **15,** 1249–1254 (2005).

207. Xiong, Z.-G. *et al.* Neuroprotection in ischemia: blocking calcium-permeable acid-sensing ion channels. *Cell* **118,** 687–698 (2004).

208. Artal-Sanz, M., Samara, C., Syntichaki, P. & Tavernarakis, N. Lysosomal biogenesis and function is critical for necrotic cell death in Caenorhabditis elegans. *J. Cell Biol* **173,** 231–239 (2006).

209. Berger, A. J., Hart, A. C. & Kaplan, J. M. G alphas-induced neurodegeneration in Caenorhabditis elegans. *J. Neurosci.* **18,** 2871–2880 (1998).

210. Korswagen, H. C., Park, J. H., Ohshima, Y. & Plasterk, R. H. An activating mutation in a Caenorhabditis elegans Gs protein induces neural degeneration. *Genes Dev* **11,** 1493–1503 (1997).

211. Lysko, P. G., Webb, C. L., Yue, T. L., Gu, J. L. & Feuerstein, G. Neuroprotective effects of tetrodotoxin as a Na+ channel modulator and glutamate release inhibitor in cultured rat cerebellar neurons and in gerbil global brain ischemia. *Stroke* **25,** 2476–2482 (1994).

212. Ingvar, M., Morgan, P. F. & Auer, R. N. The nature and timing of excitotoxic neuronal necrosis in the cerebral cortex, hippocampus and thalamus due to flurothyl-induced status epilepticus. *Acta Neuropathol.* **75,** 362–369 (1988).

213. Huang, L. & Hanna-Rose, W. EGF signaling overcomes a uterine cell death associated with temporal mis-coordination of organogenesis within the C. elegans egg-laying apparatus. *Dev Biol* **300,** 599–611 (2006).

214. Vrablik, T. L., Huang, L., Lange, S. E. & Hanna-Rose, W. Nicotinamidase modulation of NAD+ biosynthesis and nicotinamide levels separately affect reproductive development and cell survival in C. elegans. *Development* **136,** 3637–3646 (2009).

215. Labouesse, M., Sookhareea, S. & Horvitz, H. R. The Caenorhabditis elegans gene lin-26 is required to specify the fates of hypodermal cells and encodes a presumptive zinc-finger transcription factor. *Development* **120,** 2359–2368 (1994).

216. Chelur, D. S. & Chalfie, M. Targeted cell killing by reconstituted caspases. *Proc. Natl. Acad. Sci. U.S.A.* **104,** 2283–2288 (2007).

217. Malone, C. J., Fixsen, W. D., Horvitz, H. R. & Han, M. UNC-84 localizes to the nuclear envelope and is required for nuclear migration and anchoring during C. elegans development. *Development* **126,** 3171–3181 (1999).

218. Starr, D. A. *et al.* unc-83 encodes a novel component of the nuclear envelope and is essential for proper nuclear migration. *Development* **128,** 5039–5050 (2001).

219. McGee, M. D., Rillo, R., Anderson, A. S. & Starr, D. A. UNC-83 IS a KASH protein required for nuclear migration and is recruited to the outer nuclear membrane by a physical interaction with the SUN protein UNC-84. *Mol. Biol. Cell* **17,** 1790–1801 (2006).

220. Kimble, J. & Hirsh, D. The postembryonic cell lineages of the hermaphrodite and male gonads in Caenorhabditis elegans. *Dev Biol* **70,** 396–417 (1979).

221. Hodgkin, J., Horvitz, H. R. & Brenner, S. Nondisjunction Mutants of the Nematode CAENORHABDITIS ELEGANS. *Genetics* **91,** 67–94 (1979).

222. Morran, L. T., Parmenter, M. D. & Phillips, P. C. Mutation load and rapid adaptation favour outcrossing over self-fertilization. *Nature* **462,** 350–352 (2009).

223. Kiontke, K. & Fitch, D. H. A. The phylogenetic relationships of Caenorhabditis and other rhabditids. *WormBook* 1–11 (2005). doi:10.1895/wormbook.1.11.1

224. Abraham, M. C., Lu, Y. & Shaham, S. A morphologically conserved nonapoptotic program promotes linker cell death in Caenorhabditis elegans. *Dev Cell* **12,** 73–86 (2007).

225. Ambros, V. & Horvitz, H. R. Heterochronic mutants of the nematode Caenorhabditis elegans. *Science* **226,** 409–416 (1984).

226. Rougvie, A. E. & Ambros, V. The heterochronic gene lin-29 encodes a zinc finger protein that controls a terminal differentiation event in Caenorhabditis elegans. *Development* **121,** 2491–2500 (1995).

227. Harris, D. T. & Horvitz, H. R. MAB-10/NAB acts with LIN-29/EGR to regulate terminal differentiation and the transition from larva to adult in C. elegans. *Development* **138,** 4051–4062 (2011).

228. Slack, F. J. *et al.* The lin-41 RBCC gene acts in the C. elegans heterochronic pathway between the let-7 regulatory RNA and the LIN-29 transcription factor. *Mol Cell* **5,** 659–669 (2000).

229. Blum, E. S., Abraham, M. C., Yoshimura, S., Lu, Y. & Shaham, S. Control of nonapoptotic developmental cell death in Caenorhabditis elegans by a polyglutamine-repeat protein. *Science* **335,** 970–973 (2012).

230. Osterloh, J. M. *et al.* dSarm/Sarm1 is required for activation of an injury-induced axon death pathway. *Science* **337,** 481–484 (2012).

231. Gerdts, J., Summers, D. W., Sasaki, Y., DiAntonio, A. & Milbrandt, J. Sarm1-mediated axon degeneration requires both SAM and TIR interactions. *J Neurosci* **33,** 13569–13580 (2013).

232. Nguyen, C. Q., Hall, D. H., Yang, Y. & Fitch, D. H. Morphogenesis of the Caenorhabditis elegans male tail tip. *Dev Biol* **207,** 86–106 (1999).

233. Kamath, R. S., Martinez-Campos, M., Zipperlen, P., Fraser, A. G. & Ahringer, J. Effectiveness of specific RNA-mediated interference through ingested double-

stranded RNA in Caenorhabditis elegans. *Genome Biol.* **2,** RESEARCH0002 (2001).

234. Tamai, K. K. & Nishiwaki, K. bHLH transcription factors regulate organ morphogenesis via activation of an ADAMTS protease in C. elegans. *Dev Biol* **308,** 562–571 (2007).

235. Cheng, H., He, X. & Moore, C. The Essential WD Repeat Protein Swd2 Has Dual Functions in RNA Polymerase II Transcription Termination and Lysine 4 Methylation of Histone H3. *Molecular and Cellular Biology* **24,** 2932–2943 (2004).

236. Rea, S. *et al.* Regulation of chromatin structure by site-specific histone H3 methyltransferases. *Nature* **406,** 593–599 (2000).

237. Lee, J.-H. & Skalnik, D. G. Wdr82 is a C-terminal domain-binding protein that recruits the Setd1A Histone H3-Lys4 methyltransferase complex to transcription start sites of transcribed human genes. *Molecular and Cellular Biology* **28,** 609–618 (2008).

238. Schneider, J. *et al.* Molecular regulation of histone H3 trimethylation by COMPASS and the regulation of gene expression. *Mol Cell* **19,** 849–856 (2005).

239. Vitaliano-Prunier, A. *et al.* Ubiquitylation of the COMPASS component Swd2 links H2B ubiquitylation to H3K4 trimethylation. *Nat Cell Biol* **10,** 1365–1371 (2008).

240. Sun, Z.-W. & Allis, C. D. Ubiquitination of histone H2B regulates H3 methylation and gene silencing in yeast. *Nature* **418,** 104–108 (2002).

241. Wood, A., Schneider, J., Dover, J., Johnston, M. & Shilatifard, A. The Paf1 complex is essential for histone monoubiquitination by the Rad6-Bre1 complex, which signals for histone methylation by COMPASS and Dot1p. *J. Biol. Chem.* **278,** 34739–34742 (2003).

242. Dindot, S. V., Person, R., Strivens, M., Garcia, R. & Beaudet, A. L. Epigenetic profiling at mouse imprinted gene clusters reveals novel epigenetic and genetic features at differentially methylated regions. *Genome Research* **19,** 1374–1383 (2009).

243. Venkatasubrahmanyam, S., Hwang, W. W., Meneghini, M. D., Tong, A. H. Y. & Madhani, H. D. Genome-wide, as opposed to local, antisilencing is mediated redundantly by the euchromatic factors Set1 and H2A.Z. *Proc. Natl. Acad. Sci. U.S.A.* **104,** 16609–16614 (2007).

244. Miller, T. *et al.* COMPASS: a complex of proteins associated with a trithorax-related SET domain protein. *Proc. Natl. Acad. Sci. U.S.A.* **98,** 12902–12907 (2001).

245. Hsu, D. R. & Meyer, B. J. The dpy-30 gene encodes an essential component of the Caenorhabditis elegans dosage compensation machinery. *Genetics* **137,** 999–1018 (1994).

246. Ingham, P. & Whittle, R. Trithorax: A new homoeotic mutation of Drosophila melanogaster causing transformations of abdominal and thoracic imaginal segments. *Molec. Gen. Genet.* **179,** 607–614 (1980).

247. Ingham, P. W. Differential expression of bithorax complex genes in the absence of the extra sex combs and trithorax genes. *Nature* **306,** 591–593 (1983).

248. Mozer, B. A. & Dawid, I. B. Cloning and molecular characterization of the trithorax locus of Drosophila melanogaster. *Proc. Natl. Acad. Sci. U.S.A.* **86,** 3738–3742 (1989).

249. Mazo, A. M., Huang, D. H., Mozer, B. A. & Dawid, I. B. The trithorax gene, a trans-acting regulator of the bithorax complex in Drosophila, encodes a protein with zinc-binding domains. *Proc. Natl. Acad. Sci. U.S.A.* **87,** 2112–2116 (1990).

250. Tkachuk, D. C., Kohler, S. & Cleary, M. L. Involvement of a homolog of Drosophila trithorax by 11q23 chromosomal translocations in acute leukemias. *Cell* **71,** 691–700 (1992).

251. Mohan, M., Lin, C., Guest, E. & Shilatifard, A. Licensed to elongate: a molecular mechanism for MLL-based leukaemogenesis. *Nat Rev Cancer* **10,** 721–728 (2010).

252. Milne, T. A. *et al.* MLL Targets SET Domain Methyltransferase Activity to Hox Gene Promoters. *Mol Cell* **10,** 1107–1117 (2002).

253. Nakamura, T. *et al.* ALL-1 Is a Histone Methyltransferase that Assembles a Supercomplex of Proteins Involved in Transcriptional Regulation. *Mol Cell* **10,** 1119–1128 (2002).

254. Yu, B. D., Hess, J. L., Horning, S. E., Brown, G. A. & Korsmeyer, S. J. Altered Hox expression and segmental identity in Mll-mutant mice. *Nature* **378,** 505–508 (1995).

255. Xiao, Y. *et al.* Caenorhabditis elegans chromatin-associated proteins SET-2 and ASH-2 are differentially required for histone H3 Lys 4 methylation in embryos and adult germ cells. *Proc Natl Acad Sci USA* **108,** 8305–8310 (2011).

256. Dehé, P.-M. *et al.* Protein interactions within the Set1 complex and their roles in the regulation of histone 3 lysine 4 methylation. *J. Biol. Chem.* **281,** 35404–35412 (2006).

257. Vo, L. T. A., Minet, M., Schmitter, J. M., Lacroute, F. & Wyers, F. Mpe1, a Zinc Knuckle Protein, Is an Essential Component of Yeast Cleavage and Polyadenylation Factor Required for the Cleavage and Polyadenylation of mRNA. *Molecular and Cellular Biology* **21,** 8346–8356 (2001).

258. Dichtl, B. Functions for S. cerevisiae Swd2p in 3' end formation of specific mRNAs and snoRNAs and global histone 3 lysine 4 methylation. *RNA* **10,** 965–977 (2004).

259. Tabara, H. *et al.* The rde-1 gene, RNA interference, and transposon silencing in

C. elegans. *Cell* **99,** 123–132 (1999).

260. Winston, W. M., Molodowitch, C. & Hunter, C. P. Systemic RNAi in C. elegans requires the putative transmembrane protein SID-1. *Science* **295,** 2456–2459 (2002).

261. Shih, J. D. & Hunter, C. P. SID-1 is a dsRNA-selective dsRNA-gated channel. *RNA* **17,** 1057–1065 (2011).

262. Kawabe, Y.-I., Wang, Y. X., McKinnell, I. W., Bedford, M. T. & Rudnicki, M. A. Carm1 regulates Pax7 transcriptional activity through MLL1/2 recruitment during asymmetric satellite stem cell divisions. *Cell Stem Cell* **11,** 333–345 (2012).

263. Wang, K. C. *et al.* A long noncoding RNA maintains active chromatin to coordinate homeotic gene expression. *Nature* **472,** 120–124 (2011).

264. Eisenmann, D. M. Wnt signaling. *WormBook* 1–17 (2005). doi:10.1895/wormbook.1.7.1

265. Nusse, R. & Varmus, H. E. Many tumors induced by the mouse mammary tumor virus contain a provirus integrated in the same region of the host genome. *Cell* **31,** 99–109 (1982).

266. Rijsewijk, F. *et al.* The Drosophila homology of the mouse mammary oncogene int-1 is identical to the segment polarity gene wingless. *Cell* **50,** 649–657 (1987).

267. Sharma, R. P. & Chopra, V. L. Effect of the wingless (wg1) mutation on wing and haltere development in Drosophila melanogaster. *Dev Biol* **48,** 461–465 (1976).

268. Wilcox, M. & Smith, R. J. Regenerative interactions between Drosophila imaginal discs of different types. *Dev Biol* **60,** 287–297 (1977).

269. McMahon, A. P. & Moon, R. T. Ectopic expression of the proto-oncogene int-1 in Xenopus embryos leads to duplication of the embryonic axis. *Cell* **58,** 1075–1084 (1989).

270. Thomas, K. R. & Capecchi, M. R. Targeted disruption of the murine int-1 proto-oncogene resulting in severe abnormalities in midbrain and cerebellar development. *Nature* **346,** 847–850 (1990).

271. Nusse, R. *et al.* A new nomenclature for int-1 and related genes: the Wnt gene family. *Cell* **64,** 231 (1991).

272. Petersen, C. P. & Reddien, P. W. Wnt signaling and the polarity of the primary body axis. *Cell* **139,** 1056–1068 (2009).

273. Perrimon, N. & Mahowald, A. P. Multiple functions of segment polarity genes in Drosophila. *Dev Biol* (1987). doi:10.1016/0012-1606(87)90061-3

274. Wieschaus, E. & Riggleman, R. Autonomous requirements for the segment polarity gene armadillo during Drosophila embryogenesis. *Cell* **49,** 177–184

(1987).

275. Riggleman, B., Schedl, P. & Wieschaus, E. Spatial expression of the Drosophila segment polarity gene armadillo is posttranscriptionally regulated by wingless. *Cell* **63,** 549–560 (1990).

276. Noordermeer, J., Klingensmith, J., Perrimon, N. & Nusse, R. dishevelled and armadillo act in the wingless signalling pathway in Drosophila. *Nature* **367,** 80–83 (1994).

277. van Leeuwen, F., Samos, C. H. & Nusse, R. Biological activity of soluble wingless protein in cultured Drosophila imaginal disc cells. *Nature* **368,** 342–344 (1994).

278. Peifer, M. & Wleschaus, E. The segment polarity gene armadillo encodes a functionally modular protein that is the Drosophila homolog of human plakoglobin. *Cell* **63,** 1167–1178 (1990).

279. Peifer, M., Orsulic, S., Sweeton, D. & Wieschaus, E. A role for the Drosophila segment polarity gene armadillo in cell adhesion and cytoskeletal integrity during oogenesis. *Development* **118,** 1191–1207 (1993).

280. Sanson, B., White, P. & Vincent, J. P. Uncoupling cadherin-based adhesion from wingless signalling in Drosophila. *Nature* **383,** 627–630 (1996).

281. Vinson, C. R., Conover, S. & Adler, P. N. A Drosophila tissue polarity locus encodes a protein containing seven potential transmembrane domains. *Nature* **338,** 263–264 (1989).

282. Vinson, C. R. & Adler, P. N. Directional non-cell autonomy and the transmission of polarity information by the frizzled gene of Drosophila. - PubMed - NCBI. *Nature* **329,** 549–551 (1987).

283. Bhanot, P. *et al.* A new member of the frizzled family from Drosophila functions as a Wingless receptor. *Nature* **382,** 225–230 (1996).

284. Krasnow, R. E., Wong, L. L. & Adler, P. N. Dishevelled is a component of the frizzled signaling pathway in Drosophila. *Development* **121,** 4095–4102 (1995).

285. Bhat, K. M. frizzled and frizzled 2 play a partially redundant role in wingless signaling and have similar requirements to wingless in neurogenesis. *Cell* **95,** 1027–1036 (1998).

286. Chen, C. M. & Struhl, G. Wingless transduction by the Frizzled and Frizzled2 proteins of Drosophila. *Development* **126,** 5441–5452 (1999).

287. Wehrli, M. *et al.* arrow encodes an LDL-receptor-related protein essential for Wingless signalling. *Nature* **407,** 527–530 (2000).

288. Tamai, K. *et al.* LDL-receptor-related proteins in Wnt signal transduction. *Nature* **407,** 530–535 (2000).

289. Groden, J. *et al.* Identification and characterization of the familial adenomatous

polyposis coli gene. *Cell* **66,** 589–600 (1991).

290. Kinzler, K. W. *et al.* Identification of a gene located at chromosome 5q21 that is mutated in colorectal cancers. *Science* **251,** 1366–1370 (1991).

291. Rubinfeld, B. *et al.* Association of the APC gene product with beta-catenin. *Science* **262,** 1731–1734 (1993).

292. Su, L. K., Vogelstein, B. & Kinzler, K. W. Association of the APC tumor suppressor protein with catenins. *Science* **262,** 1734–1737 (1993).

293. Munemitsu, S., Albert, I., Souza, B., Rubinfeld, B. & Polakis, P. Regulation of intracellular beta-catenin levels by the adenomatous polyposis coli (APC) tumor-suppressor protein. *Proc. Natl. Acad. Sci. U.S.A.* **92,** 3046–3050 (1995).

294. Rubinfeld, B. *et al.* Binding of GSK3beta to the APC-beta-catenin complex and regulation of complex assembly. *Science* **272,** 1023–1026 (1996).

295. Zeng, L. *et al.* The mouse Fused locus encodes Axin, an inhibitor of the Wnt signaling pathway that regulates embryonic axis formation. *Cell* **90,** 181–192 (1997).

296. Behrens, J. *et al.* Functional interaction of an axin homolog, conductin, with beta-catenin, APC, and GSK3beta. *Science* **280,** 596–599 (1998).

297. Ikeda, S. *et al.* Axin, a negative regulator of the Wnt signaling pathway, forms a complex with GSK-3beta and beta-catenin and promotes GSK-3beta-dependent phosphorylation of beta-catenin. *EMBO J* **17,** 1371–1384 (1998).

298. Molenaar, M. *et al.* XTcf-3 transcription factor mediates beta-catenin-induced axis formation in Xenopus embryos. *Cell* **86,** 391–399 (1996).

299. Behrens, J. *et al.* Functional interaction of beta-catenin with the transcription factor LEF-1. *Nature* **382,** 638–642 (1996).

300. Travis, A., Amsterdam, A., Belanger, C. & Grosschedl, R. LEF-1, a gene encoding a lymphoid-specific protein with an HMG domain, regulates T-cell receptor alpha enhancer function [corrected]. *Genes Dev* **5,** 880–894 (1991).

301. van de Wetering, M. *et al.* Armadillo coactivates transcription driven by the product of the Drosophila segment polarity gene dTCF. *Cell* **88,** 789–799 (1997).

302. Brunner, E., Peter, O., Schweizer, L. & Basler, K. pangolin encodes a Lef-1 homologue that acts downstream of Armadillo to transduce the Wingless signal in Drosophila. *Nature* **385,** 829–833 (1997).

303. Peters, J. M., McKay, R. M., McKay, J. P. & Graff, J. M. Casein kinase I transduces Wnt signals. *Nature* **401,** 345–350 (1999).

304. Aberle, H., Bauer, A., Stappert, J., Kispert, A. & Kemler, R. beta-catenin is a target for the ubiquitin-proteasome pathway. *EMBO J* **16,** 3797–3804 (1997).

305. Jiang, J. & Struhl, G. Regulation of the Hedgehog and Wingless signalling

pathways by the F-box/WD40-repeat protein Slimb. *Nature* **391,** 493–496 (1998).

306. Kitagawa, M. *et al.* An F-box protein, FWD1, mediates ubiquitin-dependent proteolysis of β-catenin. *EMBO J* **18,** 2401–2410 (1999).

307. Hart, M. *et al.* The F-box protein beta-TrCP associates with phosphorylated beta-catenin and regulates its activity in the cell. *Curr. Biol.* **9,** 207–210 (1999).

308. Cavallo, R. A. *et al.* Drosophila Tcf and Groucho interact to repress Wingless signalling activity. *Nature* **395,** 604–608 (1998).

309. Salic, A., Lee, E., Mayer, L. & Kirschner, M. W. Control of beta-catenin stability: reconstitution of the cytoplasmic steps of the wnt pathway in Xenopus egg extracts. *Mol Cell* **5,** 523–532 (2000).

310. Staal, F. J. T. & Clevers, H. C. WNT signalling and haematopoiesis: a WNT-WNT situation. *Nat. Rev. Immunol.* **5,** 21–30 (2005).

311. Callahan, C. A., Muralidhar, M. G., Lundgren, S. E., Scully, A. L. & Thomas, J. B. Control of neuronal pathway selection by a Drosophila receptor protein-tyrosine kinase family member. *Nature* **376,** 171–174 (1995).

312. Yoshikawa, S., Bonkowsky, J. L., Kokel, M., Shyn, S. & Thomas, J. B. The derailed guidance receptor does not require kinase activity in vivo. *J Neurosci* **21,** RC119 (2001).

313. Inoue, T. *et al.* C. elegans LIN-18 Is a Ryk Ortholog and Functions in Parallel to LIN-17/Frizzled in Wnt Signaling. *Cell* **118,** 795–806 (2004).

314. Lu, W., Yamamoto, V., Ortega, B. & Baltimore, D. Mammalian Ryk is a Wnt coreceptor required for stimulation of neurite outgrowth. *Cell* **119,** 97–108 (2004).

315. Wouda, R. R., Bansraj, M. R. K. S., de Jong, A. W. M., Noordermeer, J. N. & Fradkin, L. G. Src family kinases are required for WNT5 signaling through the Derailed/RYK receptor in the Drosophila embryonic central nervous system. *Development* **135,** 2277–2287 (2008).

316. Hikasa, H., Shibata, M., Hiratani, I. & Taira, M. The Xenopus receptor tyrosine kinase Xror2 modulates morphogenetic movements of the axial mesoderm and neuroectoderm via Wnt signaling. *Development* **129,** 5227–5239 (2002).

317. Forrester, W. C., Dell, M., Perens, E. & Garriga, G. A C. elegans Ror receptor tyrosine kinase regulates cell motility and asymmetric cell division. *Nature* **400,** 881–885 (1999).

318. Mikels, A. J. & Nusse, R. Purified Wnt5a protein activates or inhibits beta-catenin-TCF signaling depending on receptor context. *PLoS Biol* **4,** e115 (2006).

319. Green, J. L., Inoue, T. & Sternberg, P. W. The C. elegans ROR receptor tyrosine kinase, CAM-1, non-autonomously inhibits the Wnt pathway. *Development* **134,** 4053–4062 (2007).

320. Oishi, I. *et al.* The receptor tyrosine kinase Ror2 is involved in non-canonical Wnt5a/JNK signalling pathway. *Genes Cells* **8,** 645–654 (2003).

321. Green, J. L., Inoue, T. & Sternberg, P. W. Opposing Wnt pathways orient cell polarity during organogenesis. *Cell* **134,** 646–656 (2008).

322. Nam, J.-S., Turcotte, T. J., Smith, P. F., Choi, S. & Yoon, J. K. Mouse cristin/R-spondin family proteins are novel ligands for the Frizzled 8 and LRP6 receptors and activate beta-catenin-dependent gene expression. *J. Biol. Chem.* **281,** 13247–13257 (2006).

323. Seshagiri, S. *et al.* Recurrent R-spondin fusions in colon cancer. *Nature* **488,** 660–664 (2012).

324. de Lau, W. *et al.* Lgr5 homologues associate with Wnt receptors and mediate R-spondin signalling. *Nature* **476,** 293–297 (2011).

325. Leyns, L., Bouwmeester, T., Kim, S. H., Piccolo, S. & De Robertis, E. M. Frzb-1 is a secreted antagonist of Wnt signaling expressed in the Spemann organizer. *Cell* **88,** 747–756 (1997).

326. Wang, S., Krinks, M., Lin, K., Luyten, F. P. & Moos, M. Frzb, a secreted protein expressed in the Spemann organizer, binds and inhibits Wnt-8. *Cell* **88,** 757–766 (1997).

327. Hsieh, J.-C. *et al.* A new secreted protein that binds to Wnt proteins and inhibits their activites. *Nature* **398,** 431–436 (1999).

328. Glinka, A. *et al.* Dickkopf-1 is a member of a new family of secreted proteins and functions in head induction. *Nature* **391,** 357–362 (1998).

329. Mao, B. *et al.* LDL-receptor-related protein 6 is a receptor for Dickkopf proteins. *Nature* **411,** 321–325 (2001).

330. Bafico, A., Liu, G., Yaniv, A., Gazit, A. & Aaronson, S. A. Novel mechanism of Wnt signalling inhibition mediated by Dickkopf-1 interaction with LRP6/Arrow. *Nat Cell Biol* **3,** 683–686 (2001).

331. Semënov, M. V. *et al.* Head inducer Dickkopf-1 is a ligand for Wnt coreceptor LRP6. *Curr. Biol.* **11,** 951–961 (2001).

332. Mao, B. *et al.* Kremen proteins are Dickkopf receptors that regulate Wnt/|[beta]|-catenin signalling. *Nature* **417,** 664–667 (2002).

333. Rulifson, E. J., Wu, C. H. & Nusse, R. Pathway specificity by the bifunctional receptor frizzled is determined by affinity for wingless. *Mol Cell* **6,** 117–126 (2000).

334. Holland, J. D., Klaus, A., Garratt, A. N. & Birchmeier, W. Wnt signaling in stem and cancer stem cells. *Current Opinion in Cell Biology* **25,** 254–264 (2013).

335. Anastas, J. N. & Moon, R. T. WNT signalling pathways as therapeutic targets in cancer. *Nat Rev Cancer* **13,** 11–26 (2013).

336. Goldstein, B. Establishment of gut fate in the E lineage of C. elegans: the roles of lineage-dependent mechanisms and cell interactions. *Development* **118,** 1267–1277 (1993).

337. Thorpe, C. J., Schlesinger, A., Carter, J. C. & Bowerman, B. Wnt signaling polarizes an early C. elegans blastomere to distinguish endoderm from mesoderm. *Cell* **90,** 695–705 (1997).

338. Harterink, M. *et al.* Neuroblast migration along the anteroposterior axis of C. elegans is controlled by opposing gradients of Wnts and a secreted Frizzled-related protein. *Development* **138,** 2915–2924 (2011).

339. Whangbo, J. & Kenyon, C. A Wnt signaling system that specifies two patterns of cell migration in C. elegans. *Mol Cell* **4,** 851–858 (1999).

340. Herman, M. A. & Horvitz, H. R. The Caenorhabditis elegans gene lin-44 controls the polarity of asymmetric cell divisions. *Development* **120,** 1035–1047 (1994).

341. Korswagen, H. C., Herman, M. A. & Clevers, H. C. Distinct beta-catenins mediate adhesion and signalling functions in C. elegans. *Nature* **406,** 527–532 (2000).

342. Natarajan, L., Witwer, N. E. & Eisenmann, D. M. The divergent Caenorhabditis elegans beta-catenin proteins BAR-1, WRM-1 and HMP-2 make distinct protein interactions but retain functional redundancy in vivo. *Genetics* **159,** 159–172 (2001).

343. Kidd, A. R., Miskowski, J. A., Siegfried, K. R., Sawa, H. & Kimble, J. A beta-catenin identified by functional rather than sequence criteria and its role in Wnt/MAPK signaling. *Cell* **121,** 761–772 (2005).

344. Eisenmann, D. M., Maloof, J. N., Simske, J. S., Kenyon, C. & Kim, S. K. The beta-catenin homolog BAR-1 and LET-60 Ras coordinately regulate the Hox gene lin-39 during Caenorhabditis elegans vulval development. *Development* **125,** 3667–3680 (1998).

345. Maloof, J. N., Whangbo, J., Harris, J. M., Jongeward, G. D. & Kenyon, C. A Wnt signaling pathway controls hox gene expression and neuroblast migration in C. elegans. *Development* **126,** 37–49 (1999).

346. Ishitani, T. *et al.* The TAK1-NLK-MAPK-related pathway antagonizes signalling between beta-catenin and transcription factor TCF. *Nature* **399,** 798–802 (1999).

347. Rocheleau, C. E. *et al.* WRM-1 activates the LIT-1 protein kinase to transduce anterior/posterior polarity signals in C. elegans. *Cell* **97,** 717–726 (1999).

348. Lo, M.-C., Gay, F., Odom, R., Shi, Y. & Lin, R. Phosphorylation by the beta-catenin/MAPK complex promotes 14-3-3-mediated nuclear export of TCF/POP-1 in signal-responsive cells in C. elegans. *Cell* **117,** 95–106 (2004).

349. Phillips, B. T., Kidd, A. R., King, R., Hardin, J. & Kimble, J. Reciprocal

asymmetry of SYS-1/beta-catenin and POP-1/TCF controls asymmetric divisions in Caenorhabditis elegans. *Proc. Natl. Acad. Sci. U.S.A.* **104,** 3231–3236 (2007).

350. Bänziger, C. *et al.* Wntless, a Conserved Membrane Protein Dedicated to the Secretion of Wnt Proteins from Signaling Cells. *Cell* **125,** 509–522 (2006).

351. Siegfried, E., Chou, T. B. & Perrimon, N. wingless signaling acts through zeste-white 3, the Drosophila homolog of glycogen synthase kinase-3, to regulate engrailed and establish cell fate. *Cell* **71,** 1167–1179 (1992).

352. Pai, L. M., Orsulic, S., Bejsovec, A. & Peifer, M. Negative regulation of Armadillo, a Wingless effector in Drosophila. *Development* **124,** 2255–2266 (1997).

353. Schlesinger, A., Shelton, C. A., Maloof, J. N., Meneghini, M. & Bowerman, B. Wnt pathway components orient a mitotic spindle in the early Caenorhabditis elegans embryo without requiring gene transcription in the responding cell. *Genes Dev* **13,** 2028–2038 (1999).

354. Natarajan, L., Jackson, B. M., Szyleyko, E. & Eisenmann, D. M. Identification of evolutionarily conserved promoter elements and amino acids required for function of the C. elegans beta-catenin homolog BAR-1. *Dev Biol* **272,** 536–557 (2004).

355. Herman, M. A., Vassilieva, L. L., Horvitz, H. R., Shaw, J. E. & Herman, R. K. The C. elegans gene lin-44, which controls the polarity of certain asymmetric cell divisions, encodes a Wnt protein and acts cell nonautonomously. *Cell* **83,** 101–110 (1995).

356. Herman, M. C. elegans POP-1/TCF functions in a canonical Wnt pathway that controls cell migration and in a noncanonical Wnt pathway that controls cell polarity. *Development* **128,** 581–590 (2001).

357. Siegfried, K. R. & Kimble, J. POP-1 controls axis formation during early gonadogenesis in C. elegans. *Development* **129,** 443–453 (2002).

358. Essers, M. A. G. *et al.* Functional interaction between beta-catenin and FOXO in oxidative stress signaling. *Science* **308,** 1181–1184 (2005).

359. Pawlowski, J. E. *et al.* Liganded androgen receptor interaction with beta-catenin: nuclear co-localization and modulation of transcriptional activity in neuronal cells. *J. Biol. Chem.* **277,** 20702–20710 (2002).

360. Song, L.-N. *et al.* Beta-catenin binds to the activation function 2 region of the androgen receptor and modulates the effects of the N-terminal domain and TIF2 on ligand-dependent transcription. *Molecular and Cellular Biology* **23,** 1674–1687 (2003).

361. Kouzmenko, A. P. *et al.* Wnt/beta-catenin and estrogen signaling converge in vivo. *J. Biol. Chem.* **279,** 40255–40258 (2004).

362. Armstrong, V. J. *et al.* Wnt/beta-catenin signaling is a component of osteoblastic

bone cell early responses to load-bearing and requires estrogen receptor alpha. *J. Biol. Chem.* **282,** 20715–20727 (2007).

363. Kelly, K. F. *et al.* β-catenin enhances Oct-4 activity and reinforces pluripotency through a TCF-independent mechanism. *Cell Stem Cell* **8,** 214–227 (2011).

364. Ying, L., Mills, J. A., French, D. L. & Gadue, P. OCT4 Coordinates with WNT Signaling to Pre-pattern Chromatin at the SOX17 Locus during Human ES Cell Differentiation into Definitive Endoderm. *Stem Cell Reports* (2015). doi:10.1016/j.stemcr.2015.08.014

365. Olson, L. E. *et al.* Homeodomain-Mediated β-Catenin-Dependent Switching Events Dictate Cell-Lineage Determination. *Cell* **125,** 593–605 (2006).

366. Lengerke, C. *et al.* BMP and Wnt Specify Hematopoietic Fate by Activation of the Cdx-Hox Pathway. *Cell Stem Cell* **2,** 72–82 (2008).

367. McGinnis, W., Levine, M. S., Hafen, E., Kuroiwa, A. & Gehring, W. J. A conserved DNA sequence in homoeotic genes of the Drosophila Antennapedia and bithorax complexes. *Nature* **308,** 428–433 (1984).

368. Desplan, C., Theis, J. & O'Farrell, P. H. The Drosophila developmental gene, engrailed, encodes a sequence-specific DNA binding activity. *Nature* **318,** 630–635 (1985).

369. Fainsod, A. *et al.* The homeo domain of a murine protein binds 5' to its own homeo box. *Proc. Natl. Acad. Sci. U.S.A.* **83,** 9532–9536 (1986).

370. Desplan, C., Theis, J. & O'Farrell, P. H. The sequence specificity of homeodomain-DNA interaction. *Cell* **54,** 1081–1090 (1988).

371. Postlethwait, J. H. & Schneiderman, H. A. A clonal analysis of determination in Antennapedia a homoeotic mutant of Drosophila melanogaster. *Proc. Natl. Acad. Sci. U.S.A.* **64,** 176–183 (1969).

372. Sánchez-Herrero, E., Vernós, I., Marco, R. & Morata, G. Genetic organization of Drosophila bithorax complex. *Nature* **313,** 108–113 (1985).

373. Harding, K., Wedeen, C., McGinnis, W. & Levine, M. Spatially regulated expression of homeotic genes in Drosophila. *Science* **229,** 1236–1242 (1985).

374. Dollé, P., Izpisúa-Belmonte, J. C., Falkenstein, H., Renucci, A. & Duboule, D. Coordinate expression of the murine Hox-5 complex homoeobox-containing genes during limb pattern formation. *Nature* **342,** 767–772 (1989).

375. Graham, A., Papalopulu, N. & Krumlauf, R. The murine and Drosophila homeobox gene complexes have common features of organization and expression. *Cell* **57,** 367–378 (1989).

376. Aboobaker, A. & Blaxter, M. Hox gene evolution in nematodes: novelty conserved. *Curr. Opin. Genet. Dev.* **13,** 593–598 (2003).

377. Kalis, A. K., Murphy, M. W. & Zarkower, D. EGL-5/ABD-B plays an

instructive role in male cell fate determination in the C. elegans somatic gonad. *Dev Biol* **344,** 827–835 (2010).

378. Chisholm, A. Control of cell fate in the tail region of C. elegans by the gene egl-5. *Development* **111,** 921–932 (1991).

379. Zhao, Z. *et al.* A negative regulatory loop between microRNA and Hox gene controls posterior identities in Caenorhabditis elegans. *PLoS Genet* **6,** e1001089 (2010).

380. Cadigan, K. M., Fish, M. P., Rulifson, E. J. & Nusse, R. Wingless repression of Drosophila frizzled 2 expression shapes the Wingless morphogen gradient in the wing. *Cell* **93,** 767–777 (1998).

381. Ji, N. *et al.* Feedback Control of Gene Expression Variability in the Caenorhabditis elegans Wnt Pathway. *Cell* **155,** 869–880 (2013).

382. Mentink, R. A. *et al.* Cell intrinsic modulation of Wnt signaling controls neuroblast migration in C. elegans. *Dev Cell* **31,** 188–201 (2014).

383. Clark, S. G., Chisholm, A. D. & Horvitz, H. R. Control of cell fates in the central body region of C. elegans by the homeobox gene lin-39. *Cell* **74,** 43–55 (1993).

384. Tihanyi, B. *et al.* The C. elegans Hox gene ceh-13 regulates cell migration and fusion in a non-colinear way. Implications for the early evolution of Hox clusters. *BMC Dev. Biol.* **10,** 78 (2010).

385. Salser, S. J. & Kenyon, C. Activation of a C. elegans Antennapedia homologue in migrating cells controls their direction of migration. *Nature* **355,** 255–258 (1992).

386. Morton, E. A. & Lamitina, T. Caenorhabditis elegans HSF-1 is an essential nuclear protein that forms stress granule-like structures following heat shock. *Aging Cell* **12,** 112–120 (2013).

387. Tissières, A., Mitchell, H. K. & Tracy, U. M. Protein synthesis in salivary glands of Drosophila melanogaster: relation to chromosome puffs. *J Mol Biol* **84,** 389–398 (1974).

388. Eilers, M. & Schatz, G. Binding of a specific ligand inhibits import of a purified precursor protein into mitochondria. *Nature* **322,** 228–232 (1986).

389. Gething, M. J., McCammon, K. & Sambrook, J. Expression of wild-type and mutant forms of influenza hemagglutinin: the role of folding in intracellular transport. *Cell* **46,** 939–950 (1986).

390. Copeland, C. S., Doms, R. W., Bolzau, E. M., Webster, R. G. & Helenius, A. Assembly of influenza hemagglutinin trimers and its role in intracellular transport. *J. Cell Biol* **103,** 1179–1191 (1986).

391. Chirico, W. J., Waters, M. G. & Blobel, G. 70K heat shock related proteins stimulate protein translocation into microsomes. *Nature* **332,** 805–810 (1988).

392. Deshaies, R. J., Koch, B. D., Werner-Washburne, M., Craig, E. A. & Schekman, R. A subfamily of stress proteins facilitates translocation of secretory and mitochondrial precursor polypeptides. *Nature* **332,** 800–805 (1988).

393. Palleros, D. R., Welch, W. J. & Fink, A. L. Interaction of hsp70 with unfolded proteins: effects of temperature and nucleotides on the kinetics of binding. *Proc. Natl. Acad. Sci. U.S.A.* **88,** 5719–5723 (1991).

394. Pelham, H. R. Speculations on the functions of the major heat shock and glucose-regulated proteins. *Cell* **46,** 959–961 (1986).

395. Ellis, J. Proteins as molecular chaperones. *Nature* **328,** 378–379 (1987).

396. Rothman, J. E. Polypeptide chain binding proteins: catalysts of protein folding and related processes in cells. *Cell* **59,** 591–601 (1989).

397. Ashburner, M. & Bonner, J. J. The induction of gene activity in drosophilia by heat shock. *Cell* **17,** 241–254 (1979).

398. Parker, C. S. & Topol, J. A Drosophila RNA polymerase II transcription factor binds to the regulatory site of an hsp 70 gene. *Cell* **37,** 273–283 (1984).

399. Pelham, H. R. B. A regulatory upstream promoter element in the Drosophila Hsp 70 heat-shock gene. *Cell* **30,** 517–528 (1982).

400. Pelham, H. R. & Bienz, M. A synthetic heat-shock promoter element confers heat-inducibility on the herpes simplex virus thymidine kinase gene. *EMBO J* **1,** 1473–1477 (1982).

401. Bienz, M. & Pelham, H. R. Heat shock regulatory elements function as an inducible enhancer in the Xenopus hsp70 gene and when linked to a heterologous promoter. *Cell* **45,** 753–760 (1986).

402. Sorger, P. K. & Pelham, H. R. Purification and characterization of a heat-shock element binding protein from yeast. *EMBO J* **6,** 3035–3041 (1987).

403. Sorger, P. K. & Pelham, H. R. B. Yeast heat shock factor is an essential DNA-binding protein that exhibits temperature-dependent phosphorylation. *Cell* **54,** 855–864 (1988).

404. Perisic, O., Xiao, H. & Lis, J. T. Stable binding of Drosophila heat shock factor to head-to-head and tail-to-tail repeats of a conserved 5 bp recognition unit. *Cell* **59,** 797–806 (1989).

405. Sorger, P. K. Yeast heat shock factor contains separable transient and sustained response transcriptional activators. *Cell* **62,** 793–805 (1990).

406. Jakobsen, B. K. & Pelham, H. R. Constitutive binding of yeast heat shock factor to DNA in vivo. *Molecular and Cellular Biology* **8,** 5040–5042 (1988).

407. Sorger, P. K. & Nelson, H. C. Trimerization of a yeast transcriptional activator via a coiled-coil motif. *Cell* **59,** 807–813 (1989).

408. Westwood, J. T., Clos, J. & Wu, C. Stress-induced oligomerization and chromosomal relocalization of heat-shock factor. *Nature* **353,** 822–827 (1991).

409. Westwood, J. T. & Wu, C. Activation of Drosophila heat shock factor: conformational change associated with a monomer-to-trimer transition. *Molecular and Cellular Biology* **13,** 3481–3486 (1993).

410. Sarge, K. D., Murphy, S. P. & Morimoto, R. I. Activation of heat shock gene transcription by heat shock factor 1 involves oligomerization, acquisition of DNA-binding activity, and nuclear localization and can occur in the absence of stress. *Molecular and Cellular Biology* **13,** 1392–1407 (1993).

411. Baler, R., Dahl, G. & Voellmy, R. Activation of human heat shock genes is accompanied by oligomerization, modification, and rapid translocation of heat shock transcription factor HSF1. *Molecular and Cellular Biology* **13,** 2486–2496 (1993).

412. Zou, J., Guo, Y., Guettouche, T., Smith, D. F. & Voellmy, R. Repression of heat shock transcription factor HSF1 activation by HSP90 (HSP90 complex) that forms a stress-sensitive complex with HSF1. *Cell* **94,** 471–480 (1998).

413. Ali, A., Bharadwaj, S., O'Carroll, R. & Ovsenek, N. HSP90 interacts with and regulates the activity of heat shock factor 1 in Xenopus oocytes. *Molecular and Cellular Biology* **18,** 4949–4960 (1998).

414. Rabindran, S. K., Wisniewski, J., Li, L., Li, G. C. & Wu, C. Interaction between heat shock factor and hsp70 is insufficient to suppress induction of DNA-binding activity in vivo. *Molecular and Cellular Biology* **14,** 6552–6560 (1994).

415. Raychaudhuri, S. *et al.* Interplay of acetyltransferase EP300 and the proteasome system in regulating heat shock transcription factor 1. *Cell* **156,** 975–985 (2014).

416. Jurivich, D. A., Sistonen, L., Kroes, R. A. & Morimoto, R. I. Effect of sodium salicylate on the human heat shock response. *Science* **255,** 1243–1245 (1992).

417. Cotto, J. J., Kline, M. & Morimoto, R. I. Activation of heat shock factor 1 DNA binding precedes stress-induced serine phosphorylation. Evidence for a multistep pathway of regulation. *J. Biol. Chem.* **271,** 3355–3358 (1996).

418. Xia, W. & Voellmy, R. Hyperphosphorylation of heat shock transcription factor 1 is correlated with transcriptional competence and slow dissociation of active factor trimers. *J. Biol. Chem.* **272,** 4094–4102 (1997).

419. Jurivich, D. A., Pachetti, C., Qiu, L. & Welk, J. F. Salicylate triggers heat shock factor differently than heat. *J. Biol. Chem.* **270,** 24489–24495 (1995).

420. Liu, X. D. & Thiele, D. J. Oxidative stress induced heat shock factor phosphorylation and HSF-dependent activation of yeast metallothionein gene transcription. *Genes Dev* **10,** 592–603 (1996).

421. Mivechi, N. F. & Giaccia, A. J. Mitogen-activated protein kinase acts as a negative regulator of the heat shock response in NIH3T3 cells. *Cancer Research*

55, 5512–5519 (1995).

422. Knauf, U., Newton, E. M., Kyriakis, J. & Kingston, R. E. Repression of human heat shock factor 1 activity at control temperature by phosphorylation. *Genes Dev* **10,** 2782–2793 (1996).

423. Chu, B., Soncin, F., Price, B. D., Stevenson, M. A. & Calderwood, S. K. Sequential phosphorylation by mitogen-activated protein kinase and glycogen synthase kinase 3 represses transcriptional activation by heat shock factor-1. *J. Biol. Chem.* **271,** 30847–30857 (1996).

424. Kline, M. P. & Morimoto, R. I. Repression of the heat shock factor 1 transcriptional activation domain is modulated by constitutive phosphorylation. *Molecular and Cellular Biology* **17,** 2107–2115 (1997).

425. Kim, J., Nueda, A., Meng, Y. H., Dynan, W. S. & Mivechi, N. F. Analysis of the phosphorylation of human heat shock transcription factor-1 by MAP kinase family members. *J. Cell. Biochem.* **67,** 43–54 (1997).

426. Chu, B., Zhong, R., Soncin, F., Stevenson, M. A. & Calderwood, S. K. Transcriptional activity of heat shock factor 1 at 37 degrees C is repressed through phosphorylation on two distinct serine residues by glycogen synthase kinase 3 and protein kinases Calpha and Czeta. *J. Biol. Chem.* **273,** 18640–18646 (1998).

427. Holmberg, C. I. *et al.* Phosphorylation of serine 230 promotes inducible transcriptional activity of heat shock factor 1. *EMBO J* **20,** 3800–3810 (2001).

428. Xia, W., Guo, Y., Vilaboa, N., Zuo, J. & Voellmy, R. Transcriptional activation of heat shock factor HSF1 probed by phosphopeptide analysis of factor 32P-labeled in vivo. *J. Biol. Chem.* **273,** 8749–8755 (1998).

429. Hung, J. J., Cheng, T. J., Lai, Y. K. & Chang, M. D. Differential activation of p38 mitogen-activated protein kinase and extracellular signal-regulated protein kinases confers cadmium-induced HSP70 expression in 9L rat brain tumor cells. *J. Biol. Chem.* **273,** 31924–31931 (1998).

430. Jedlicka, P., Mortin, M. A. & Wu, C. Multiple functions of Drosophila heat shock transcription factor in vivo. *EMBO J* **16,** 2452–2462 (1997).

431. Xiao, X. *et al.* HSF1 is required for extra-embryonic development, postnatal growth and protection during inflammatory responses in mice. *EMBO J* **18,** 5943–5952 (1999).

432. Mezger, V., Renard, J. P., Christians, E. & Morange, M. Detection of heat shock element-binding activities by gel shift assay during mouse preimplantation development. *Dev Biol* **165,** 627–638 (1994).

433. Wang, Z. & Lindquist, S. Developmentally regulated nuclear transport of transcription factors in Drosophila embryos enable the heat shock response. *Development* **125,** 4841–4850 (1998).

434. Sarge, K. D., Bray, A. E. & Goodson, M. L. Altered stress response in testis. *Nature* **374,** 126 (1995).

435. Ovsenek, N. & Heikkila, J. J. DNA sequence-specific binding activity of the heat-shock transcription factor is heat-inducible before the midblastula transition of early Xenopus development. *Development* **110,** 427–433 (1990).

436. Trinklein, N. D., Murray, J. I., Hartman, S. J., Botstein, D. & Myers, R. M. The role of heat shock transcription factor 1 in the genome-wide regulation of the mammalian heat shock response. *Mol. Biol. Cell* **15,** 1254–1261 (2004).

437. Birch-Machin, I. *et al.* Genomic analysis of heat-shock factor targets in Drosophila. *Genome Biol.* **6,** R63 (2005).

438. Mendillo, M. L. *et al.* HSF1 drives a transcriptional program distinct from heat shock to support highly malignant human cancers. *Cell* **150,** 549–562 (2012).

439. Verma, P., Pfister, J. A., Mallick, S. & D'Mello, S. R. HSF1 protects neurons through a novel trimerization- and HSP-independent mechanism. *J Neurosci* **34,** 1599–1612 (2014).

440. Stephanou, A., Isenberg, D. A., Nakajima, K. & Latchman, D. S. Signal transducer and activator of transcription-1 and heat shock factor-1 interact and activate the transcription of the Hsp-70 and Hsp-90beta gene promoters. *J. Biol. Chem.* **274,** 1723–1728 (1999).

441. Xie, Y., Chen, C., Stevenson, M. A., Auron, P. E. & Calderwood, S. K. Heat shock factor 1 represses transcription of the IL-1beta gene through physical interaction with the nuclear factor of interleukin 6. *J. Biol. Chem.* **277,** 11802–11810 (2002).

442. Xiao, H., Perisic, O. & Lis, J. T. Cooperative binding of Drosophila heat shock factor to arrays of a conserved 5 bp unit. *Cell* **64,** 585–593 (1991).

443. Tang, Z. *et al.* MEK Guards Proteome Stability and Inhibits Tumor-Suppressive Amyloidogenesis via HSF1. *Cell* **160,** 729–744 (2015).

444. Kim, H. P. *et al.* Heat shock protein-70 mediates the cytoprotective effect of carbon monoxide: involvement of p38 beta MAPK and heat shock factor-1. *J. Immunol.* **175,** 2622–2629 (2005).

445. Smith, S. T. *et al.* Modulation of heat shock gene expression by the TAC1 chromatin-modifying complex. *Nat Cell Biol* **6,** 162–167 (2004).

446. Chen, Y. *et al.* Identification of mixed lineage leukemia 1(MLL1) protein as a coactivator of heat shock factor 1(HSF1) protein in response to heat shock protein 90 (HSP90) inhibition. *J Biol Chem* **289,** 18914–18927 (2014).

447. Prahlad, V., Cornelius, T. & Morimoto, R. I. Regulation of the cellular heat shock response in Caenorhabditis elegans by thermosensory neurons. *Science* **320,** 811–814 (2008).

448. Kumsta, C. *et al.* Integrin-linked kinase modulates longevity and thermotolerance in C. elegans through neuronal control of HSF-1. *Aging Cell* **13,** 419–430 (2014).

449. Chiang, W.-C., Ching, T.-T., Lee, H. C., Mousigian, C. & Hsu, A.-L. HSF-1 regulators DDL-1/2 link insulin-like signaling to heat-shock responses and modulation of longevity. *Cell* **148,** 322–334 (2012).

450. Bond, U. & Schlesinger, M. J. Ubiquitin is a heat shock protein in chicken embryo fibroblasts. *Molecular and Cellular Biology* **5,** 949–956 (1985).

451. Ovsenek, N. & Heikkila, J. J. Heat shock-induced accumulation of ubiquitin mRNA in Xenopus laevis embryos is developmentally regulated. *Dev Biol* **129,** 582–585 (1988).

452. Ungewickell, E. The 70-kd mammalian heat shock proteins are structurally and functionally related to the uncoating protein that releases clathrin triskelia from coated vesicles. *EMBO J* **4,** 3385–3391 (1985).

453. Chappell, T. G. *et al.* Uncoating ATPase is a member of the 70 kilodalton family of stress proteins. *Cell* **45,** 3–13 (1986).

454. Rothman, J. E. & Schmid, S. L. Enzymatic recycling of clathrin from coated vesicles. *Cell* **46,** 5–9 (1986).

455. Valastyan, J. S. & Lindquist, S. Mechanisms of protein-folding diseases at a glance. *Dis Model Mech* **7,** 9–14 (2014).

456. Ciechanover, A. & Kwon, Y. T. Degradation of misfolded proteins in neurodegenerative diseases: therapeutic targets and strategies. *Experimental & Molecular Medicine* **47,** e147 (2015).

457. Jin, X., Moskophidis, D. & Mivechi, N. F. Heat shock transcription factor 1 is a key determinant of HCC development by regulating hepatic steatosis and metabolic syndrome. *Cell Metab.* **14,** 91–103 (2011).

458. Pfaffenbach, K. T. & Lee, A. S. The critical role of GRP78 in physiologic and pathologic stress. *Current Opinion in Cell Biology* **23,** 150–156 (2011).

459. Kenific, C. M. & Debnath, J. Cellular and metabolic functions for autophagy in cancer cells. - PubMed - NCBI. *Trends Cell Biol* **25,** 37–45 (2015).

460. Strecker, T. R., Kongsuwan, K., Lengyel, J. A. & Merriam, J. R. The zygotic mutant tailless affects the anterior and posterior ectodermal regions of the Drosophila embryo. *Dev Biol* **113,** 64–76 (1986).

461. Strecker, T. R., Merriam, J. R. & Lengyel, J. A. Graded requirement for the zygotic terminal gene, tailless, in the brain and tail region of the Drosophila embryo. *Development* **102,** 721–734 (1988).

462. Pignoni, F. *et al.* The Drosophila gene tailless is expressed at the embryonic termini and is a member of the steroid receptor superfamily. *Cell* **62,** 151–163 (1990).

463. Steingrímsson, E., Pignoni, F., Liaw, G. J. & Lengyel, J. A. Dual role of the Drosophila pattern gene tailless in embryonic termini. *Science* **254,** 418–421 (1991).

464. Monaghan, A. P. *et al.* Defective limbic system in mice lacking the tailless gene. *Nature* **390,** 515–517 (1997).

465. Zhang, C.-L., Zou, Y., He, W., Gage, F. H. & Evans, R. M. A role for adult TLX-positive neural stem cells in learning and behaviour. *Nature* **451,** 1004–1007 (2008).

466. Fernandes, J. S. & Sternberg, P. W. The tailless Ortholog nhr-67 Regulates Patterning of Gene Expression and Morphogenesis in the C. elegans Vulva. *PLoS Genet* **3,** e69 (2007).

467. Sarin, S., Antonio, C., Tursun, B. & Hobert, O. The C. elegans Tailless/TLX transcription factor nhr-67 controls neuronal identity and left/right asymmetric fate diversification. *Development* **136,** 2933–2944 (2009).

468. Verghese, E. *et al.* The tailless ortholog nhr-67 functions in the development of the C. elegans ventral uterus. *Dev Biol* **356,** 516–528 (2011).

469. Kato, M. & Sternberg, P. W. The C. elegans tailless/Tlx homolog nhr-67 regulates a stage-specific program of linker cell migration in male gonadogenesis. *Development* **136,** 3907–3915 (2009).

470. Schwarz, E. M., Kato, M. & Sternberg, P. W. Functional transcriptomics of a migrating cell in Caenorhabditis elegans. *Proc Natl Acad Sci USA* **109,** 16246–16251 (2012).

471. Yu, R. T., McKeown, M., Evans, R. M. & Umesono, K. Relationship between Drosophila gap gene tailless and a vertebrate nuclear receptor Tlx. *Nature* **370,** 375–379 (1994).

472. Ekker, S. C. *et al.* The degree of variation in DNA sequence recognition among four Drosophila homeotic proteins. *EMBO J* **13,** 3551–3560 (1994).

473. la Fuente van Bentem, de, S., Mentzen, W. I., la Fuente, de, A. & Hirt, H. Towards functional phosphoproteomics by mapping differential phosphorylation events in signaling networks. *Proteomics* **8,** 4453–4465 (2008).

474. Kim, D. H. A Conserved p38 MAP Kinase Pathway in Caenorhabditis elegans Innate Immunity. *Science* **297,** 623–626 (2002).

475. Tanaka-Hino, M. *et al.* SEK-1 MAPKK mediates Ca2+ signaling to determine neuronal asymmetric development in Caenorhabditis elegans. *EMBO Rep.* **3,** 56–62 (2002).

476. Nakata, K. *et al.* Regulation of a DLK-1 and p38 MAP kinase pathway by the ubiquitin ligase RPM-1 is required for presynaptic development. *Cell* **120,** 407–420 (2005).

477. Hammarlund, M., Nix, P., Hauth, L., Jorgensen, E. M. & Bastiani, M. Axon regeneration requires a conserved MAP kinase pathway. *Science* **323,** 802–806 (2009).

478. Courey, A. J., Holtzman, D. A., Jackson, S. P. & Tjian, R. Synergistic activation by the glutamine-rich domains of human transcription factor Sp1. *Cell* **59,** 827–836 (1989).

479. Gerber, H. P. *et al.* Transcriptional activation modulated by homopolymeric glutamine and proline stretches. *Science* **263,** 808–811 (1994).

480. Friedman, M. J. *et al.* Polyglutamine domain modulates the TBP-TFIIB interaction: implications for its normal function and neurodegeneration. *Nat Neurosci* **10,** 1519–1528 (2007).

481. Bonn, S. *et al.* Cell type-specific chromatin immunoprecipitation from multicellular complex samples using BiTS-ChIP. *Nat Protoc* **7,** 978–994 (2012).

482. Zhou, Z., Hartwieg, E. & Horvitz, H. R. CED-1 is a transmembrane receptor that mediates cell corpse engulfment in C. elegans. *Cell* **104,** 43–56 (2001).

483. Kimble, J. E. & White, J. G. On the control of germ cell development in Caenorhabditis elegans. *Dev Biol* **81,** 208–219 (1981).

484. Zhang, S., Banerjee, D. & Kuhn, J. R. Isolation and culture of larval cells from C. elegans. *PLoS ONE* **6,** e19505 (2011).

485. Cox, G. N., Kusch, M. & Edgar, R. S. Cuticle of Caenorhabditis elegans: its isolation and partial characterization. *J. Cell Biol* **90,** 7–17 (1981).

486. Seglen, P. O. Preparation of isolated rat liver cells. *Methods Cell Biol.* **13,** 29–83 (1976).

487. Mello, C. C., Kramer, J. M., Stinchcomb, D. & Ambros, V. Efficient gene transfer in C.elegans: extrachromosomal maintenance and integration of transforming sequences. *EMBO J* **10,** 3959–3970 (1991).

488. Frøkjær-Jensen, C. *et al.* Random and targeted transgene insertion in Caenorhabditis elegans using a modified Mos1 transposon. *Nat Chem Biol* **11,** 529–534 (2014).

489. Tursun, B., Cochella, L., Carrera, I. & Hobert, O. A Toolkit and Robust Pipeline for the Generation of Fosmid-Based Reporter Genes in C. elegans. *PLoS ONE* **4,** e4625 (2009).